NTNU – Trondheim
Norwegian University of
Science and Technology

Numerical Simulation of an Ekofisk Single Well Chemical Tracer Test

Mari Mikalsen

Petroleum Geoscience and Engineering
Submission date: June 2014
Supervisor: Jan-Åge Stensen, IPT
Co-supervisor: Robert Moe, ConocoPhillips

Norwegian University of Science and Technology
Department of Petroleum Engineering and Applied Geophysics

NTNU ConocoPhillips

Numerical Simulation of an Ekofisk Single Well Chemical Tracer Test

Master Thesis by

Mari Mikalsen

June 2014

Acknowledgements

This master thesis is the final part of the Master of Science program in Petroleum Engineering at the Norwegian University of Science and Technology (NTNU). The thesis was written in co-operation with ConocoPhillips Scandinavia AS. I would like to thank them for the motivating and interesting project.

Next, I would like to thank Dr. Robert W. Moe for being my mentor at ConocoPhillips. I would like to thank him for his excellent technical guidance, constructive support and interesting discussions.

Also, I would like to thank Arvid Østhus for taking a special interest in my thesis; giving me constructive feedback and guidance all the way through.

Thanks to Ole Eeg for his full support and assistance.

Further, I would like to thank my supervisor at NTNU, Jan Åge Stensen, for his support during this thesis.

A special thanks to all the graduates at ConocoPhillips. Without all the lunch breaks, good conversation and countless coffee breaks, I would have lost my mind.

Finally, I would like to thank my family and friends for the support and understanding during the course of this thesis.

Abstract

The Ekofisk field in the North Sea has been undergoing waterflood since 1987. It has proved to efficiently recover oil by means of spontaneous imbibition. The plan is to continue waterflooding until the end of the license in 2028. The challenge lies in how to recover the residual oil left immobile after the waterflood. The average oil saturation in the flooded parts of the reservoir is approximately 30 %. Surfactant flooding has now been proposed as an option, and is showing promising results in the laboratory. An enhanced imbibition study by injection of low concentration surfactants was conducted in the mid-1990s. The study was terminated in 1997 due to lab measurements of unsatisfactory high adsorption, making it un-economical. Further studies on surfactants were not done until 2011. The most attractive feature of the surfactant this time around is its ability to lower IFT enough to free immobile oil from the pores. Both the economics and understanding of the surfactant process have improved significantly over the last 20 years, making it an option once again.

Current plans involve the implementation of a single well chemical tracer test in 2015 to confirm the lab results on the effect the surfactant flood has on the residual oil. Several simulation studies were conducted in this thesis to determine the expected injection rates and the volumes necessary to execute an efficient pilot test. Particular attention is paid to the influence of surfactant adsorption and the effect of geological features in the test area. Adsorption proved to have a particular large effect on the acting distance of the surfactant slug.

Based on history matching and other specific simulation studies, the expected injection rate was determined to be 35 bbl/day for a 20 feet high perforation interval. With this rate a total of 6 months to complete the SWCTT was required with the predetermined slug volumes.

Sammendrag

Ekofiskfeltet I Nordsjøen har blitt vannflømmet siden 1987. Det har vist seg å være svært effektivt med tanke på å utvinne olje ved hjelp av spontan imbibering. Planen er å fortsette vannflømmingen av feltet frem til lisensen går ut i 2028. Utfordringen ligger i hvordan å utvinne den residuelle oljen som blir forlatt immobil i porene. Den gjennomsnittlige oljemetningen i de flømmede områdene av reservoaret er omtrent 30 %. Surfaktant har nå blitt foreslått som en mulighet, og viser lovende resultater fra kjerneflømminger. Et økt-imbibering studie ved injeksjon av lav-konsentrasjon surfaktant ble utført på midten av 1990-tallet. Studiet ble avsluttet i 1997 etter at laboratoriemålinger viste utilfredsstillende høye adsorpsjonsverdier som gjorde hele prosjektet uøkonomisk. Videre studier ble ikke gjort før i 2011. Den mest attraktive egenskapen til surfaktanten i denne omgang var dens evne til å redusere IFT nok til å frigjøre oljen fra porene. Både det økonomiske aspektet og forståelsen av prosessen bak flømming med surfaktant har økt betraktelig i løpet av de siste 20 årene, og gjør det til et alternativ nok en gang.

Nåværende planer er å implementere en ènbrønns kjemisk tracer test i 2015 for å bekrefte laboratorieresultatene om effekten surfaktant har på den residuelle oljemetningen. Flere simuleringsstudier ble utført i denne oppgaven for å bestemme forventede injeksjonsrater og nødvendige volumer for å gjennomføre en vellykket pilottest. Spesiell oppmerksomhet ble rettet mot adsorpsjon av surfaktant og effekten av geologiske egenskaper i testområdet. Adsorpsjon viste seg å ha en spesielt stor effekt på virkningslengden av surfaktanten.

Basert på historietilpasning og andre spesifikke simuleringsstudier, ble den forventede raten bestemt til 35 bbl/dag for et 20 fots høyt perforeringsintervall. Med denne raten tok det totalt 6 måneder å fullføre pilottesten med de forhåndsbestemte volumene.

Table of Contents

List of Figures

List of Tables

1 Introduction

The petroleum industry in Norway is by far superior when it comes to creating value, Government income and export value. The oil and gas industry has produced values of 9000 billion NOK since the start of oil production on the North Continental Shelf (NCS) (Force Report 2011). Production has slowly decreased since the Norwegian oil production peaked in year 2000, and action is needed to maintain production levels. According to NPD (Norwegian Petroleum Directorate) the total production of oil and gas on the NCS was 226 MSm^3 oil equivalents in 2012. The decline in oil production was 8.5 % from the previous year, while gas production increased with 13% during the same time period. The forecast is that production will continue on the same level as 2012 towards 2020, and then decrease towards 2030; with increasing gas production and decreasing oil production (Miljødirektoratet 2013).

More than half of the world`s remaining oil exists in carbonate (chalk and limestone) reservoirs (Zahid *et al.* 2010). The low permeability chalk reservoirs in the southern part of the North Sea are characterized by intense fracturing caused by tectonic activities. They are classified as naturally fractured reservoirs. Standard recovery methods yield a significantly lower recovery in fractured chalk reservoirs compared to sandstone reservoirs. The potential enhanced oil recovery target is accordingly higher (Ersland *et al.* 2010).

In this thesis the terms enhanced oil recovery (EOR) and improved oil recovery (IOR) are defined in accordance with the Norwegian Petroleum Directorate (NPD). IOR is defined as any processes applied to improve sweep efficiency to extract more of the mobile oil fraction. EOR is defined as processes aiming to improve production by targeting the immobile part of the oil.

The entire reservoir on the Ekofisk field is currently under waterflood, both vertically and laterally. The current plan is to continue the water injection until end of license in 2028. While waterflooding at Ekofisk has been a huge success, it is recognized that there is a large

potential for EOR. ConocoPhillips is currently looking at several possible EOR options and the possibility of moving towards a Single Well Chemical Tracer Test by 2015.

Single Well Chemical Tracer Tests are widely used in the oil industry as the first field pilot. The method needs careful planning and the results can be challenging to interpretate. Numerical simulation is used to help design the pilot and for understanding the pilot results. Design parameters could include injection volumes and rates, volume needed in the back production and the size of the pilot.

The main objective of this thesis is to provide input to the design of a field test and to make sensitivity runs to estimate the impact of heterogeneity on the results by use of the ConocoPhillips in-house simulator, PSim. Also, to build a 2D sector model and match the Ekofisk waterflood for the selected injector-producer pair, use the model to run initial single well chemical tracer test sensitivities and use the input and results from the 2D model in a 2D radial model and simulate a field test. Run a sensitivity study including impact of fractures, flow out of zone, temperature, etc.

This thesis starts with an introduction to the Ekofisk field history and background. Further, the theory of particular interest for surfactant flooding is presented. A literature review of surfactant flooding is featured in the succeeding chapter. Next, factors influencing recovery are discussed; followed by a general description the EOR process and different EOR techniques.

The key part of the thesis starts with an introduction to the Ekofisk model, followed by a chapter discussing the concepts of a single well chemical tracer test including a simulation study. Further, simulation studies of surfactant flooding in a 2D sector model and a 2D radial model are presented. Finally, conclusions, discussion and thoughts around future work and limitations are brought forward.

2 Ekofisk Field History and Background

The greater Ekofisk Area comprises of eight fields in the North Sea, of which four are shut-in; Cod, West Ekofisk, Albuskjell and Edda. The four fields currently producing are Ekofisk, Eldfisk, Tor and Embla. ConocoPhillips Skandinavia AS operates the Greater Ekofisk Area with an ownership of 35.11 % in production license (PL) 018. The partners are Total E&P Norge AS (39.90 %), Eni Norge AS (12.39 %), Statoil Petroleum AS (7.60 %) and Petoro AS (5.00%). The PL018 license is currently valid until 2028 (ConocoPhillips n.d). In 2013 production from Ekofisk accounted for 8.4% of the total oil production on the Norwegian Continental Shelf (SSB 2014).

2.1 Field Discovery

Ekofisk was discovered in 1969 in Block 2/4, located in the Central Graben; south in the Norwegian sector of the North Sea (Figure 2.1). This particular discovery came at a time when companies had started to become discouraged after unsuccessful exploration; abandoning the search in the area. Even after the discovery of Ekofisk, reactions were negative because the reservoir consisted of chalky limestone. It was only after four subsea completed wells were drilled in 1971 and showed promising results, that other companies turned believers (Van den Bark & Thomas 1980).

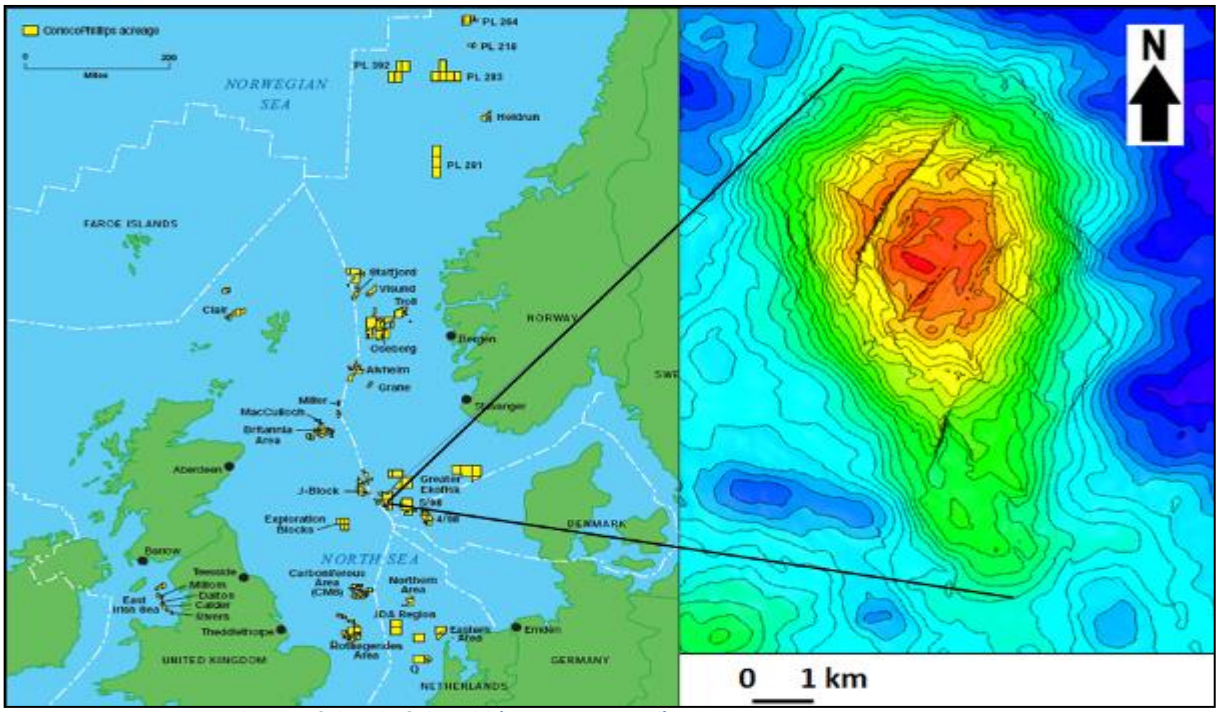

Figure 2.1 Location and map of the Ekofisk Field (COPNO Internal).

2.2 Geology

The Ekofisk field is an elongated anticline with the major axis running North-South, and covering around 12 000 acres. It consists of two overlying chalk formations – Ekofisk (Danian age) and Tor (Maastrichtian age) – separated by a tight zone below the lower Ekofisk formation (Figure 2.2). Roughly two thirds of the 7.1 billion STB oil in place is located in the Ekofisk formation (Hermansen *et al.* 2000). The tight zone is 50 feet thick, and forms an impermeable barrier between the two formations in the major part of the field. Communication between the two formations is limited to the highly fractured areas on the crest (Hallenbeck *et al.* 1991). The top of the Ekofisk formation is located at a depth of 9 600 ft. Both formations have thicknesses varying between 300 and 500 ft.

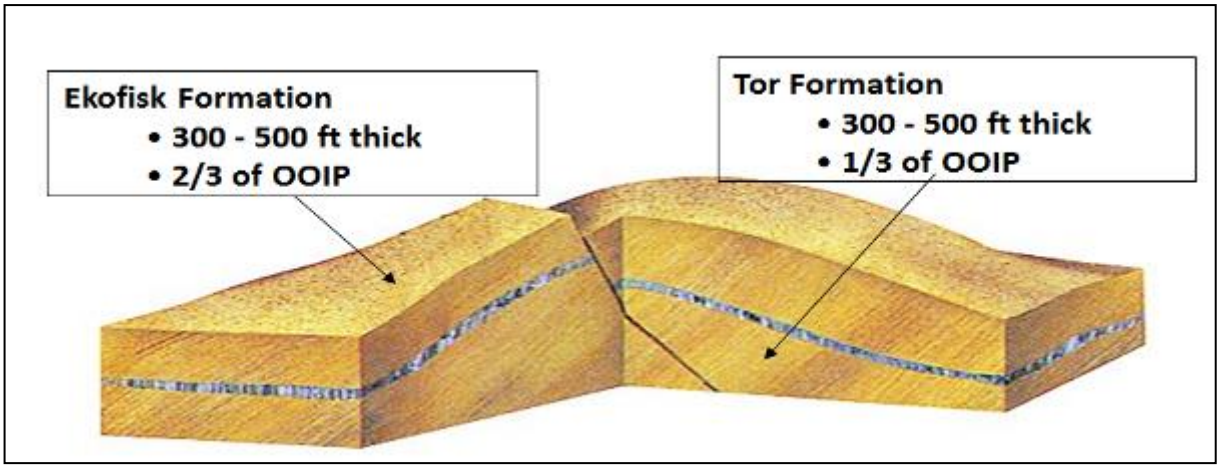

Figure 2.2 Cross sectional view of the Ekofisk Formation and the Tor Formation (COPNO Internal).

The chalk is naturally fractured with matrix permeability up to 5 md, and with an effective permeability near 100 md. The Ekofisk formation is dominated by tectonic fractures, while most of the fractures in the Tor formation are stylolite-associated. The other two fracture types dominating the Ekofisk field are irregular and healed fractures. Figure 2.3 shows the two main types of fractures; tectonic and stylolite.

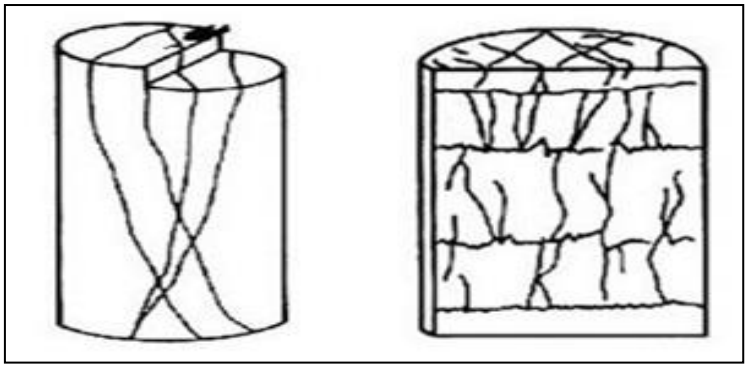

Figure 2.3 Tectonic (Left) and Stylolite (Right) fractures (COPNO Internal).

The overlying Ekofisk formation has somewhat higher porosity than the underlying Tor formation; respectively 30% to 48% against 30% to 40% (Sulak 1990). The initial reservoir pressure was 7135 psia at a depth of 10 400 ft. The field originally contained undersaturated volatile oil at a bubble point pressure of 5560 psia at an initial temperature of 268 °F (Hermansen *et al.* 2000).

2.3 Field Development

The Ekofisk field was developed in stages. Exploration progressed simultaneously with development plans; hence the conditions for development changed. The first stage was started in 1971, and consisted of test production from the discovery well and three appraisal wells. Reports from this phase stated that the reservoir was as good as, or even better than first assumed. This gained the confidence needed to move on to phase II – drilling 30 new wells from three platforms and installing production facilities to handle 300 000 STB/D (Boyce 1972).

In 1974 production through permanent facilities was initiated. In addition to the three drilling platforms, the field terminal platform and living quarters, and a one-million-barrel concrete storage tank was installed. The storage tank allowed production to continue when weather conditions prevented offshore loading. An oil pipeline to Teesside, England became operational in 1975, and in 1977 a gas pipeline to Emden, Germany was a reality (Sulak 1990). Production peaked in October 1976 at 350 000 STB/D, before rapidly decreasing.

Based on positive results from laboratory studies and a water injection pilot, it was in 1983 decided to commence water injection into the Tor Formation. In 1987 water injection began from the water-injection platform 2/4 K with an injection capacity of 375 000 BWPD and 30 well slots. A water injection pilot was also initiated into the Lower Ekofisk Formation, and showed promising signs. 11 additional injectors and 16 producers were drilled in early 1990 to realize water injection into Lower Ekofisk. Further expansion was done, and water injection capacity was raised to 500 000 BWPD. In 1992 it was decided to start water

injection into the Upper Ekofisk Formation as well, and water injection capacity was further increased to 820 000 BWPD by use of a converted drilling rig.

Figure 2.4 shows the platforms and drilling rigs currently operating on Ekofisk. In addition to the surface facilities, two subsea installations – Victor Alpha and Victor Bravo – are installed. During the last 40 years of production, more than 400 wells have been drilled (COPNO Internal).

Figure 2.4 Current platforms on Ekofisk (COPNO Internal).

In 1987, prior to the implementation of the waterflood, oil production rates were as low as 70 000 STB/D. In March 1990 the response from the waterflood was characterized by sharply increased oil rates, declining GOR and low water cuts. The average water injection into Ekofisk was as of March 2014 just below 400 000 BPD, divided between 32 active injectors. As of March 2014 the oil production rates from Ekofisk were approximately 140 000 STB/D (COPNO Internal).

Only 18% of the original oil in place (OOIP) in the Ekofisk field was initially estimated to be recoverable. The discovery of reservoir compaction increased this primary recovery estimate to 24%, because it led to increased recovery by compaction drive (Sulak 1990). In year 2000 the oil recovery estimate from Ekofisk was 38 % of the OOIP (Hermansen *et al.* 2000). As of 2014 an estimated recovery factor of 51 % seems possible by 2029 (COPNO Internal).

2.4 Subsidence

Seabed subsidence at the Ekofisk field was discovered in 1984. This was a result of reservoir compaction from hydrocarbon extraction, leading to a massive decline in reservoir pressure. Decreased pore pressure lead to an increase in effective stress, causing the weak chalk to compact by pore collapse. It was first thought that natural conditions had caused the sea level to rise, and the subsidence was not taken seriously. The belief at the time was that compaction of the reservoir would lead to decreased productivity, and since productivity was not decreasing, the reservoir could not be compacting. By 1984 the seabed beneath the Ekofisk complex had subsided by more than 10 feet, and measurements confirmed that the platforms were indeed sinking (Sulak 1990). Figure 2.5 shows the seabed subsidence rates from year 1992 to 2008 for the hotel (red), the Ekofisk Alpha platform (green) and the Ekofisk Bravo platform (blue).

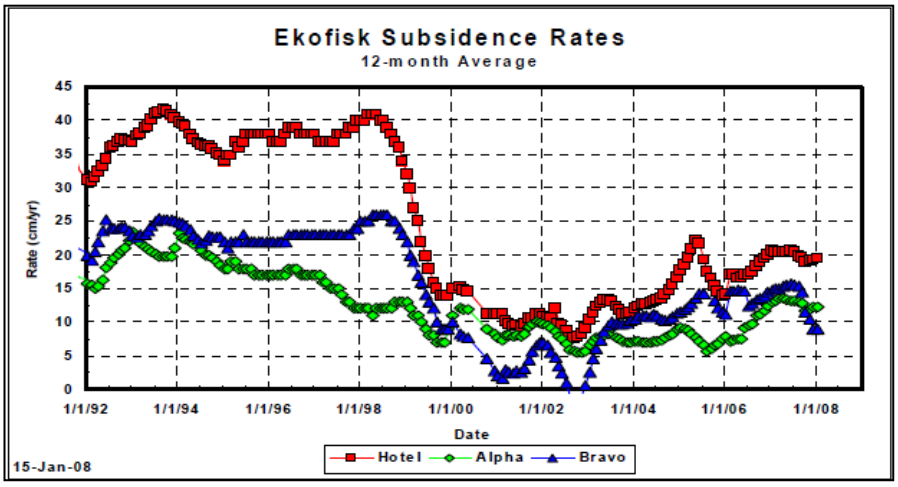

Figure 2.5 Subsidence rates from 1992 – 2008 (COPNO Internal).

The main problem and concern regarding the subsidence was the protection of the platforms and the storage tank. The solution to secure the concrete tank was to build a protective barrier around it. Figure 2.5 shows pictures of the protective wall around the storage tank in years 1974, 1985 and 2006, and the degree of subsidence. The holes in the wall are 1.3 meters for scale. For the platforms, a major jack up project was executed during the summer of 1987. At the time the Ekofisk Center Complex consisted of six steel platforms and inter-connected bridges; all elevated 6 meters to be out of harm's way from storm waves.

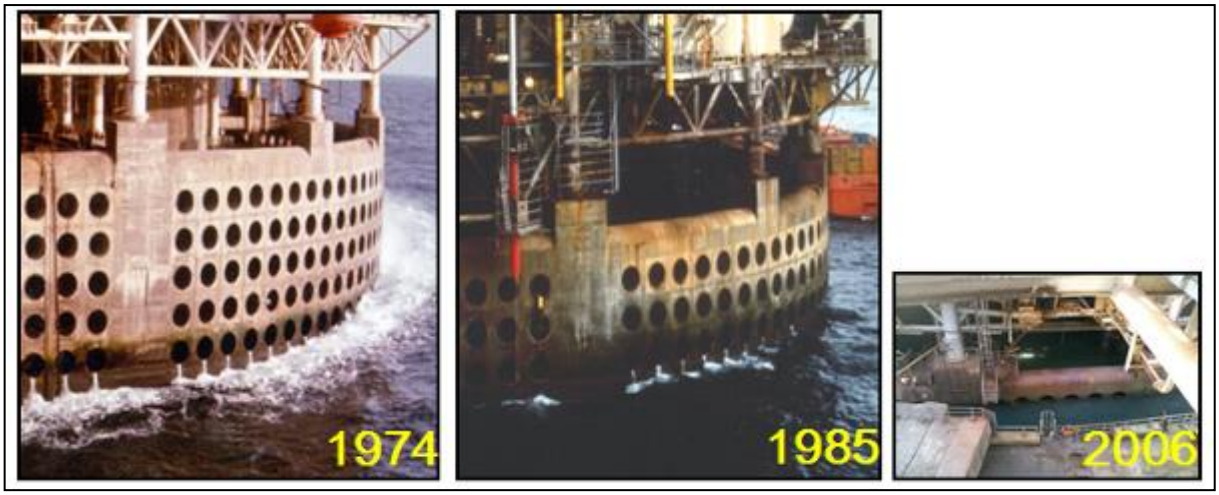

Figure 2.6 Subsidence of the concrete protective wall around the storage tank (COPNO Internal).

The field wide water injection process has slowed down the subsidence rate. The decreasing subsidence trend indicates good pressure support by the injected water. Although the Ekofisk formation has been repressurized to a pressure greater than the bubble point of oil, subsidence will continue with a rate of 15 cm/year in the water flooded areas. Estimated subsidence by 2050 is 12 – 16 meters (COPNO Internal). The reason will be discussed in subchapter 2.5.1. Compaction and subsidence are also issues for well integrity. There is great well failure potential involved in the process of compaction; e.g. buckling of the wellbore. A consequence of well collapse is that the process of P&A (Plug & Abandonment) of a well becomes highly more difficult to implement. Seabed pipelines are also at risk when the compaction leads to seabed subsidence.

2.5 Production from Chalk Reservoirs

The average recovery factor (RF) for carbonate reservoirs is far less than for sandstone reservoirs. The worldwide RF for carbonate reservoirs is only 30%. Most of the reservoirs are highly fractured, and almost 90% are oil-wet to neutral-wet; prohibiting oil displacement by spontaneous imbibition of water. Contrary to sandstone behavior, carbonate reservoirs appear to become increasingly oil-wet as the reservoir temperature decreases (Austad *et al*. 2008).

In the North Sea the dominant oil-containing carbonate formation is chalk. The early invasion of oil into these chalks is the reason for the natural fracture system and high porosity. The Ekofisk chalk is very poorly cemented between grains. The main production mechanism for fractured chalk reservoirs undergoing waterflood is spontaneous imbibition. The imbibition process is affected by several parameters; rock characteristics (porosity, permeability), fluid properties (density, viscosity and interfacial tension), wettability, thermodynamic conditions, initial saturations and boundary conditions. Wettability varies through the Ekofisk field. The Tor formation is water-wet, while conditions for the Lower and Upper Ekofisk formations are mixed-wet to nearly oil-wet. Because of this, the nature of spontaneous water imbibition is different for the formations (Austad & Milter 1997).

The injection of seawater proved to imbibe efficiently into the Ekofisk and Tor chalk matrix; regardless of the low matrix permeability. The most crucial wetting parameter for carbonates is the acid number, AN. The acid number represents the amount of carboxylic acids present in the crude oil. At natural pH the initial interface between chalk and water is positively charged, while the interface between oil and water is negatively charged. Thus, the disjoining pressure in the water film becomes negative, and oil contacts the chalk surface; making it naturally oil-wet (Austad *et al*. 2008).

Cuiec *et al*. (1994) established the importance of capillary forces and the existence of a predominant countercurrent mechanism at constant and high interfacial tension (IFT). Their research concluded that as IFT was lowered, the final recovery increased. A chalk core experiment showed that the water volume imbibed into a given end was equal to the oil volume produced by the same end. It was confirmed that the oil was produced by countercurrent flows into the fractures, and that no cocurrent flow occurred during spontaneous imbibition. At high IFT`s (41 mN/m) no additional oil was displaced when a forced imbibition was performed after a spontaneous imbibition, confirming that no mobile oil was trapped in the core after the process (Cuiec *et al*. 1994).

Capillary forces are the main driving forces in spontaneous imbibition. The capillary number, N_C, expresses the ratio of viscous to capillary forces, and is given in eq.2.1;

$$N_C = \frac{V\,\mu}{\sigma} \tag{2.1}$$

Where μ is the fluid viscosity, *V* is the fluid velocity and σ the interfacial tension. In forced displacements the goal is to mobilize the residual oil saturation. This can be done by lowering the IFT to raise the capillary number enough to overcome the capillary forces. Viscous forces will then dominate, and allow oil to flow. The capillary number has to exceed the critical capillary number in order to mobilize residual oil. The relationship is illustrated by the graph in Figure 2.7;

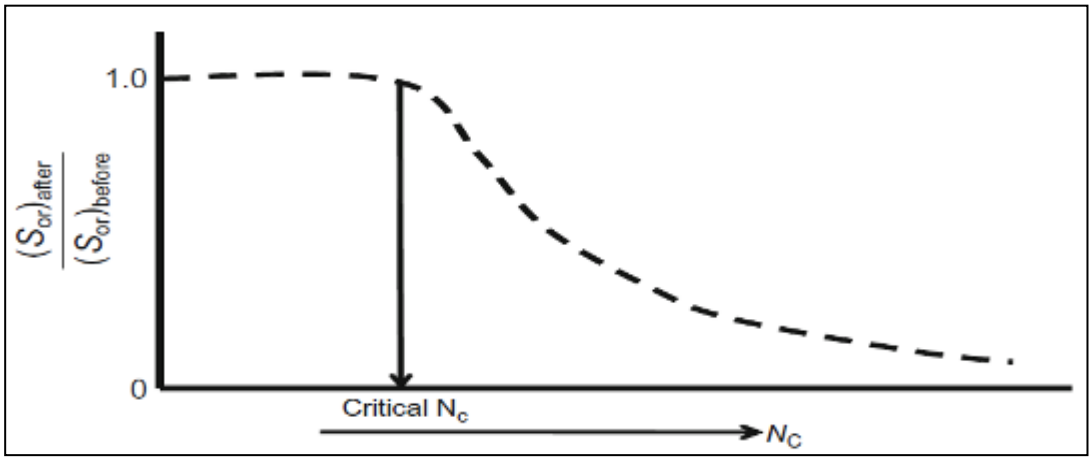

Figure 2.7 Effect of N_C on residual oil saturation (Ahmed & Meehan 2012).

In water-wet chalks the fluid flow is countercurrent at high IFT; governed by capillary forces. At low IFT (0.02 mN/m) imbibition goes from being capillary dominated to being gravity dominated. The oil production in the gravity dominated regime is slow compared to the production driven by capillary forces. At low IFT a larger fraction of the oil is produced by the slow gravity process. For field applications this may mean too long of a delay. The crossover point from capillary forced imbibition to gravity dominated imbibition can be scaled according to the inverse Bond number, N_B^{-1}, which is the ratio between capillary and gravity forces;

$$N_B^{-1} = C\,\frac{\sigma\sqrt{\varphi/k}}{\Delta\rho\, g\, H} \tag{2.2}$$

Where *C* is a constant related to pore geometry, σ is the interfacial tension, ϕ is the porosity, *k* is the permeability, Δρ is the difference in density between the two immiscible phases, *g* is the acceleration due to gravity and *H* is the core length. The work done by Austad & Milter

(1997) concluded that for $N_B^{-1}>5$ the imbibition process is driven by capillary forces and exhibits countercurrent flow. For $N_B^{-1}<<1$ the imbibition is driven by gravity forces; exhibiting vertical cocurrent flow.

The Lower Ekofisk formation is believed to be mixed-wet, and displays similar trends as the water-wet Tor formation. The expulsion of oil at low IFT is however extremely slow for mixed-wet conditions. Compared to the water-wet cores, the crossover point takes place at an earlier stage for the mixed-wet cores; meaning more oil is produced in the slow gravity forced region.

Further experiments done by Austad & Milter (1997) showed that spontaneous imbibition into nearly oil-wet chalk is possible with the use of a cationic surfactant. The resulting countercurrent flow points to the surfactant turning the chalk more water-wet during the imbibition process.

2.5.1 Water Weakening in Chalks

Permeability studies conducted by Newman (1983) showed that a significant permeability reduction occurs in chalk when it is saturated with sea water. The reduction is mainly caused by the extensive amount of compaction in the chalk. This effect is called water weakening. In the same study the effluent of the injection water was analyzed, showing increased calcium concentration. It was suggested that this was dissolution of calcium carbonate from the chalk matrix. The solubility of chalk in water is low, and decreases with increasing temperature. Dissolution only occurs if the injected water is not in chemical equilibrium with the chalk. Considering that dissolution can cause mechanical failure, it should be avoided.

Even though the Ekofisk formation has been repressurized to a pressure greater than the bubble point of oil, subsidence will continue with a rate of 15 cm/year in the water flooded areas. This strongly indicates the water weakening effect on the chalk matrix. Studies done by Austad *et al*. (2008) showed that fluids containing Ca^{2+}, Mg^{2+} and SO_4^{2-} have a specific

impact on chalk at high temperatures. These three ions are regarded potential determining ions.

At low temperatures Ca^{2+} has a higher affinity towards the chalk surface than Mg^{2+}, and is more strongly adsorbed on the chalk surface. At higher temperatures (>158 °F) Mg^{2+} becomes active, and Ca^{2+} is substituted at the surface by Mg^{2+} (Figure 2.8). Because Mg^{2+} is a smaller ion than Ca^{2+}, stress is caused at the chalk grain contact. This proved to weaken the chalk and lead to an increase in compaction by $CaSO_4$ precipitation. SO_4^{2-} was determined to be acting as a catalyst for this substitution process (Austad *et al*. 2008).

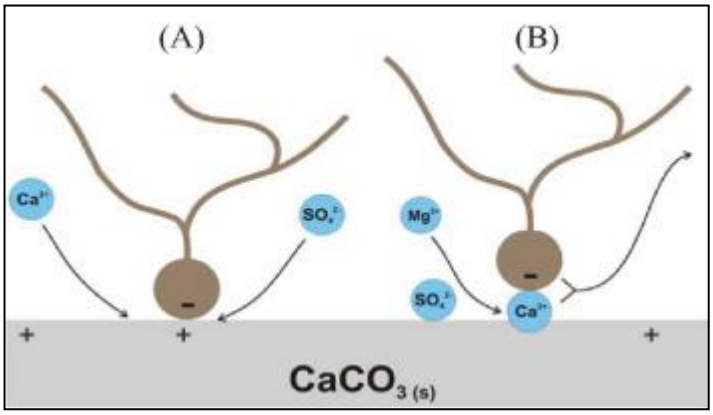

Figure 2.8 Illustration showing ion interaction and substitution at (A) low temperature and (B) high temperature (Austad *et al.* 2008).

The studies done by Austad and his co-workers concluded that without SO_4^{2-} present, substitution of Ca^{2+} by Mg^{2+} would not take place at the grain contact. Compaction could be dramatically decreased by removing SO_4^{2-} from the seawater. With reduced compaction comes reduced compaction drive; the contributor to 40% of the drive mechanism for Ekofisk. The risks associated with compaction need to be weighed against the potential loss of oil recovery from reduced compaction drive.

2.6 EOR Screening for Ekofisk

Jensen *et al*. (2000) evaluated and ranked several possible EOR technologies for application on the Ekofisk field, with focus on relative oil recovery potential. Since Ekofisk is a very large field, an incremental recovery of only 1% represents around 80 MMBOE. This will mean that major value is added (COPNO Internal). Figure 2.9 shows a pie chart of the total resources in

Ekofisk. 39 % of the OOIP had been produced by 2014. The ultimate recovery at the end of 2028 is estimated to be 51 %. The remaining oil fraction after 2028 will then be 49 %.

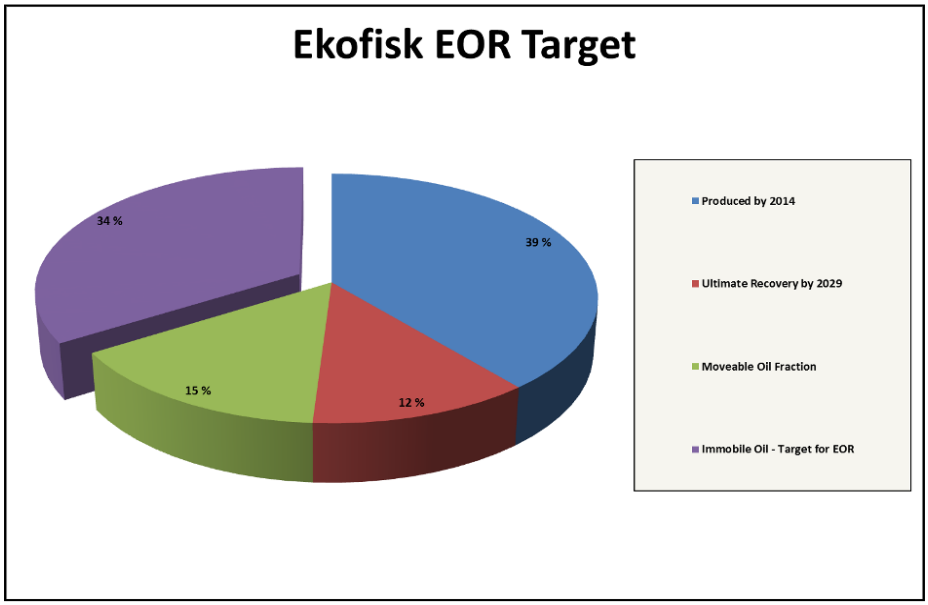

Figure 2.9 Ekofisk EOR target (COPNO Internal).

Considering that the average values of initial water saturation (S_{wi}) and residual oil saturation (S_{or}) are respectively 10 % and 30 %, the maximum sweep for Ekofisk can be calculated by use of equation 5.5. The equation will be explained in Chapter 5;

$$Maximum\,Sweep\,Efficiency = \frac{0.9 - 0.3}{0.3} \times 100\% = 66\%$$

Out of these 66 %, 51 % should already have been recovered by 2029; leaving a mobile oil fraction of 15 %. This means that approximately 77 % of the mobile oil will be recovered by 2029. The immobile oil fraction (purple) will then be 34 %. With regards to the definition of EOR, it is the immobile oil which is the target for enhanced recovery.

The high immobile oil fraction and the volumes it represents, makes the field a good candidate for EOR. Several studies have been done throughout its existence. The key issue with an EOR agent is its ability to contact and mobilize the waterflood residual oil in the highly fractured chalk system. The incremental oil recovery from gas injection schemes could be drastically lower than predicted by simulation studies if the injected gas prefers to flow through the fracture system; staying clear of matrix flow. This situation with non-matrix flow

could occur if matrix flow is prohibited by capillary threshold entry pressures or rate-limited by gas-water diffusion (Jensen *et al*. 2000).

Figure 2.10 shows the waterflood and EOR investigation that has been going on for the Ekofisk field since 1973.

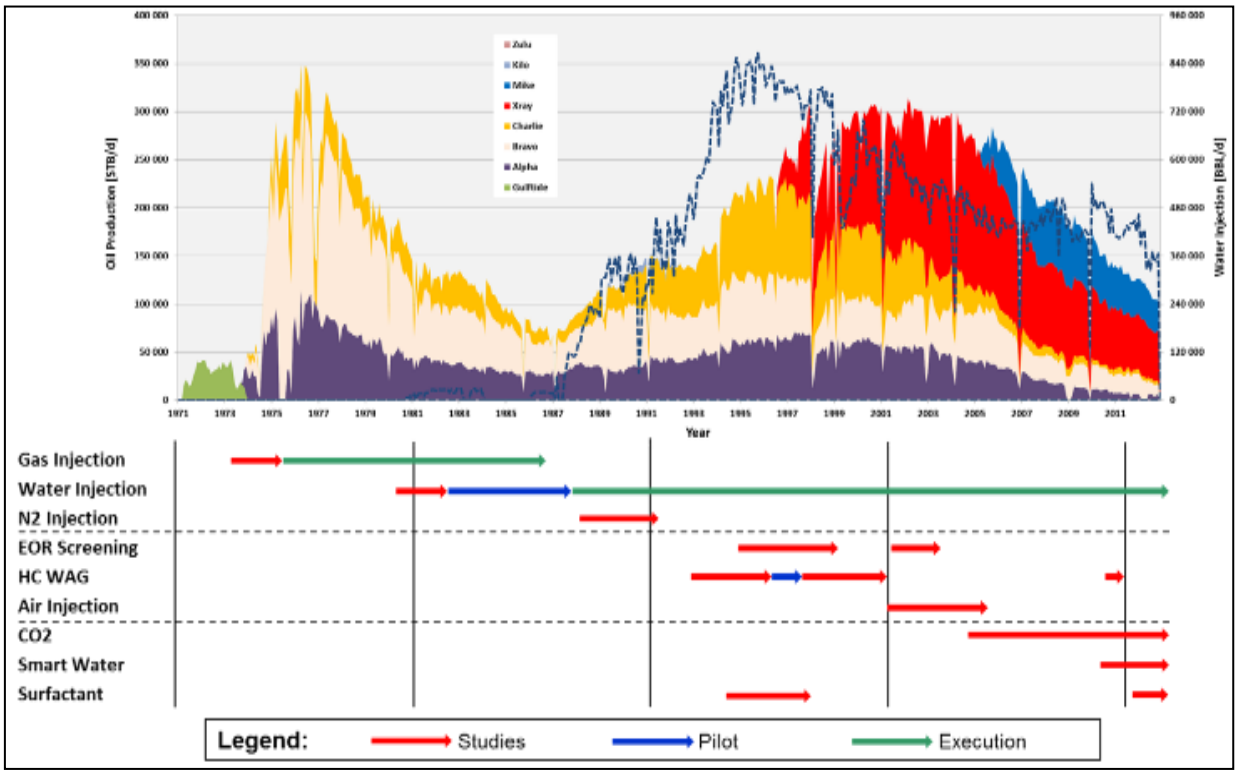

Figure 2.10 Historical EOR studies and waterflood for Ekofisk (COPNO Internal).

Since 1975 swing gas has been re-injected into the crestal areas of the field. As of June 2000, 21% (1.3 Tscf) of the cumulative produced gas had been re-injected. Tracer tests done from 1986 to 1988 proved that the gas covered a large area, and that no immediate production of free gas was experienced. In the late 1980s a nitrogen study was conducted, showing non-favorable economics. The nitrogen only extracted the lightest components from the oil; leaving the remaining oil less mobile, with higher viscosity and IFT.

The investigation into the possibility of implementing a WAG pilot was initiated in 1993. The studies of injecting hydrocarbon gas alternate water showed promising results, and a pilot test was planned. The pilot was executed in 1996, but was found to be both technically and economically challenging. The many years of injecting cold seawater had created a cold region around the injecting wells. This cold region caused the formation of hydrates in-situ in

the reservoir, and injectivity dropped to zero in a matter of hours. Following the pilot, studies were done to find ways in which hydrate formation could be avoided, but no real solutions were discovered (Jensen *et al*. 2000).

In addition to the HC-WAG pilot and the waterflood pilot in the early 1980s, two other pilots have been performed on Ekofisk. This was a water-shut-off pilot and a produced water pilot; where neither of which has been published with results in the literature.

After the failed pilot test, a number of other EOR techniques were studied; air injection, CO_2 WAG injection, smart water and surfactants. Air injection to create spontaneous ignition around the cooled water injectors was studied between 2001 and 2006. The incremental oil recovery from air injection proved to be the highest of the methods in the screening study done by Jensen and his co-workers. Air injection was at the end ruled out due to the large risk and uncertainty involved. Producing large amounts of oxygen together with oil and gas creates a potential explosion hazard.

CO_2 is not a likely option today due to the lack of CO_2 availability and the potential need for extensive field re-development. Some of the equipment on Ekofisk dates back to the start of the field's life, which would make corrosion a huge problem. The large amount of fractures in the field also present problems for a possible CO_2 flood, because it could lead to early breakthrough of CO_2. With the temperature profile created by injecting cold seawater, there is also a potential risk of hydrate formation. This will cause injectivity losses similar to those experienced in the WAG pilot. The subsidence increases the potential for well failure, which increases the risk of leakage. There is also a high potential for CO_2 leakage due to the fact that more than 400 wells have been drilled during the last 40 years of production. A safe aquifer would be needed for containment assurance. As of today, CO_2 flooding is looked at as a possibility for the future. A multi-well pilot would need to be carried out before a full field implementation. Smart Water has been studied over the last couple of years, but is currently not at a level where it is possible to quantify the EOR effect.

In the mid- to late 1990s an enhanced imbibition study by injection of low concentration surfactants was conducted. The study was terminated in 1997 due to lab measurements of unsatisfactory high adsorption, making it un-economical. The high adsorption was especially

seen in the vicinity of existing water injection wells, where reservoir temperatures were reduced. Further studies on surfactants were not done until 2011. Both the economics and understanding of the surfactant process have improved significantly over the last 20 years, making it an option once again.

3 Theory

This chapter addresses the rock and fluid properties of particular interest for surfactant flooding. This includes porosity, permeability, matrix-fracture interaction, interfacial tension, wettability, relative permeability, saturation and spontaneous imbibition.

The two main parameters that determine the efficiency of surfactant flood as an EOR technique are interfacial tension and wettability alteration. The two parameters play a crucial part in the ability to recover what is left of the oil in the reservoir; reducing the residual oil saturation.

3.1 Rock Properties

3.1.1 Porosity

Porosity is defined as the ratio of pore volume (void space) to the bulk volume of the rock (Lake 1989);

$$\varphi = \frac{V_p}{V_b} \tag{3.1}$$

Where φ is porosity, V_p the pore volume, and V_b the bulk volume. The porosity is normally in the range of 10% to 40% (Lake 1989) for naturally occurring media; the rock phase clearly occupying the largest fraction of any medium. For a rock containing all equally sized grains, the grain size does not affect porosity. Grain size distribution and sorting however, play an important role. Well sorted grains produce a much higher porosity than does poorly sorted grains. Porosity can be divided into primary and secondary porosity. Basically, primary porosity is formed when the sediments are first deposited, while secondary porosity is formed by geological processes that take place after deposition (e.g. digenesis). The porosity of sandstone is normally primary, while limestone typically has secondary porosity. Furthermore, porosity can be divided into interconnected (effective) porosity and disconnected porosity. The latter is of no concern to EOR, as the oil in disconnected pores cannot be contacted by any displacing agent (Zolotukhin & Ursin 2000).

Porosity is as high as 48 % in some parts of the Ekofisk formation. The high porosity can be explained by the early invasion of oil into the reservoir rock; preventing the porosity from being lowered by digenesis.

3.1.2 Permeability

Permeability is as important to EOR processes as porosity, and is defined as a medium`s capability to transmit fluids through its network of interconnected pores (Zolotukhin & Ursin 2000). From this we can draw out that a medium can be porous yet not permeable, if there are no interconnected pores across the whole medium for fluid to flow through. On the other hand, a medium cannot be permeable without being porous. Permeability is usually calculated by using Darcy`s equation for fluid flow through porous medium;

$$k = \frac{q\,\mu}{A}\frac{\Delta P}{\Delta x} \tag{3.2}$$

Where *k* is permeability measured in units of darcies (D) or millidarcies (mD), *q* is flow rate, μ is viscosity, *A* is surface area and $(\Delta P/\Delta x)$ is the pressure gradient. In most reservoir rock, primarily sandstone, there is a strong correlation between porosity and permeability. This correlation is often used to determine permeability, as it is more difficult to measure than porosity. It should also be noted that permeability is much more uncertain than porosity. While porosity only varies a few percent spatially in a typical formation, permeability can vary by three or more factors of 10 (Lake 1989).

The permeability of the Ekofisk formation, and chalk reservoirs in general, can be divided into two categories; matrix permeability and fracture permeability. Typical matrix permeability for Ekofisk is in the range of 0.02 – 10 md, with 5 md as the average. Faults or fractures in chalk are not associated with flow barriers as they are in sandstone. Fracture permeability is substantially higher than matrix permeability, and effective permeability is in the range of 1 md to 100 md (COPNO Internal).

3.1.1.1 Matrix-fracture Interaction (Single vs. Dual Porosity Model)

The dual porosity model involves both porosity and permeability. Naturally fractured reservoirs typically have two distinct porosities; primary in the matrix and secondary in the fractures. These two different porosities can be represented by corresponding homogeneous porosity systems. The matrix contributes significantly to the storage capacity of hydrocarbons, but has negligible contribution to the flow capacity. The concept of dual porosity was developed based on the need to model the behavior of such matrix regions, and distinguish them from fractures (Warren & Root 1963). The fractures provide an easy path for fluid flow, but have limited hydrocarbon storage capacity. Figure 3.1 shows an idealized representation of a matrix-fracture system. There are two distinct fluid flow types. The first is the flow from the matrix to the fractures, and then to the wellbore. The other is the direct fluid flow from the fractures to the wellbore.

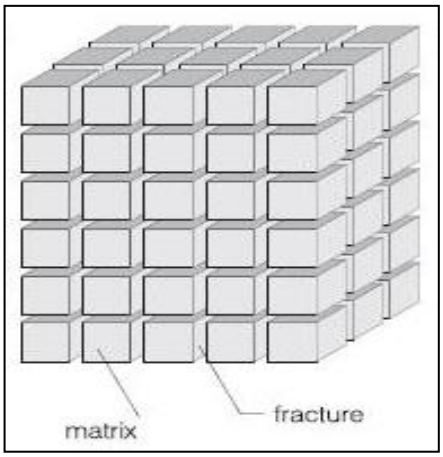

Figure 3.1 Idealized matrix-fracture system (Warren & Root 1963).

Although a dual porosity model gives a more accurate representation than a single porosity model, limitations with regard to computational resources make it impractical for full field simulation problems. For this reason, a single-porosity model is used for the Ekofisk model. By aligning the grid with the major fractures and adjusting the transmissibility between the grid cells in the fracture, an approach to the real situation is achieved.

3.2 Fluid-Rock Interaction

3.2.1 Interfacial Tension

Interfacial tension (IFT) exists when two immiscible fluids are in contact with each other. A clearly defined interface, only a few molecular diameters thick, arises between the two fluids. This happens because the attractive forces between the molecules internally in one phase are larger than the attraction to the molecules in the other phase. This means that the molecules on the surface of a drop will experience a net inward attraction. This attraction ensures that the surface area of the drop is made as small as possible.

The definition of the IFT between two fluids, σ, is the force per unit length (newtons/meter), and is often expressed as dynes/centimeter. This is numerically equal to millinewtons per meter (mN/m). IFT is a measure of miscibility; the lower the IFT, the closer the two phases are to being miscible (Tiab & Donaldson 2012). The action of the IFT is to reduce the size of the sphere unless it is opposed by a great enough pressure difference ($P_2 - P_1$). Figure 3.2 shows the forces acting on a spherical cap.

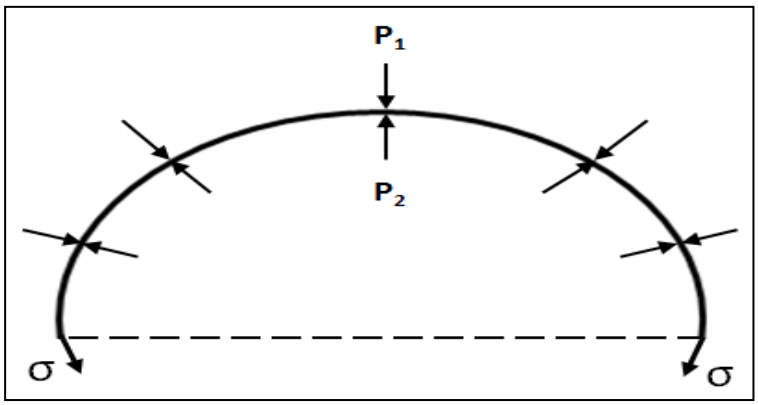

Figure 3.2 Capillary equilibrium of a spherical cap (Tiab & Donaldson 2012).

The mechanical equilibrium of the interface is governed by the Laplace equation;

$$P_2 - P_1 = \sigma\left(\frac{1}{r_1} + \frac{1}{r_2}\right) \quad (3.3)$$

Where P_1 is the external pressure acting on the spherical cap, P_2 is the internal pressure, ($P_2 - P_1$) is the capillary pressure (P_c), σ is the interfacial tension between the two phases, and r_1, r_2 are the principal radii of the curvature.

3.2.2 Wettability

Wettability is the preferential affinity of the solid matrix for either the aqueous phase or the oil phase. It is the tendency of a fluid to spread on or adhere to a solid surface in the presence of other immiscible fluids (Elshahawi *et al*. 1999). Wettability determines the fluid distribution in a porous medium, and is important for waterflood behavior as well as enhanced recovery. Wettability controls the capillary pressure and relative permeability behavior; hence also the rate of oil displacement and overall recovery.

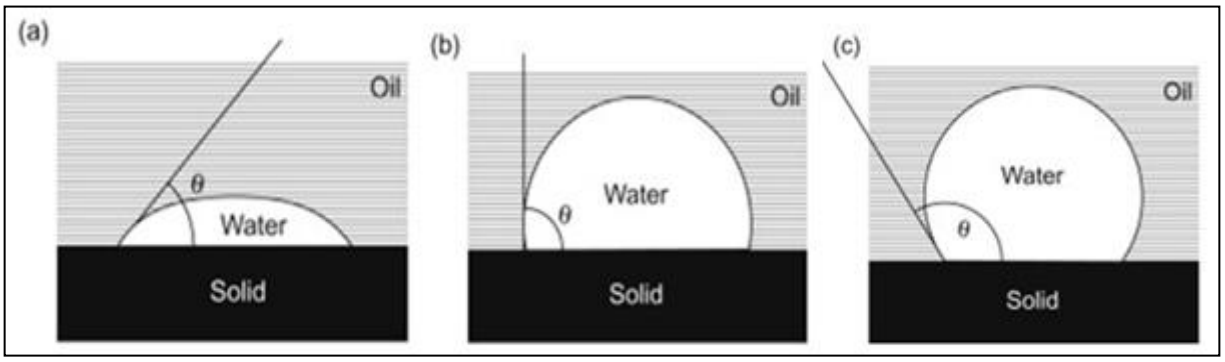

Figure 3.3 Wettability at solid-fluid interface. (a) Water-wet system (b) Neutrally-wet system (c) Oil-wet system (Tiab & Donaldson 2012).

The wettability of a reservoir rock can be quantified by the contact angle between the rock surface and the fluid-fluid interphase; a value larger than 90° suggesting a water-wet system, and a value less than 90° indicating an oil-wet system. For contact angle values close to 90°, the system is referred to as mixed-wet or neutral. The contact angle, θ, is given by Equation 3.4;

$$\cos\theta = \frac{\sigma_{so} - \sigma_{sw}}{\sigma_{wo}} \tag{3.4}$$

Where σ_{so} is the IFT between the solid and oil, σ_{sw} is the IFT between the solid and water, and σ_{wo} is the IFT between water and oil.

3.3 Relative Permeability

Relative permeability is a dimensionless term created to adapt Darcy equation to account for multiphase flow conditions. If only one fluid is present in the rock, the relative permeability

of this fluid will be 1. Relative permeability is defined as the ratio of the phase permeability to the absolute permeability, and is a number between 0 and 1;

$$k_{ri} = \frac{k_i}{k} \tag{3.5}$$

Where *i* is the phase, k_{ri} is the relative permeability of the phase, and k is the absolute permeability. Calculating relative permeabilities allows for comparison between different abilities of fluid to flow in presence of each other. The relative permeability to a phase decreases as the saturation of the phase decreases. When k_{ri} approaches zero, the phase can no longer flow. This corresponds to the critical phase saturation, S_{ci}; defined as the lowest level of saturation at which a phase is left immobile (Cinar 2013).

Endpoint relative permeability is also an important property, defined as the k_r of a phase at the other phase`s residual saturation. Endpoint $k_r$ is denoted by an *o* in superscript, and is a measure of the rock wettability. The wetting phase`s k_r^o will be smaller than the non-wetting phase`s k_r^o. Another good indication of wettability is the crossover point of a relative permeability curve (where $k_{r1} = k_{r2}$). (Lake 1989)

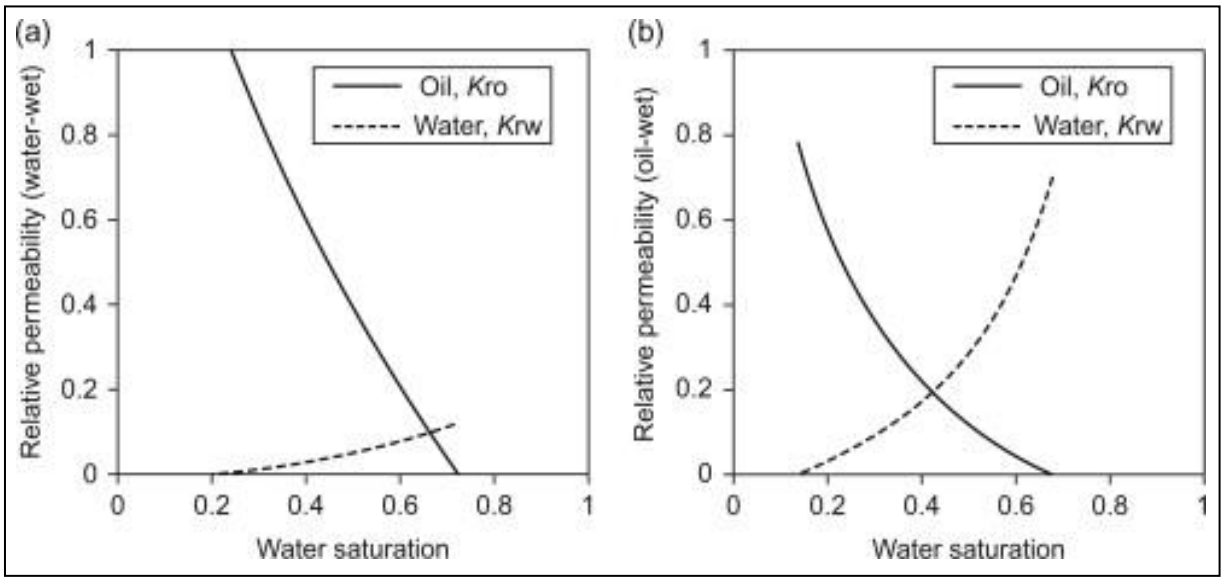

Figure 3.4 Typical water-oil relative permeability curves for (a) water-wet & (b) oil-wet system (Tiab & Donaldson 2012).

Figure 3.4 shows the relative permeability curves for strongly water-wet rock to the left, and a strongly oil-wet rock to the right. For strongly water-wet rock the crossover point is larger than S_w=50%, while it is smaller than S_w=50% for strongly oil-wet rock.

3.3.1 Pseudo Relative Permeability Curves

A large number of grid cells are needed to simulate large field models. Pseudo relative permeability curves are used to reduce the dimensionality of the models. They are also used to account for intra-cell rock property variations. Pseudo relative permeability curves are most affected by the dip angle of the reservoir, but are also highly dependent on layer thickness and PVT properties (Saud & Abdulaziz 1998).

Pseudo relative permeability curves can be applied to two-dimensional reservoir simulator models to approximate the three-dimensional solution. The pseudo curves account for vertical heterogeneity, known as stratification. The properties needed to calculate the pseudo relative permeability curves are permeability, thickness, porosity, connate water saturation, residual oil saturation and the end point relative permeabilities of the different layers in the model (Hearn 1971).

3.4 Saturation

The saturation, S, of a particular fluid phase *i* in a rock is the fraction V_i of the total pore volume (PV) this fluid occupies;

$$S_i = \frac{V_i}{PV} \tag{3.6}$$

It is believed that before the invasion of petroleum, the pores are completely filled with water. As oil or gas migrates to take the waters place, it does not manage to replace all the water. To determine the quantity of oil and gas, it is necessary to determine the different saturations of water, oil and gas in the pore space. There are especially three important saturation terms worth mentioning:

- S_{wi} is the initial water saturation in the reservoir. This is the mentioned water that is not displaced as oil migrates upwards to fill the pores.
- S_{wirr} is the irreducible water saturation, and refers to the lowest water saturation that can be achieved when displacing water with oil or gas.

- S_{or} is the residual oil saturation, and is defined as the oil which cannot move during fluid flow in primary or secondary recovery. EOR methods aim to increase recovery by reducing this value.

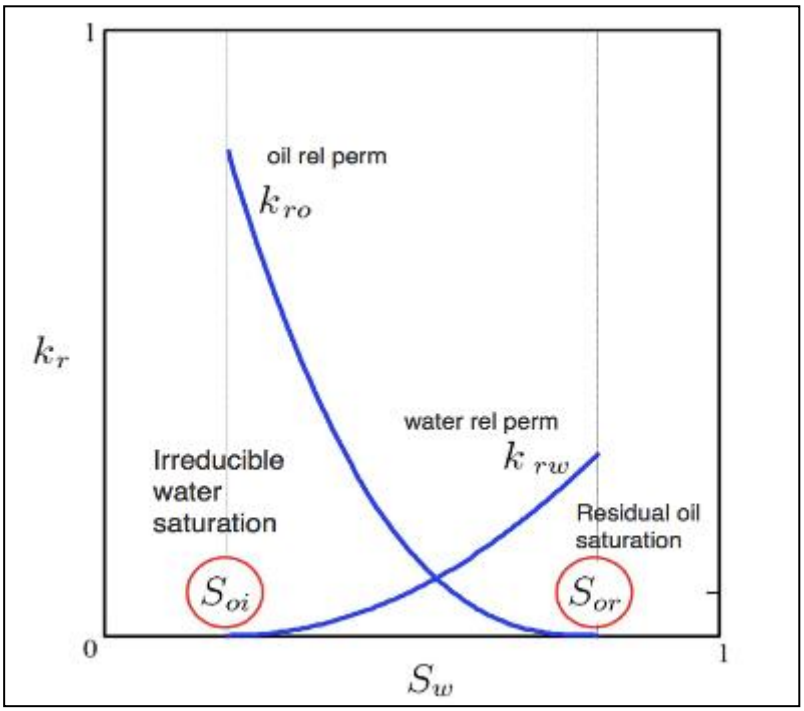

Figure 3.5 Two-phase relative permeability curves; water-oil system – imbibition.

The total saturation of a rock should always add up to unity. For two-phase flow of oil and water, the simple equation for saturation becomes;

$$S_w + S_o = 1 \tag{3.7}$$

For three-phase flow of oil, gas and water, the same equation becomes;

$$S_w + S_o + S_g = 1 \tag{3.8}$$

Where the saturations are S_w for water, S_o for oil and S_g for gas.

3.4.1 Spontaneous Imbibition

Imbibition is defined as the exchange between oil in the matrix and water in the fractures as a result of capillary action. Imbibition can be divided into spontaneous and forced displacement. Spontaneous imbibition is especially important for highly heterogeneous reservoirs, such as fractured-matrix reservoirs. Water will be imbibed into the matrix from

fractures with a countercurrent flow of oil into the fractures. The oil is then free to flow towards the production wells through the fracture network (Morrow & Mason 2001). If a rock is oil-wet, water needs to be forced into the rock in order to displace oil. This process corresponds to forced imbibition. The spontaneous and forced parts of a capillary imbibition curve are indicated in Figure 3.6.

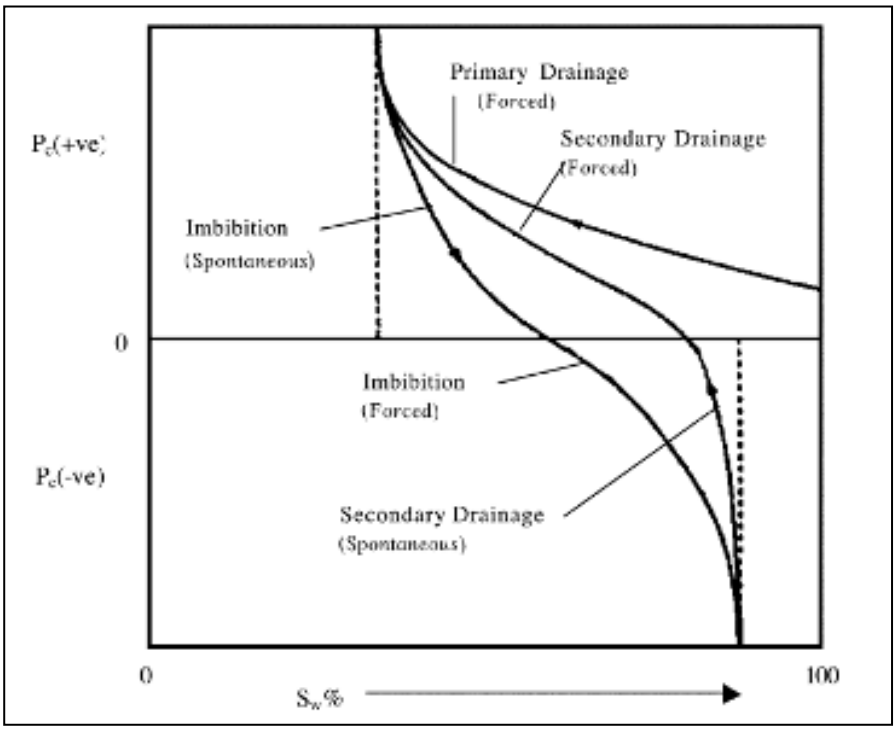

Figure 3.6 Spontaneous and forced imbibition and drainage capillary pressure curves (Morrow & Mason 2001).

4 Literature

Development of mature fields has become popular due to the decline in new field discoveries and the currently high oil prices. Average recovery factors for carbonate reservoirs are 30 % (Sheng 2013). Prior to the major increase in oil prices this oil was often not economically viable to extract by applying EOR methods. However, with the change in economics and the ever increasing demand for oil, the times have changed.

Chemical EOR is generally applied to fields that have undergone waterflooding over a long period of time, and have significant water cuts. For reservoirs with low temperatures and low salinity brines, EOR chemicals have been applied for over 80 years. The challenge lies in developing chemicals for high temperature and high salinity reservoirs. The majority of production comes from exactly reservoirs with high temperature and high salinity; representing a vast potential for chemical EOR. Oil production from EOR is today less than 5% worldwide (Siggel *et al*. 2012). Most of these 5 % come from thermal methods or use of miscible gas rather than chemical flooding.

Two issues are critical in the development of mature fields: determining the main reasons for the low production or high ROS, and finding the optimum economical solution with minimal risk.

4.1 Surfactant Flooding

Surfactants are surface active agents, meaning that they act on the rock surface. In a surfactant flood the aim is to alter the rock wettability and/or lower the interfacial tension (IFT) between water and oil to recover the capillary-trapped oil after waterflooding. These capillary trapped oil droplets can constitute more than half of the residual oil. An efficient surfactant can reduce IFT by a factor of 10^4 (Zolotukhin & Ursin 2000).

Some challenges related to field application of surfactants is finding a suitable surfactant for specific reservoir conditions. The surfactant needs to demonstrate optimal phase behavior at reservoir conditions. The most challenging properties to handle are reservoir pressure,

reservoir temperature and brine salinity. Other factors for a surfactant flood to be successful are low cost of the chemical, manageable logistics, good injectivity and low adsorption. Optimizing a surfactant flood is a compromise between achieving ultralow IFT, low retention and sufficient injectivity (Sheng 2013).

Surfactants are often used in combination with alkali and polymer to form an alkaline-surfactant-polymer (ASP) flood. Figure 4.1 illustrates the sequence of an ASP flood.

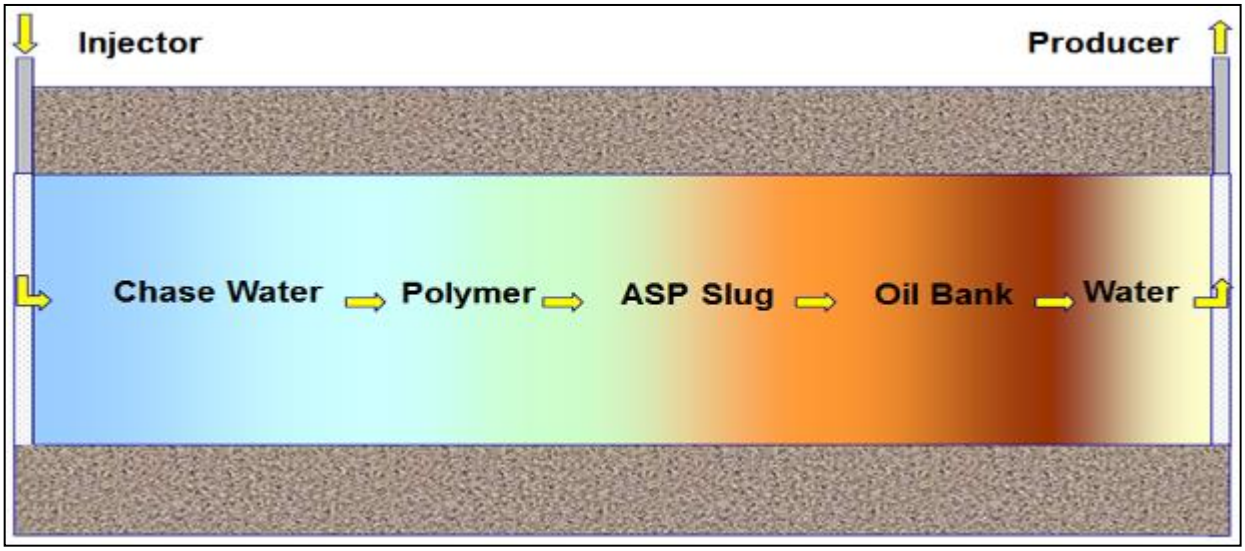

Figure 4.1 Representation of an ASP flooding sequence (COPNO Internal).

The target reservoir is usually first flooded with a preflush bank of water to flush the formation brine out of the reservoir. This can reduce the amount of chemicals needed and create optimum conditions for the surfactant flood. The ASP slug is then injected to mobilize the trapped oil and reduce the residual saturation; creating a new oil bank. The volume chemicals required is typically between 15 % and 30 % of the pore volume (Ahmed & Meehan 2012). This slug is followed by a polymer slug which aims to provide mobility control; improving the sweep efficiency. Without this mobility buffer there is a risk of water fingering through the ASP slug; diluting and dispersing the slug. If the concentration of the chemical slug falls below a certain value, it will no longer work as designed. Finally, chase water is injected to drive the new oil bank towards the producer. Chase water is injected until the economic limit of the project is reached (Ahmed & Meehan 2012). The economic limit is typically a specified water cut or oil rate.

4.1.1 Types of Surfactants

A typical surfactant monomer consists of a nonpolar portion and a polar portion, making it attracted to both water and oil. The nonpolar portion has a strong affinity for oil, and the polar portion a strong affinity for water; giving the surfactant a distinct dual nature. It is because of this dual nature it has the ability to alter rock wettability. A surfactant monomer is often represented by a tadpole symbol, with the polar part being the head and the nonpolar part being the tail. The nature of the polar portion classifies the surfactant as one of four groups; anionic, cationic, nonionic or amphoteric (Lake 1987). The most widely used surfactants for EOR purposes are cationic and anionic. Cationic surfactants have a positively charged head group, while it is negatively charged for anionic surfactants (Figure 3.2). Nonionic surfactants mainly serve as cosurfactants to improve system phase behavior (Sheng 2011).

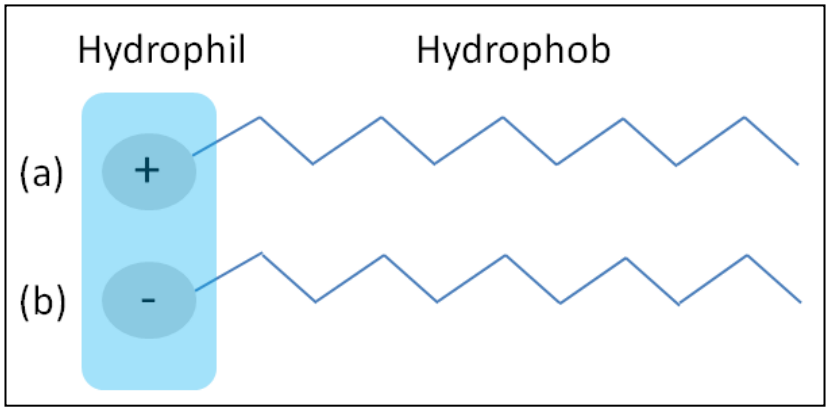

Figure 4.2 Representation of (a) cationic surfactant and (b) anionic surfactant.

Cationic surfactants are efficient in altering wettability from oil-wet to mixed-wet or water-wet. By means of electrostatic forces they interact with anionic crude oil compounds adsorbed on the chalk. Cationic monomers form ion-pairs with the negatively charged carboxylates of crude oil; desorbing them from the chalk. Once the adsorbed material is released from the surface, the chalk becomes more water-wet. This process of wettability alteration is irreversible, as the ion-pairs are only soluble in the oil-phase (Sheng 2013).

Anionic surfactants do not desorb the negative oil compounds in the same irreversible manner as the cationic surfactants. However, they can create a surfactant double-layer between the oil and the chalk, which has demonstrated to slowly displace oil spontaneously (Sheng 2013). Because the bonds of the double-layer are weak it is not regarded a

permanent wettability alteration. The main goal of anionic surfactants is reducing the IFT. Anionic surfactants are often combined with nonionic surfactants to increase their tolerance to salinity (Sheng 2011).

Several surfactant formulations have been developed for Ekofisk conditions in the Bartlesville laboratory. The current formulations are anionic surfactants with sulphonate groups (COPNO Internal).

4.1.2 Microemulsion Phase Behavior

Winsor (1954) classified surfactant/oil/water microemulsions as Type I (oil in water), Type II (water in oil) or Type III (bicontinuous oil and water in a third phase known as the middle phase microemulsion). Type III exhibits the lowest IFT, and is related to the term optimum salinity developed by Healy & Reed (1974). They showed how phase volumes in microemulsion systems could be correlated with IFT`s and oil recovery. The goal since then has been to maximize oil recovery under these optimum conditions, and to maintain them as long as the surfactant flows through the reservoir (Robertson 1988).

A microemulsion is defined by Healy & Reed (1974) as “a stable, translucent micellar-solution of oil and water that may contain electrolytes, and one or more amphiphilic compounds” (surfactants, alcohols, etc.). According to this definition a microemulsion distinguishes itself from an emulsion by not necessarily having a distinct external phase. A microemulsion has at least three components – oil, water and surfactant – which can be represented by a ternary diagram, as showed in Figure 4.3. Differences among the various microemulsions and surfactant flooding processes simply reduce to variations in location of injection composition on the ternary diagram.

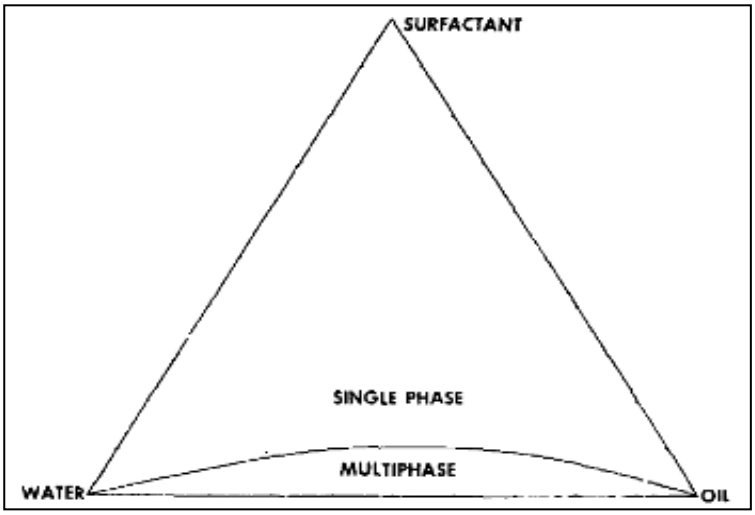

Figure 4.3 Ternary diagram of microemulsion system (Healy & Reed 1974).

As long as the composition of the microemulsion slug allows it to stay in the single-phase region, displacement will be miscible, and all of the oil is recovered. Once the composition enters the multi-phase region, displacement of the slug will be immiscible. Two important criteria for a microemulsion to effectively recover oil were made clear by Healy; the multiphase region should be minimal to prolong miscible displacement in the single-phase region, and the IFT in the multiphase region should be low to enhance immiscible displacement.

There are at least two reasons for considering IFT in regards to microemulsion systems. One is that whenever IFT is measured between water and oil in the presence of surfactant, there is a large possibility that one or both phases are microemulsions. The second reason is that once a microemulsion bank enters the multiphase region, oil recovery is driven by low IFT immiscible displacement. Furthermore, IFT depends on both salinity and cosurfactant concentration, and can vary almost three orders of magnitude within a given multiphase region. Salinity determines the IFT distribution, and affects the size, shape and connectivity of the multiphase region (Healy & Reed 1974).

4.1.3 Optimum Salinity for Ultralow IFT

Surfactant flooding in combination with low salinity water has revealed a boosting effect on enhanced oil recovery in recent research. There are three main advantages of the low salinity environment; it may reduce re-trapping of mobilized oil, reduce adsorption/retention and make more low cost surfactants available for use (Skauge 2013).

The purpose of reducing IFT to ultralow values is to mobilize the disconnected oil droplets typically left behind after a waterflood; considered residual oil. Ultralow IFT generally only exists in a narrow salinity range near the optimum salinity. To achieve this, the approach suggested for Ekofisk is one where a salinity gradient is applied. The active region containing the surfactant is flanked by overoptimum salinity ahead, and underoptimum salinity behind. This way, the salinity profile is certain to pass through the optimal salinity somewhere in the displacement front region (Hirasaki *et al*. 2011). Figure 4.4 shows a visual representation of the salinity gradient. The x-axis represents the distance from injector to producer, and is plotted against salinity on the y-axis.

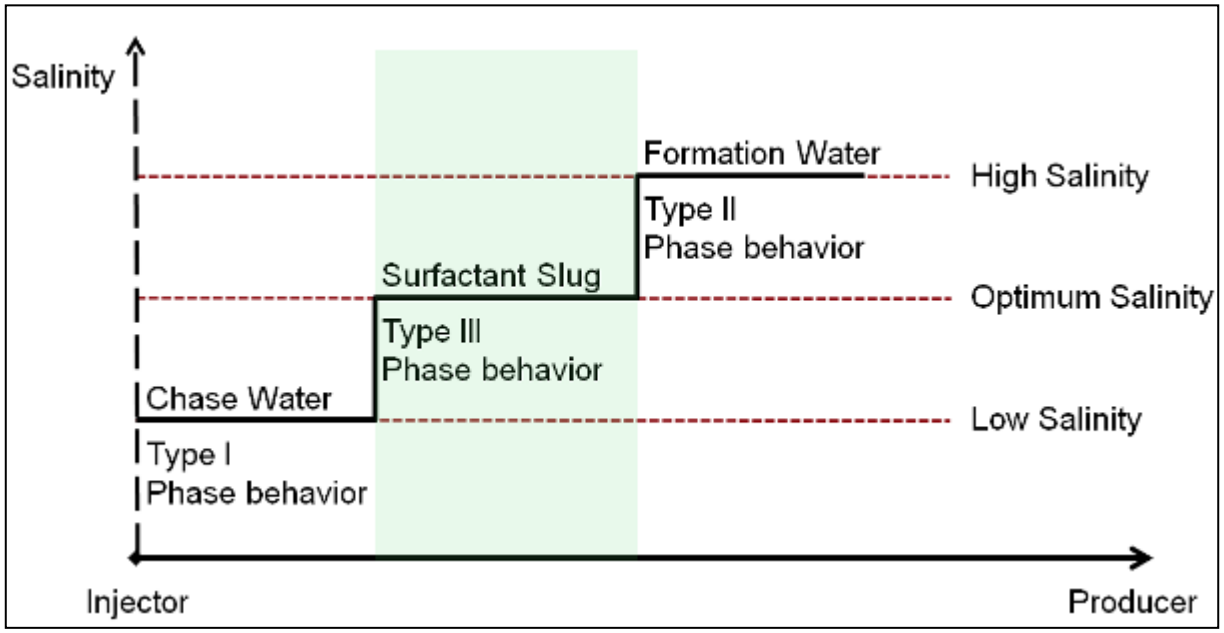

Figure 4.4 Salinity gradient (COPNO Internal).

The salinity gradient works in the following manner:

1. The system is overoptimum ahead of the active region. This retards the surfactant by partitioning into the oil phase.

2. The residual oil displacement takes place as the system passes through the active region of ultralow IFT (Winsor III).
3. The system is underoptimum behind the active region. Lower-phase microemulsion takes place, and the surfactant propagates with water velocity.

The surfactant slug is in practice injected in a near- to underoptimum salinity environment. By applying this practice, the gradient ensures that if overoptimum conditions are for some reason reached during the process, the lower salinity behind the surfactant slug will still allow optimal conditions to be achieved; releasing surfactant trapped in the oil.

Optimum salinity is a function of surfactant concentration and water oil ratio (WOR) for an alkaline/surfactant system. It is also dependent on the soap/surfactant ratio, unless the soap content is negligible or the soap and surfactant have the same optimum salinity. The soap/surfactant gradient exists because the soap is generated in-situ, while the surfactant is introduced with the injected fluid (Hirasaki *et al*. 2011).

4.1.4 Surfactant Retention

The propagation of surfactant through the reservoir is limited by its retention. Surfactant retention includes phase trapping, unfavorable phase behavior and adsorption. It is an important factor to consider because it leads to loss of surfactant as the slug moves through the reservoir. The economic viability of a surfactant flood is highly dependent on the volume chemicals required in the process. It should also be noted that if the surfactant slug is highly dispersed it may no longer work as designed. If the concentration of surfactant falls below a critical value, it will no longer form microemulsions and obtain the desirable effects associated with the Type III behavior. Grigg & Mikhalin (2007) claimed that surfactant loss through partitioning into the oil phase and through adsorption onto the rock surface often consumes more than 90 % of the surfactant in the system. The partitioning of surfactant into crude oil can be responsible for as much as 30 % of the losses, while adsorption is responsible for the major part of retention. Retention varies widely depending on surfactant

structure, mineralogy, brine salinity and hardness, wettability, pH, microemulsion viscosity, temperature, crude oil, co-solvent and mobility control among others (Solairaj *et al*. 2012).

The research done by Solairaj and his co-workers concluded that surfactant retention would be low for an optimized surfactant formulation with good mobility control and a favorable salinity gradient. They further stated that retention decreases with increasing pH, acid number, temperature or oil reactivity.

Adsorption of surfactant on solid surfaces can modify surface hydrophobicity, charge and other key parameters important for the interfacial processes in enhanced oil recovery. The forces generally controlling adsorption are covalent bonding, electrostatic attraction, hydrogen bonding, solvation and desolvation. Which forces that dominate a surfactant-solid system depends on the solid and surfactant type, surfactant concentration, electrolyte, pH, temperature etc. Adsorption of anionic surfactant is for instance higher on a positively charged surface than on a negatively charged surface, while cationic surfactants adsorb more on negatively charges surfaces (Zhang & Somasundaran 2006). This is due to the fact that anionic surfactants have a negatively charged head group, while it is positively charged for cationic surfactants.

4.2 Recent Advances in Surfactant EOR

Of the petroleum present in known reservoirs, it is currently considered that about one third of it is economically recoverable. Improving recovery by use of surfactants was an idea already in 1927, but early results were not encouraging, and the process mechanisms were not understood. In the 1960s the interest in surfactant EOR was revitalized through miscible flooding research, and the results were more promising. It was however not initially recognized that process success also depended on maintaining ultralow IFT at the rear of the slug, where it was displaced by an aqueous polymer solution and became a Winsor 1 microemulsion (Hirasaki *et al.* 2011). As described by Winsor (1954) there are three phases of microemulsion behavior; lower-phase (I), upper-phase (II) and middle-phase (III).

Surfactants work in means of wettability alteration and/or producing ultralow IFT. By altering the wettability, imbibition is increased. Achieving ultralow IFT by lowering the capillary number makes it possible to displace oil from preferentially oil-wet carbonate matrix to fractures by oil/water gravity drainage. The process depends on the surfactant forming microemulsions in the oil and water phases to be able to free the trapped oil. Work by Pennel *et al*. (1996) revealed that at typical reservoir velocities, IFT between crude oil and brine had to be reduced from values of 20 to 30 mN/m to values in the range of 0.001 to 0.1 mN/m to achieve low residual oil saturation values (<0.05) (Hirasaki *et al.* 2011). In the 1970s systematic variations of IFT when changing variables as salinity, oil composition and temperature were found.

As salinity increased, it was discovered that the surfactant was able to solubilize an increasing amount of oil and decreasing amount of water. The point where the surfactant microemulsion solubilized equal amounts of oil and water was called the optimum salinity. The appearance of a middle-phase microemulsion depends on the amounts of water, oil and surfactant present (Hirasaki *et al.* 2011). In order to have a successful displacement process, the injected surfactant slug must first achieve ultralow IFT to mobilize residual oil and create an oil bank. The oil and water should both flow as continuous phases. Secondly, to prevent mobilized oil from being re-trapped by capillary forces, ultralow IFT must be maintained at the displacement front.

Prior to the work of Abe *et al*. (1986) it was thought that alcohol was necessary as a cosolvent to have a microemulsion with an anionic surfactant. It was later proved that by using a branched surfactant, microemulsion without a cosolvent was possible at room temperature. Although it is not necessary, the use of a cosolvent can alter the optimal salinity required to achieve ultralow IFT. A disadvantage of using alcohol is that it decreases solubilization of oil and water in microemulsions; increasing the minimum obtainable value of IFT with a given surfactant.

The long-term stability of a surfactant at reservoir conditions is a requirement for any surfactant. Surfactant hydrolysis is limited up to temperatures of 50-60 °C at slightly alkaline

pH levels and a modest concentration of calcium (Hirasaki *et al.* 2011). For reservoirs at higher temperatures, surfactants with other head groups will be needed.

The process of combining surfactants with alkali to optimize surfactant effect was presented by Nelson *et al*. (1984). The role of the alkali is to reduce surfactant adsorption as the slug propagates through the reservoir. Also, alkali generates soap in situ; allowing the surfactant to be injected at lower salinities, which further reduces the adsorption of the chemical. This allows for a smaller volume of surfactant to be used. However, adsorption is only one component of surfactant retention. A more significant process can be found in the phase trapping of surfactants. In order to have an effective process in a fractured oil-wet reservoir, the combined effect of surfactant and alkali in shifting matrix wettability towards water-wet is of the essence.

Formation wettability can be altered by pH, surfactants that adsorb on the minerals or remove adsorbed naphthenic acids, and acids or bases. Since carbonate formations are likely to be fractured, they will depend on spontaneous imbibition or buoyancy for displacement of oil from the matrix to fractures. Spontaneous imbibition is the process where the wetting fluid is drawn into a porous medium by capillary action. When low IFT is achieved with a surfactant, capillary pressure is reduced to negligible values; eliminating the process of spontaneous imbibition. Under these conditions, gravity becomes an important contributor. For a given system, temperature is an important factor for wettability alteration and rate of imbibition oil recovery (Hirasaki *et al.* 2011).

4.3 Environmental Regulations of EOR Chemicals

Offshore installations create major challenges related to the handling and discharge of back-produced water containing EOR chemicals. Use of chemicals in the Norwegian sector of the North Sea is subjected to restrictions by the Norwegian Environmental Regulations. Use and discharge of EOR chemicals needs to be approved by Klif (Climate and Pollution Directorate). The chemicals are classified into four groups based on their level of ecotoxicity. The groups are green, yellow, red and black; black being the most toxic, least biodegradable and with the highest risk of bioaccumulation. Both the red and black chemicals are harmful, and should only be chosen if they are necessary for technical and safety reasons. There is a zero

discharge policy for red and black chemicals on the Norwegian sector. As seen from Figure 4.5, the use of these chemicals has decreased to a very low level the last couple of years. In 2012 the total discharge was 10.4 tons.

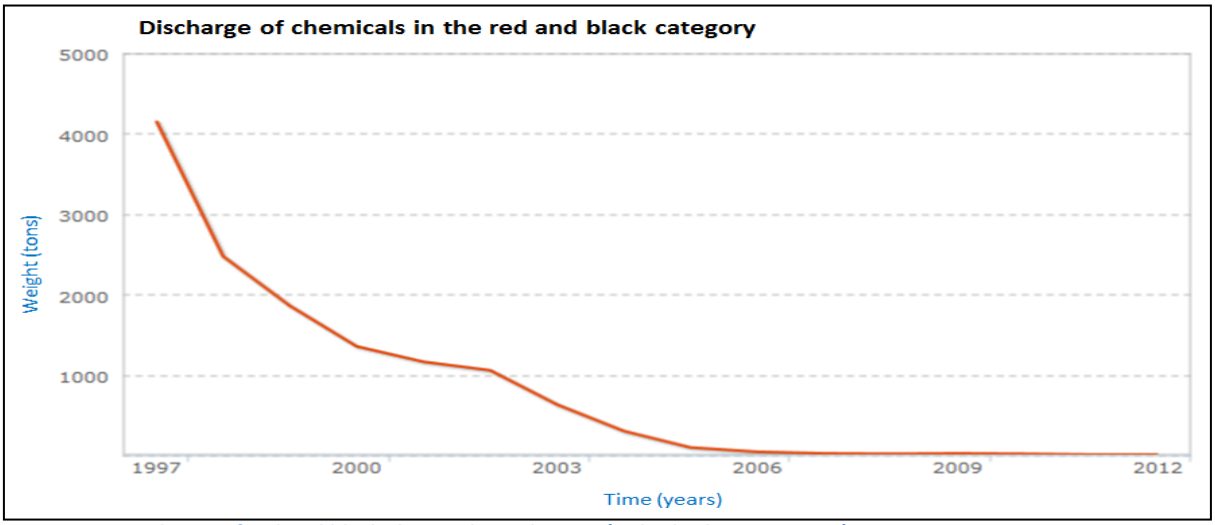

Figure 4.5 Discharge of red and black chemicals on the NCS (Miljødirektoratet 2013).

Extensive implementation of chemical EOR techniques on the NCS will lead to a large increase in the usage of toxic chemicals. Still, it must not be forgotten that a 1% increase in production of the proven resources on Norwegian fields equals a gross value of 270 billion NOK (FORCE report 2011). The economic impact of implementing EOR techniques can be remarkable both for operator, licenses and the Norwegian society.

The environmental challenges are related to the handling of chemicals during chemicals preparation, injection, back production and discharge to sea. The zero discharge policy is not necessarily a show stopper for the use of red and black chemicals for EOR purposes. The chemical bearing produced water can be re-injected, or the chemicals can be separated from the water. Looking at it from a holistic perspective, EOR techniques often reduce water cuts, which can lead to reduced CO_2 emission.

5 Factors Influencing Recovery

A number of factors influence the overall recovery of a reservoir. Horikx *et al*. (2013) presented twelve factors most important for oil recovery in chalk oil fields, and also subdivided them;

- Lateral Reservoir Qualities:
  - Faulting & macro-fracturing
  - Lateral permeability variation
- Vertical Reservoir Qualities:
  - Net to gross
  - Vertical connectivity
  - Vertical permeability profile
- Dynamic Aspects:
  - Moveable oil fraction
  - Wettability
  - Compaction drive potential
  - Gas cap & bubble point
  - Oil Mobility
- Geography & Economics:
  - Location of field
  - Effective oil column

The more general displacement mechanisms are presented in the subchapters below.

5.1 Displacement efficiency and Volumetric sweep efficiency

Displacement efficiency (E_D) and volumetric sweep efficiency (E_V) are equally important to the total recovery of oil. E_D is a function of time, fluid viscosities, relative permeabilities and capillary pressure. E_V is a function of time, viscosities, well arrangements, heterogeneity, gravity and capillary forces. All efficiencies are numbers between 0 and 1 (Lake 1989).

Displacement efficiency is defined as the ratio of oil displace to the amount of oil contacted by the displacing agent, assuming constant oil density;

$$E_D = \frac{Amount\ of\ oil\ displaced}{Amount\ of\ oil\ contacted\ by\ displacing\ agent} = \frac{S_{oi} - S_{o,avg}}{S_{oi} - S_{or}} \quad (5.1)$$

Where S_{oi} is the initial oil saturation, $S_{o,avg}$ is the average oil saturation of the swept zone and S_{or} is the residual oil saturation in the swept zone. A higher E_D will be achieved by reducing $S_{o,avg}$.

Volumetric sweep refers to the reservoir`s volume that can be invaded by a displacing agent. Volumetric sweep is the product of areal and vertical sweep efficiency; respectively E_A and E_I;

$$E_V = E_A \times E_I \quad (5.2)$$

E_A and E_I both depend on each other, and a large mobility ratio is detrimental to both efficiencies. Areal sweep (Equation 5.3) refers to the horizontal area that can be swept, while vertical sweep (Equation 5.4) refers to the cross-sectional area that can be invaded;

$$E_A = \frac{Area\ contacted\ by\ displacing\ agent}{Total\ area} \quad (5.3)$$

$$E_I = \frac{Cross-sectional\ area\ contacted\ by\ displacing\ agent}{Total\ cross-sectional\ area} \quad (5.4)$$

E_A is normally determined from displacement in scaled physical models. It depends on well pattern, and increases as the flow pattern approaches linear flow. It also increases with increased injection time and decreasing mobility ratio. Other factors determining areal sweep are fluid mobilities, areal heterogeneities and the total injection volume (Ahmed & Meehan 2012). E_I is a measure of the flood`s effectiveness in overcoming heterogeneities in the vertical direction, and is controlled by gravity-, capillary- and viscous forces in varying degree (Cinar 2013).

Furthermore, the volumetric sweep efficiency is defined as the ratio of oil contacted to the amount of oil initially in place. It can also be defined as the moveable oil fraction;

$$E_V = \frac{Amount\ of\ oil\ contacted\ by\ displacing\ agent}{Amount\ of\ oil\ initially\ in\ place} = \frac{S_{oi} - S_{or}}{S_{oi}} \quad (5.5)$$

5.2 Recovery Factor

Recovery factor E_R is the product of displacement efficiency E_D and volumetric sweep efficiency E_V;

$$E_R = E_D \times E_V \quad (5.6)$$

Taking typical values of connate water and residual oil saturations should give an ultimate displacement efficiency of 50% - 80% of contacted oil in a waterflood. Based on empirical equations and figures, the volumetric sweep should be around 40% - 60% for a waterflood (Lake 1989). This would give a resulting recovery factor between 16% and 48%; meaning that over half of the original oil in place could be left in the ground after an even so successful waterflood.

6 The EOR Process in General

EOR is oil recovery by means of injecting materials not normally present in the reservoir. This definition does not restrict EOR to a particular phase, as it can be implemented at any stage of the reservoirs life. There are three main stages of recovery. Primary recovery is defined as recovery by natural drive mechanisms; e.g. water drive (aquifer influx), gas cap drive, solution gas or gravity assisted drainage. Secondary recovery is mechanisms that aim to maintain reservoir pressure, such as gas- or water injection. Any technique applied after secondary recovery is referred to as tertiary recovery (Lake 1989).

Polymer flooding is not considered an EOR technique in accordance with the definition of EOR in this thesis. The aim with polymer flooding is improving the sweep efficiency; not to reduce the residual oil saturation. Polymer flooding falls into the category of IOR. It is all the same included in this chapter as it is more often than not referred to as an EOR technique.

Waterflooding as a secondary recovery method has become very common, and is the most frequently applied recovery technique in North Sea reservoirs. Injecting water helps both to maintain reservoir pressure and increase recovery over natural driving forces, but still yields low sweep efficiency and a poor production performance in most reservoirs. This is mainly due to the impact of reservoir heterogeneities, problems related to well siting and spacing, as well as the unfavorable mobility ratio between the displacing fluids (water, gas) and displaced fluids (oil). Channeling of water or gas through more permeable flow paths causes early breakthrough of the injectant as well as high water cuts.

EOR methods can be classified into three main categories; thermal, solvent and chemical methods. Thermal methods include steam drive, steam soak and in-situ combustion. Solvent methods refer to injection of natural gas, CO_2, air, nitrogen or flue gas, among others, with the aim to extract incremental oil by changing the phase behavior of the crude oil. The last category of chemical methods involves flooding the reservoir with polymer, micellar polymer, surfactants, foam or alkaline (high-pH) chemicals. In recent years several of these methods have been combined in attempt to gain an even more efficient incremental

recovery (e.g. Alkaline-surfactant-polymer flooding). Smart Water and Low Salinity flooding also fall into the category of chemical EOR because the water used is chemically altered.

Oil volumes can be divided into resources and reserves. Resources are an estimate of the amounts of oil and gas that are believed to be physically contained in discovered and undiscovered accumulations. Reserves are defined as the part of the resources which is commercially recoverable in known reservoirs; given present economics and technology. As oil and gas prices change, or new technology is presented, present reserves may be added or deducted;

$$Present\ Reserves = Past\ Reserves + Additions\ to\ reserves - Production\ from\ reserves \quad (6.1)$$

The four methods of adding to reserves are (1) Discovering new fields, (2) Discovering new reservoirs, (3) Extending reservoirs in known fields, and (4) Redefining reserves because of change in economics and/or extraction technology. EOR clearly falls into the two last categories. Since the discovery of new fields and reservoirs is limited, the need for additions by means of EOR is clear. Figure 6.1 shows the remaining oil resources and reserves in Norwegian fields at the end of 2013. The remaining in-place resources make up half or more of the total resources in most of the fields. This creates a vast potential for EOR processes.

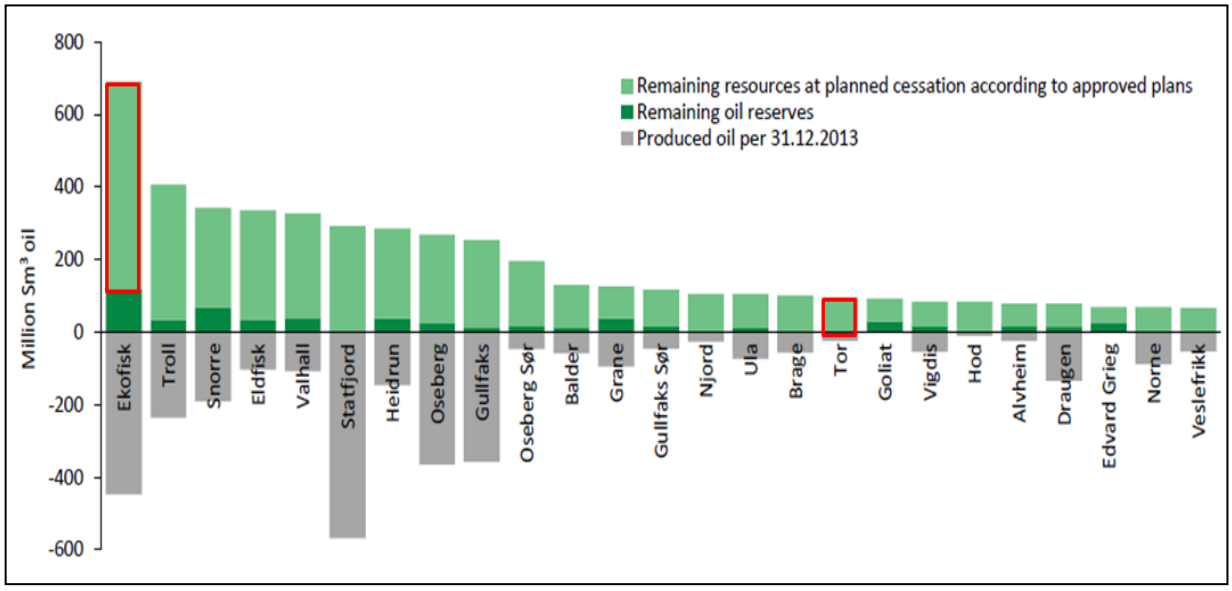

Figure 6.1 Oil resources and reserves for the 25 largest Norwegian oil fields (NPD).

Only Statfjord has produced more oil than Ekofisk by the start of 2014. The figure clearly shows that Ekofisk has the largest quantities of both remaining reserves and resources.

Incremental oil is the increased oil recovery by implementing EOR processes compared to the recovery from doing nothing or from continued waterflood. Incremental oil recovered is the measure of the success of any EOR project.

The goal with implementing EOR is often to mobilize more oil than is possible with only water flooding/ primary production, and reducing the residual oil saturation. This is achieved by increasing the volumetric and displacement sweep efficiencies. Different types of EOR processes achieve this in different ways. Techniques involving thermal recovery methods aim to reduce the oil viscosity to make it flow more easily. Polymer flooding gives a more favorable mobility ratio, reducing viscous fingering and thereby increasing sweep efficiency. Alkaline flooding aims to reduce the effect of capillary forces and alter the rock wettability, and is often used in combination with surfactants. A surfactant flood aims to alter the rock wettability and/or change the interfacial tension (IFT) between water and oil; freeing more oil to flow.

In order for an EOR fluid to have the desired effect, it needs to get in contact with the trapped oil. This has proved to be a special problem in naturally fractured reservoirs. The main volume of oil is located inside the matrix, which is separated from the fracture network. Because of this, there is major difficulty in getting EOR fluids to contact and displace oil. There is no real way to assure matrix flow in an EOR process (Miller 2010).

7 EOR Methods with Basis in Waterflooding

Most chemical EOR techniques have their basis in water flooding. Not only is water a good means of transporting chemicals, it is also good for dissolving them. These EOR techniques can be implemented either before or after a field is flooded with water. Adding chemicals to water can slow down water breakthrough and reduce water cut significantly, making a project economically viable for a longer period of time; thereby extending field life.

7.1 The Screening Criteria

Not every reservoir will be adequate for implementing EOR methods. Both geological and geographical conditions need to be analyzed under varying reservoir conditions to determine the applicability of EOR methods. Table 7.1 features a list of screening criteria retrieved from a paper by Taber *et al*. (1997).

Table 7.1 The screening criteria (Taber *et al*. 1997).

EOR Method	API Gravity (°)	Viscosity (cp)	Compo-sition	Oil Sat. (%)	Rock Type	Net Thic. (ft)	Avg. Perm (md)	Depth (ft)	T (°F)
N_2 or flue gas	>35, 48	<0.4, 0.2	High % of C_1 –C_7.	>40, 75	Sandstone/ carbonate	Thin unless dipping	Not critical	>6,000	Not critical
HC	>23, 41	<3, 0.5	High % of C_2-C_7	>30, 80	Sandstone/ carbonate	Thin unless dipping	Not critical	>4,000	Not critical
Miscible-CO_2	>22, 36	<10, 1.5	High % of C_5-C_{12}	>20, 55	Sandstone/ carbonate	Wide range	Not critical	>2,500	Not critical
Immiscible gases	>12	<600	Not Critical	>35, 70	Not critical	Not critical if dipping / good ver. perm	Not critical	>1,800	Not critical
Micellar/polymer, ASP, Alkaline flooding	>20, 35	<35, 13	Light-Inter. org acids for alkaline	>35, 53	Sandstone preferred	Not critical	>10, 450	<9,000, 3,250	<200, 80
Polymer flooding	>15	<150; >10	Not critical	>50, 80	Sandstone preferred	Not critical	>10, 800	<9,000	<200, 140
Combustion	>10, 16	<5,000, 1,200	Some asphalts	>50, 72	High poro sand/sands tone	>10	>50	<11,500, 3,500	>100, 135
Steam	>8 to 13.5	<200,000, 4,700	Not critical	>40, 66	High poro sand/sands tone	>20	>200, 2,540	<4,500, 1,500	Not critical

Each reservoir will have to be screened to see if it matches the requirements for one or several methods. A project will require a choice of injection fluid and an overall process to maximize the incremental oil, while still making a profit. With this said, a reservoir may fit

the screening criteria for several different EOR methods, and it is up to the engineers to choose the best one for their exact purpose of the project. The best option will depend on several factors: oil price, injection fluid price, cost of chemicals, environmental regulations, available facilities and so on. The screening criteria are based on field experience, and are not set in stone. New technology and successful pilots or projects can require the screening criteria to be reevaluated and changed.

7.2 Chemical EOR Methods

7.2.1 Polymer Flooding

A big issue with water flooding is the amount and extent of viscous fingering, and the poor sweep efficiency that is achieved. Polymer flooding is an IOR technique that aims to increase the viscosity of water. By adding polymer to the injection water, water viscosity increases, and the mobility ratio becomes close to or even smaller than unity. The mobility ratio is defined as the mobility of the displacing phase (water) over the mobility of the displaced phase (oil);

$$Mobility\ Ratio, M = \frac{\lambda_w}{\lambda_o} = \frac{\mu_O k_W}{\mu_W k_O} = \frac{\mu_O k k_{rW}}{\mu_W k k_{rO}} \tag{7.1}$$

As the mobility decreases, viscous fingering is reduced. The fingers become smaller and more branched, resulting in a much larger area being swept at breakthrough. Less oil is bypassed, and this results in increased areal-, vertical- and displacement sweep efficiencies; leading to an overall higher recovery (Sheng 2012). Figure 7.1 shows a comparison of sweep efficiency in water flooding and polymer flooding. The top three images display the waterflood, while the bottom three images display the polymer flood. The sweep efficiency is clearly higher for the polymer flood. Also, the breakthrough for the polymer flood occurs at a much later time than for the water flood.

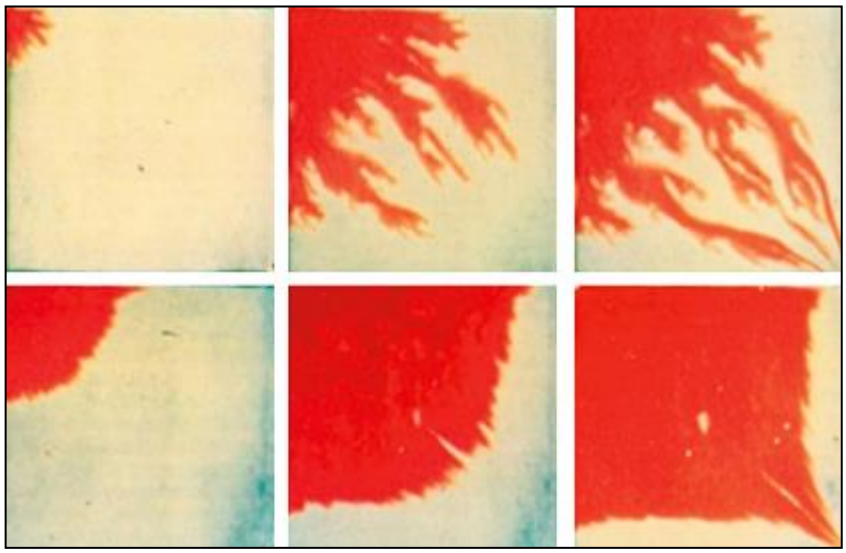

Figure 7.1 Comparison of sweep efficiency in water flooding (top) and polymer flooding (bottom) (Sheng 2012).

7.2.2 Alkaline Flooding

Alkaline flooding is flooding the reservoir with high-pH chemicals with aim to reduce the effect of capillary forces and alter the wettability. When an alkaline solution reacts with acid in the crude oil, soap is generated in situ. The principal mechanism of alkaline flooding is reducing the IFT between oil and water. Another mechanism is emulsification. Both the formations of oil-in-water and water-in-oil emulsions can effectively improve oil recovery. Alkaline solution is able to infiltrate the residual oil and created some discontinuous water ganglia inside the oil phase to form water-in-oil emulsion. This causes an increase in the resistance to flow in water fingers; diverting the injected water to unswept regions and improving oil recovery. The formation and flow of these emulsions can result in significant reduction in water-phase relative permeability (Surkalo 1990) and (Wang *et.al* 2010). Alkali is often used in combination with surfactants to optimize the effect of the surfactant.

7.2.3 Low Salinity Waterflooding

Low salinity waterflooding (LSW) falls into the category of EOR because the water in this process is altered in some way. LSW is the injection of water with lower salinity than the initial formation brine salinity. By applying LSW, some chemically and physically processes are provoked. Together these processes tend to enhance the recovery of oil in some reservoirs. The amount of incremental oil produced is, however, very dependent on the initial reservoir properties. EOR by LSW is a fairly new and unpredictable method. It has been

successful for some pilot tests and projects, but the criteria for it being applicable are not fully understood. Three conditions seem to be especially important for a LSW to be effective; the presence of a significant clay fraction, connate water and the exposure of crude oil to create mixed wettability conditions (Morrow & Buckley 2011). Initial wettability and end point saturations also play an important role (Ashraf *et al*. 2010).

7.2.4 Smart Water

Smart Water is water with altered composition; not unlike the process of LSW. Smart Water is made by modifying the ion composition of the water. Because this EOR method does not require the use of chemicals, it is regarded environmental friendly. Smart Water can improve wetting properties of oil reservoirs and optimize fluid flow and oil recovery. The concept is developed by studying the chemical mechanisms happening during a waterflood. Addition of sulfate ions (SO_4^-) in seawater has proved to have a positive effect on spontaneous imbibition and total oil recovery in chalk. Two other ions are also active in this process; Mg^{2+} and Ca^{2+} (Austad 2013).

7.2.5 Microbial EOR

Microbial EOR (MEOR) is EOR by means of using resident microbes or introducing microbes to the reservoir for the purpose of mobilizing trapped oil by reducing IFT, selectively plugging of high permeability zones and reducing oil viscosity. The only essential difference between MEOR and chemical EOR is in the method of introducing the recovery-enhancing chemicals into the reservoir. Microbes produce chemicals in-situ in the reservoir by feeding on a carbon source. Using residual oil as a carbon source would make the cost and logistics of field implementation closer to that of a waterflood than to that of a chemical EOR process (Bryant & Lockhart 2002).

Another technology involving microbes is microbial permeability profile modification (MPPM). This method aims to restrict flow in watered-out channels, and forcing injection water into unswept channels. MPPM technology differs from most MEOR methods by its reliance on the in-situ micro flora rather than on injecting microbes into the reservoir (Brown *et.al.* 2002).

8 The Ekofisk Model

This chapter presents the Ekofisk simulation model. Included is a history match of the water flooding sequence in the observation well (C11), a short introduction to PSim, a relative permeability study and a 2D Ekofisk Sector model study.

8.1 History Matching

History matching is the act of changing a model to make it reproduce the past behavior of a reservoir. By achieving this history match, the model can be used to predict future behavior with a high degree of certainty. In this case the aim was to match the waterflooding sequence of the different layers in a specific well located in the middle of the Ekofisk Field. The reservoir pressure was also matched, but to a higher degree of uncertainty.

The observation well C11 was the main point of study in this part of the research. Water breakthrough data from C11 was used to history match a 2D simulation model constructed in PSim. Breakthrough times were matched by altering permeability and transmissibility in x- and z-directions. Also, to get the spontaneous imbibition effect observed in the Lower Ekofisk formation, capillary pressure data was added. A critical property to match was the degree of dispersion of the displacement front. The observation suggested a very sharp front; a region going from initial water saturation to being swept to residual oil saturation (S_{orw}) in a short period of time. To imitate this behavior, a relative permeability study was conducted by using a 2D homogenous sector model.

8.2 PSim

PSim is the ConocoPhillips in-house simulator, used for simulating black oil and compositional problems in single-porosity reservoirs. One of its features is the tracer option for oil, water and gas phases. This feature is useful in equity situations as well as in tracking injected water and gas streams. Traced components can be any of the fluid components, including water. PSim will be used in this thesis for both the 2D Sector Model and the 2D Radial Model (COPNO Internal).

8.3 2D Homogenous Sector Model

The sector model is a 2D model with 35 cells in x-direction and 200 cells in z-direction, giving it a total of 7000 cells. Each cell is 70 feet wide in the x-direction, and 5 feet high in the z-direction. This makes the model 2450 feet wide and 1000 feet high. The top 27 cells make up an overburden which is not subjected to the waterflood. The top of the model is located at a depth of 9373 feet. The distance between the injector and producer is 1960 feet. Both producer and injector are perforated each 10 feet. The observation well without perforations in located between the injector and producer, 1120 feet from the injector.

In the relative permeability study all layers in the model were given the same properties; creating a synthetic homogeneous reservoir. Porosity was set to 30 % and initial water saturation was set to 10 %. Permeabilities in both directions were set to 5 md; the average matrix permeability for Ekofisk Chalk. The transmissibility was fixed to 0.5 in x-direction, and 0.1 in z-direction. By altering either k_{rw} or k_{ro} one at a time, the effect of the change could be seen clearly. Figure 8.1 shows the relative permeability curves for the four different scenarios constructed; low k_{ro}, high k_{ro}, low k_{rw} and high k_{rw}. The end-points were kept the same, to not alter the S_{orw} values.

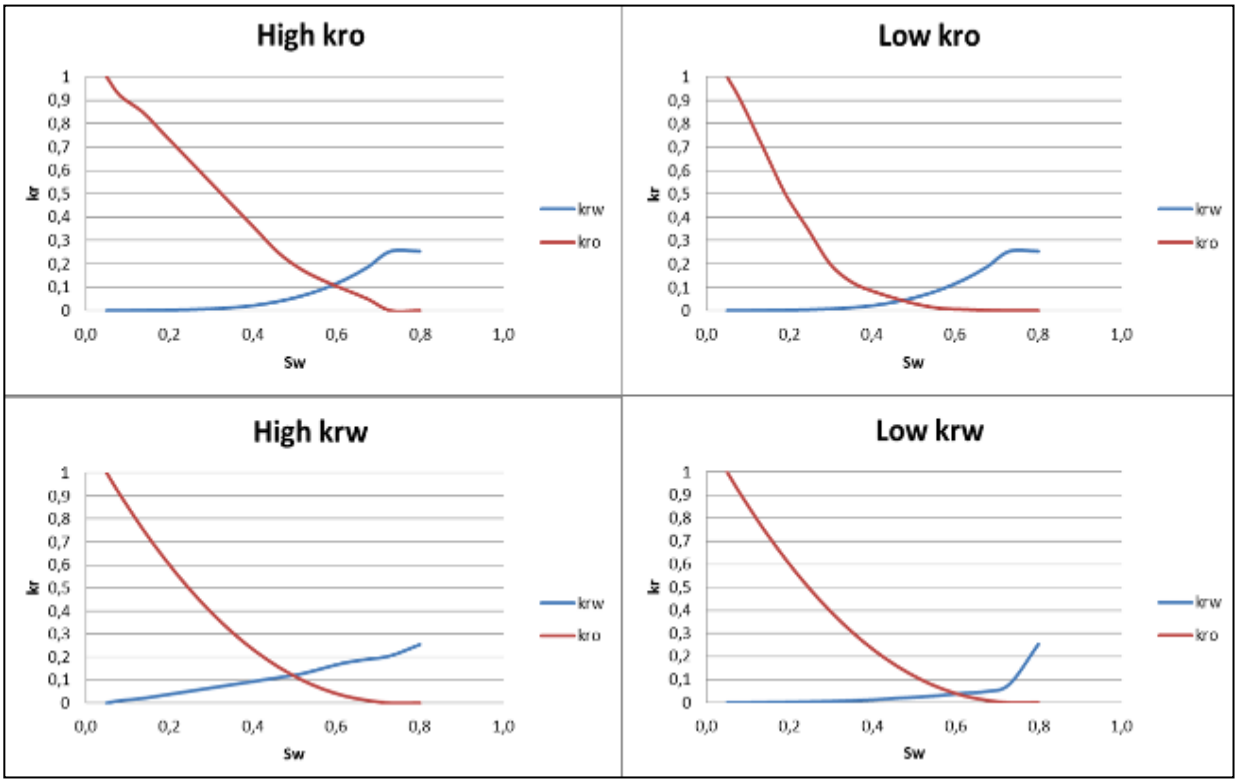

Figure 8.1 Two-phase relative permeability curves.

For the two cases of low k_{ro} and high k_{rw} the crossover point is at a water saturation of around 0.5, suggesting neutrally wet conditions. For the other two cases, high k_{ro} and low k_{rw}, the crossover point is at a water saturation of around 0.6, indicating slightly water wet conditions. Figure 8.2 shows the fractional flow curves (in blue) for the same four scenarios plotted against water saturation. The tangent lines (in red) show the expected water saturation behind the sweep front, and are based on a water viscosity of 0.4 cp and an oil viscosity of 0.2 cp (applicable viscosities for Ekofisk). The two cases of high k_{ro} and low k_{rw} have the highest water saturation in the swept zone, meaning less oil is left behind as the displacement front propagates through the reservoir. This coincides better with the noted displacement in the observation well than that for the cases of low k_{ro} and high k_{rw}. The two latter cases show somewhat lower water saturation behind the displacement front.

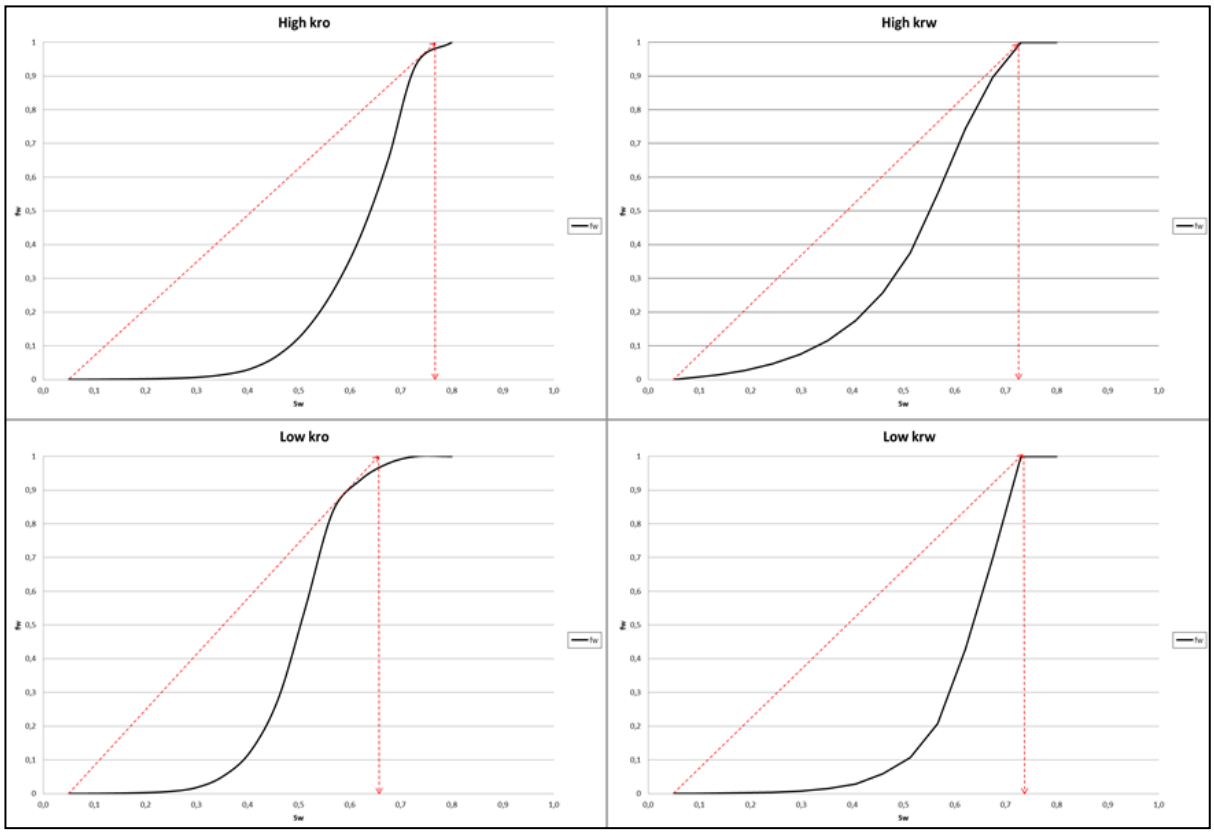

Figure 8.2 Fractional flow curves for the four scenarios of relative permeability data.

By implementing the four sets of relative permeability data into a simple homogeneous 2D model, the displacement can be observed in a more visual manner. The results can be seen in Figure 8.3. The images represent a simple waterflood case; the injector to the left of the image injecting water that flows towards a producer in the far right (outside of the image). The blue box is a representation of the location of the observation well. Colder colors (blue)

represent higher degree of water saturation. All four figures are captured at the same time in the flooding process. The two clearest things to draw out from the visualization are that (1) the water saturation behind the displacement front varies for the cases, and (2) the velocity of the front is different for each of the cases.

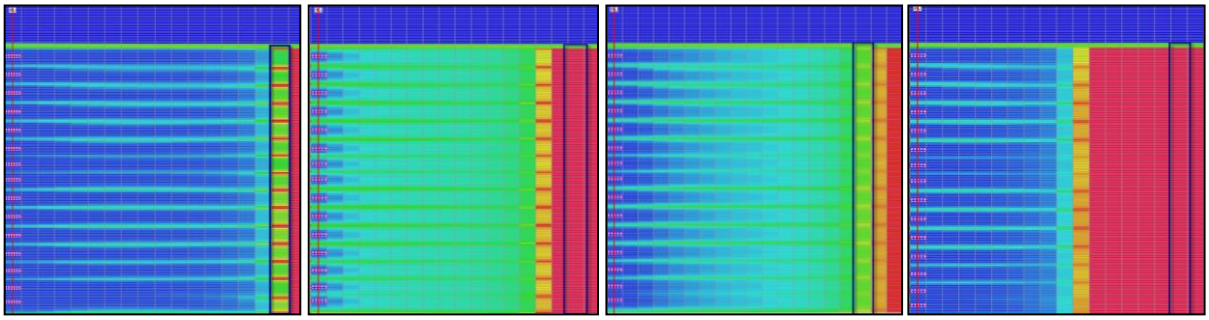

Figure 8.3 Saturation profile for high kro, low kro, high krw & low krw (from left to right).

The case with low k_{rw} exhibits the slowest velocity of the front. This is due to the fact that when the relative permeability to water decreases, so does the effective permeability to water, making it flow with more difficulty. The two middle cases both show very dispersed displacement, and were discarded for further use in the model. A combination of high k_{ro} and low k_{rw} seemed to be the most appropriate data to apply to the model. The result is presented in Figure 8.4. Embedded in the lower right corner is the water saturation scale applied to the images (Figure 8.3 and 8.4). The displacement is close to a piston displacement, and the water saturation in the swept zone is close to the residual. The dispersion observed between the perforations is caused by the injector not being placed in the first cell of the model. For this first part of the study this makes no difference. The injector was moved to the first cell later in the simulation study.

Figure 8.4 Saturation profile for low krw and high kro.

8.4 2D Ekofisk Sector Model

By applying Ekofisk porosities and initial water saturations to the appropriate layers, the 2D Ekofisk sector model was built. Porosities in the model vary between 15 % and 43 %, with the major part being greater than 30 %. The initial water saturation range is from 5 % to 10 %. The tight zone in the middle of the formation is called the thief zone. This zone and the formation under and above it were given special properties. The thief zone has high fracture density, and water breakthrough here was seen in 1994. This water has then spontaneously imbibed into the formations under and above. This behavior can be seen in Figure 8.5, which shows the flooding sequence in the observation well C11. Flooding starts in 1986. The three main breakthrough times to match for C11 were decided to be year 2001, 2006 and 2012 (marked with red boxes). In 2006 and 2012 all layers of interest in C11 were flooded with water.

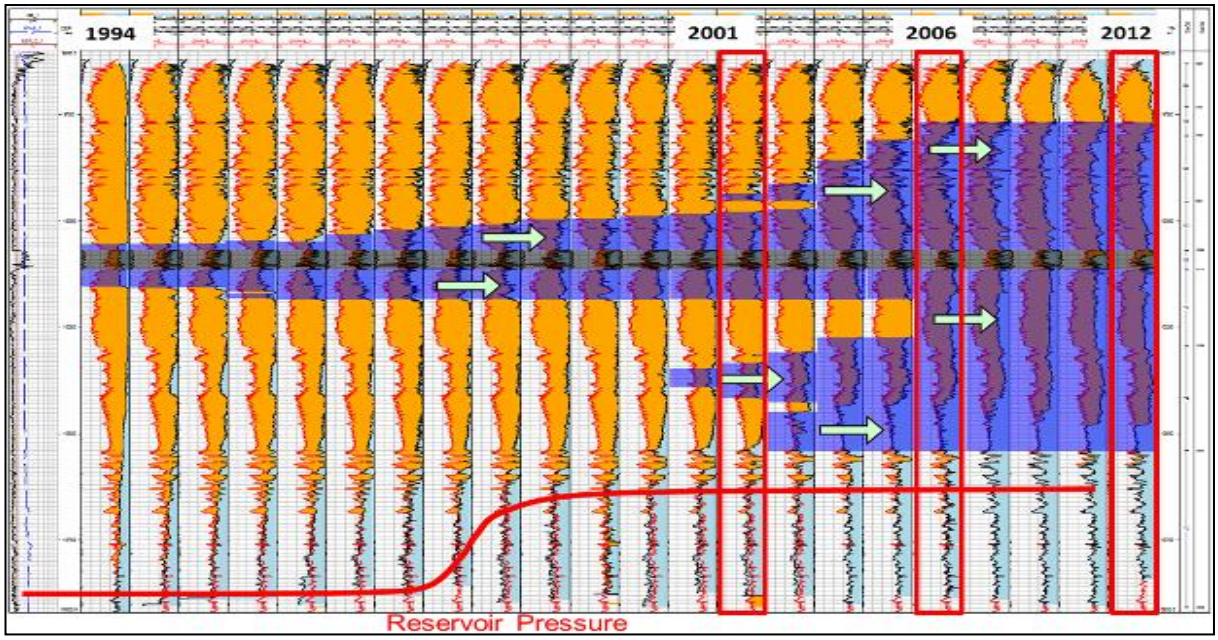

Figure 8.5 Water flooding sequence and reservoir pressure in the observation well, 1994-2012 (COPNO Internal).

Figure 8.5 also shows the reservoir pressure profile at C11, represented by the full red line at the bottom of the figure. Reservoir pressure is a fairly uncertain parameter. It is estimated that the pressure buildup started around 1998, and that the reservoir pressure at C11 is presently somewhere between 5000 psia and 6000 psia.

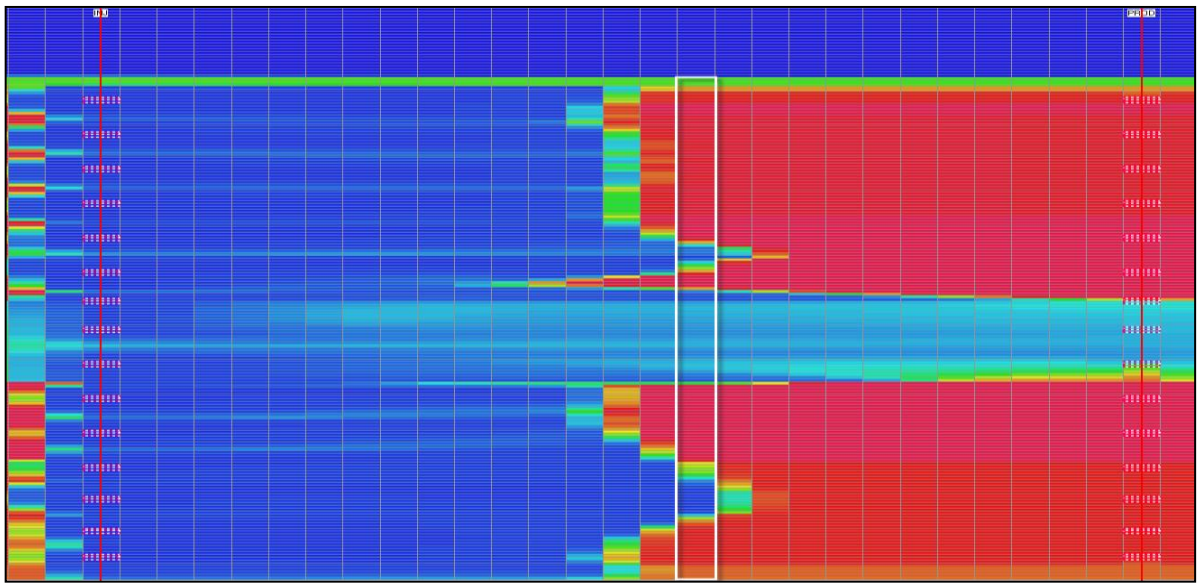

Figure 8.6 Water saturation distribution in year 2001 for the 2D Ekofisk sector model.

Figures 8.6 and 8.7 feature the history matched model in years 2001 and 2006, respectively. The white box marks the location of C11. The relative permeability data of high k_{ro} and low k_{rw} is applied. The figures present the water saturation distribution. Comparing with the observation data in Figure 8.5, the flooding sequence coincides well. In 2001, one zone is flooded in both the Ekofisk Formation and the Tor Formation. In 2006 all the layers are fully flooded with water. The spontaneous imbibition of water into the Lower Ekofisk Formation can also be observed in the model. Horizontal permeability in the formations ranges from 7 md to 46 md. The corresponding permeability of the brittle tight zone was set to 100 md.

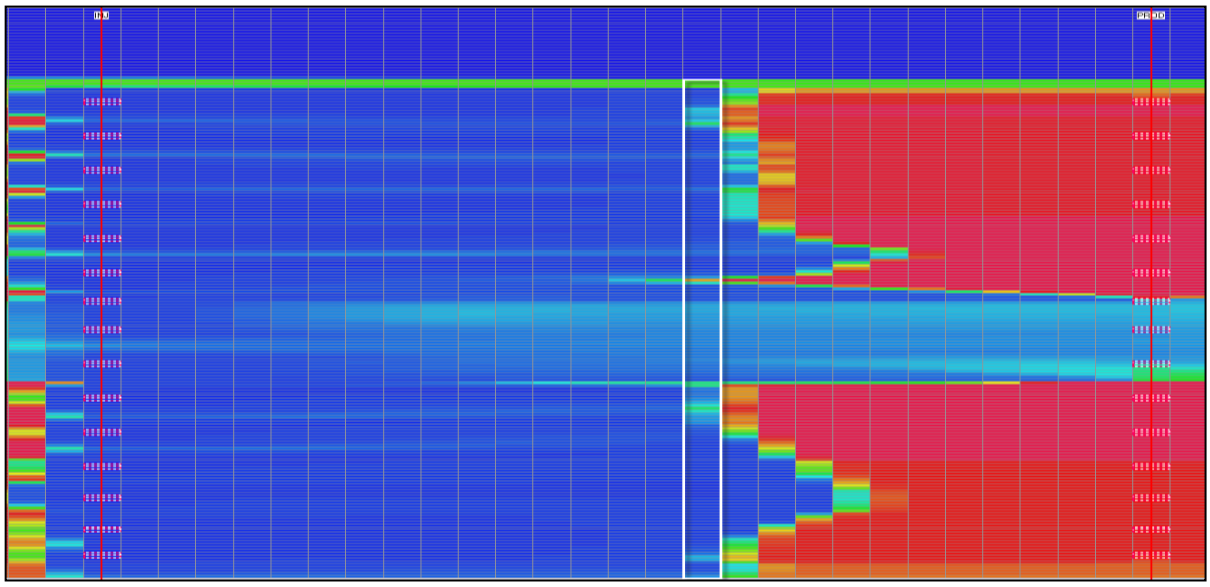

Figure 8.7 Water saturation distribution in year 2006 for the 2D Ekofisk sector model.

A history file with observed water saturations and pressures over time for C11 was created to better match the model to the actual data. In the history file the water saturation was for

simplicity set to 0.3 for unflooded layers, and similarly to 0.7 for the flooded layers. These values are not accurate, but were chosen to simply distinguish between flooded and unflooded layers. Figures 8.8 through 8.10 present plots of water saturation (fraction) against true vertical depth (feet) in years 2001, 2006 and 2012. The water saturation data from the history file is presented with dashed black lines, and the corresponding model data is represented by full blue lines.

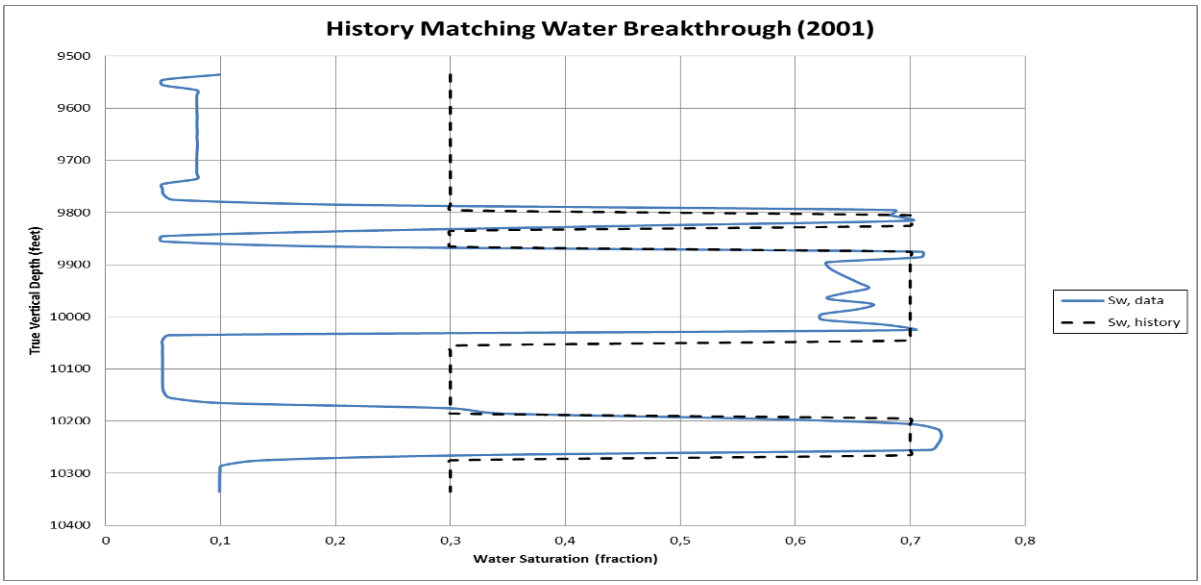

Figure 8.8 Water saturation data from sector model and history file in year 2001.

Figure 8.8 suggests that the match for the water saturation in year 2001 is good. The layers at the right depth have been flooded to the residual oil saturation. Seeing that the history data values are not actual data, the match is sufficient.

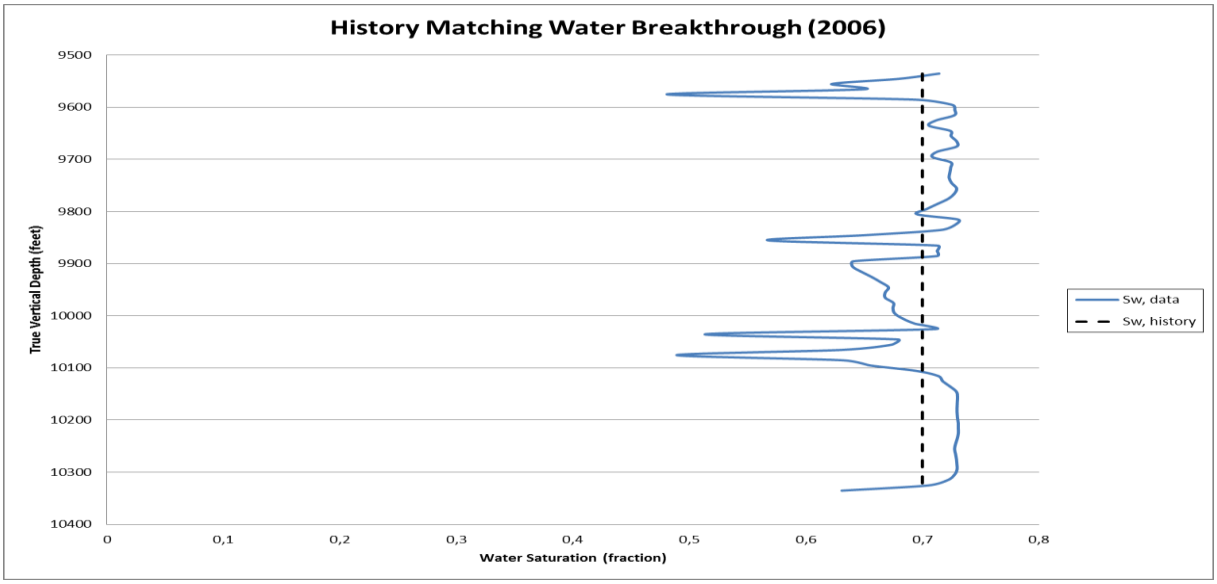

Figure 8.9 Water saturation data from sector model and history file in year 2006.

Figure 8.9 shows the same type of data from year 2006. At this time the well should be completely flooded. The match is good enough, although all layers have not reached the maximum obtainable water saturation for the waterflood.

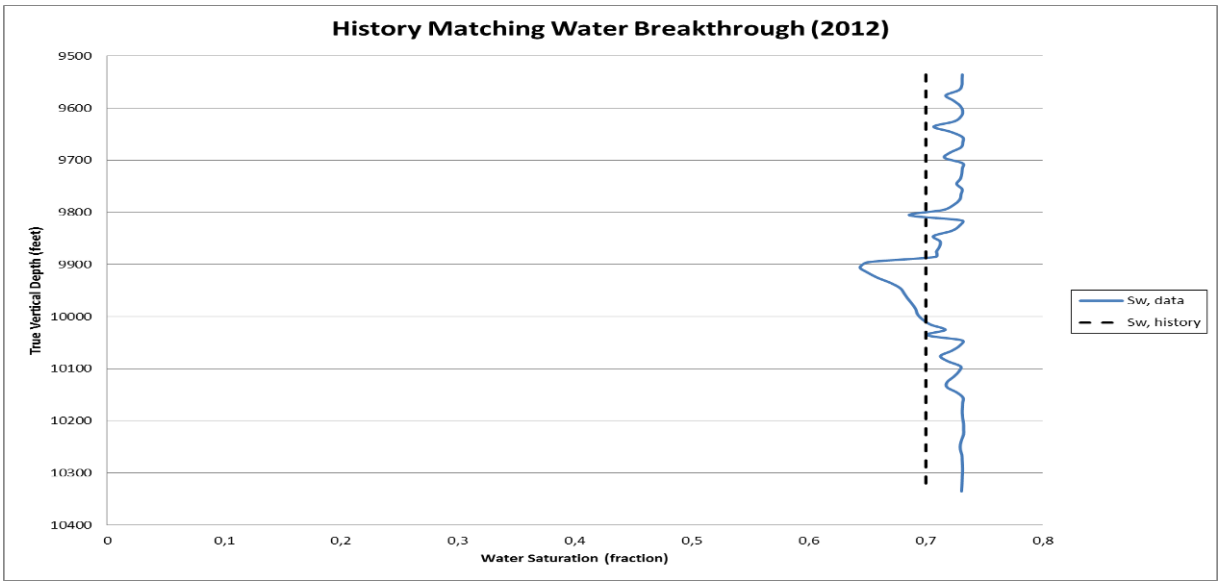

Figure 8.10 Water saturation data from sector model and history file in year 2012.

Figure 8.10 shows the water breakthrough data from year 2012. At this time the model has managed to completely flood all layers of the well. The only exception is the tight zone, which is really not of interest in this study.

Figure 8.11 shows the history matched pressure data for years 2001 (blue), 2006 (red) and 2012 (green). Reservoir pressure (psia) is plotted against true vertical depth (feet). The dashed vertical black line is the history data for pressure, set to an approximated value of 5000 psia. The figure shows that in 2001 the pressure has not quite built up to this value. Based on the pressure curve in Figure 8.5 the pressure should be at least 5000 psia in 2001. The pressure is somewhat higher in year 2006 than in year 2001, but has still not reached the value of 5000 psia. In 2012 the pressure has built up to over 5000 psia in most part of the well, and is a good enough match for the purpose of the further study.

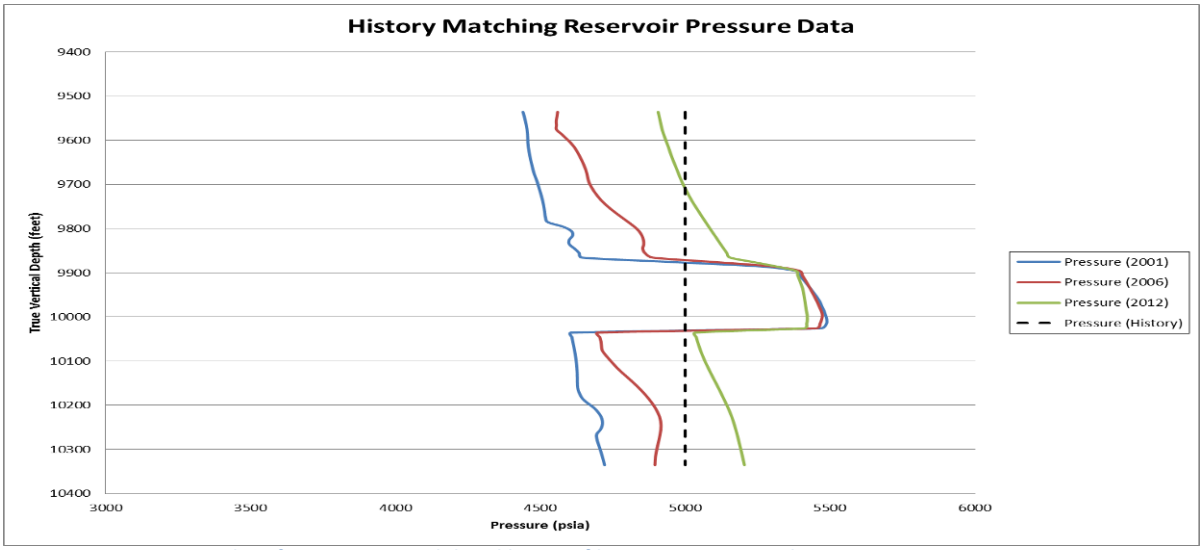

Figure 8.11 Pressure data from sector model and history file in 2001, 2006 and 2012.

In Figure 8.12 water saturation is plotted against time for a selected cell at a depth of 9773 feet located in the observation well. It can be seen from the profile that the saturation front is sharp, and completely flooding the selected cell in a short period of time. The residual oil saturation after the waterflood seems to be 25 %. The typical S_{orw} for water-wet chalk in the Ekofisk field is around 30 %. The deviation lies in the slight change of the relative permeability curves. However, in some parts of the field the S_{orw} is lower than 30 %. This suggests that the deviation from water-wet chalk yields an increased recovery. The Ekofisk formation is found at the depth of which the data in Figure 8.12 is retrieved. Since the conditions for the Ekofisk formation is moderately water-wet to near neutral wet, the result of a S_{orw} around 25 % is not necessarily wrong.

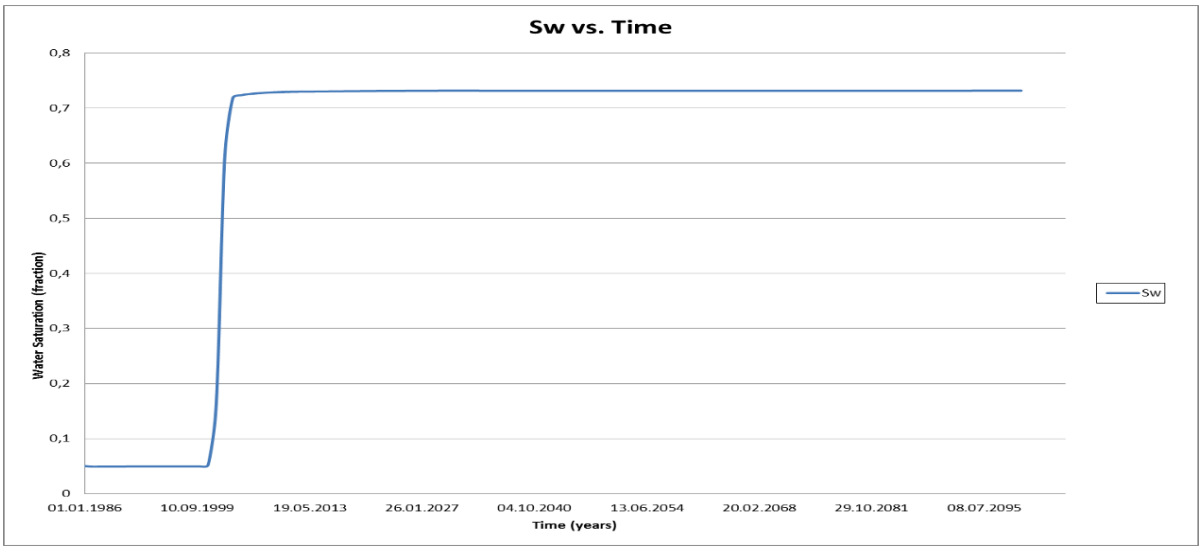

Figure 8.12 Water saturation plotted against time for C11 at a depth of 9773 feet.

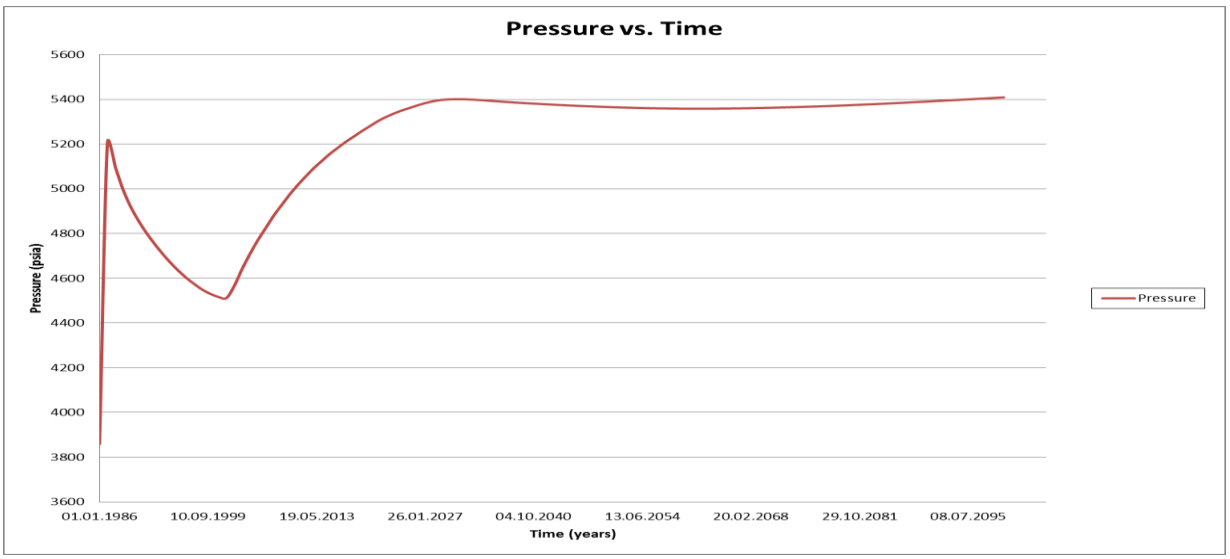

Figure 8.13 Pressure plotted against time for C11 at a depth of 9773 feet.

The pressure profile, pressure plotted against time, is presented in Figure 8.13. The same cell as in Figure 8.12 is used. The pressure build up starts in year 2003, which is somewhat late compared to the data from the observation well. Judging from the profile, a reservoir pressure of 5000 psia is not reached until year 2011. It reaches a plateau pressure of 5400 psia in year 2029. Considering that the pressure buildup profile in Figure 8.5 is an average representation of the whole well, the model is not necessarily wrong. It should be sufficient to reach a pressure greater than 5000 psia by 2014 for the purpose of this study.

If a cell at a greater depth is considered, as in Figure 8.14, the profile looks different due to gravity effects. At this depth the pressure build up starts in year 1999, which is not far from the reality. The pressure is 5000 psia in year 2006, and reaches a plateau value of 5350 psia by 2025.

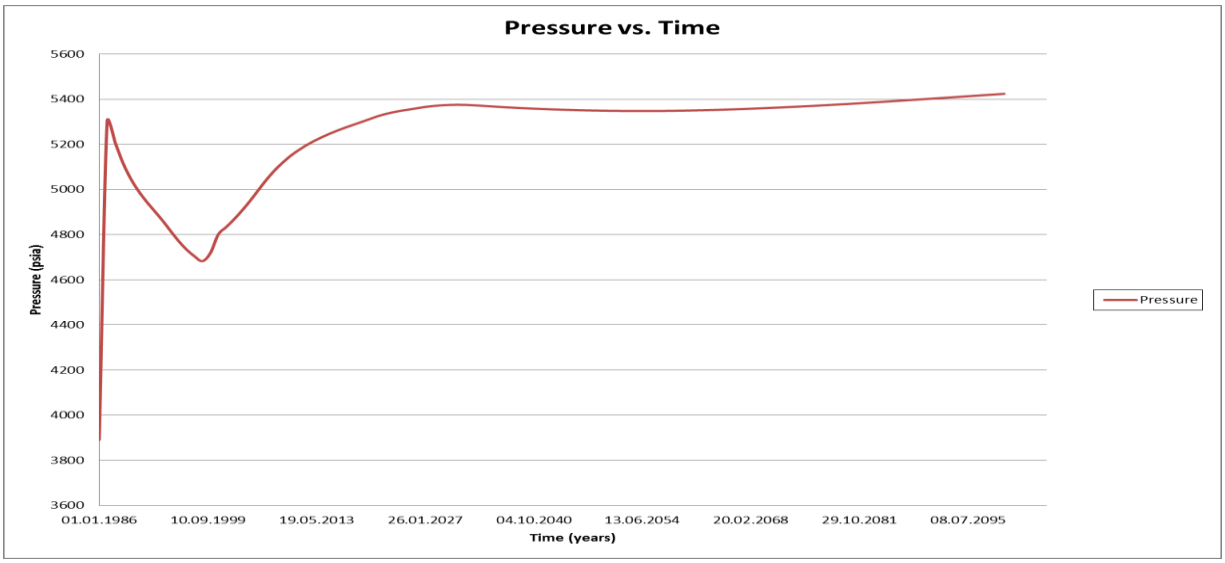

Figure 8.14 Pressure plotted against time for C11 at a depth of 9873 feet.

8.4.1 Grid Refinement

For the simulation of the single well chemical tracer test only a small section of the history matched model is to be used. A 20 feet interval of C11 in z-direction is to be perforated, and the tracer is to be displaced 30 feet into the reservoir on both sides of the well. This 20 feet times 60 feet interval, plus a buffer zone, making it 70 feet times 40 feet, was decided to have grid cells the size of 1 foot in each direction. An image of the fine grid and its location (in grey) can be seen in Figure 8.15. The fine grid, featuring a porosity map, is presented on the right hand side. The yellow layers have a porosity of 35 %, while the red layers have 40 % porosity. The fine grid is flanked by gradually increasing grid block sizes to make the model more stable.

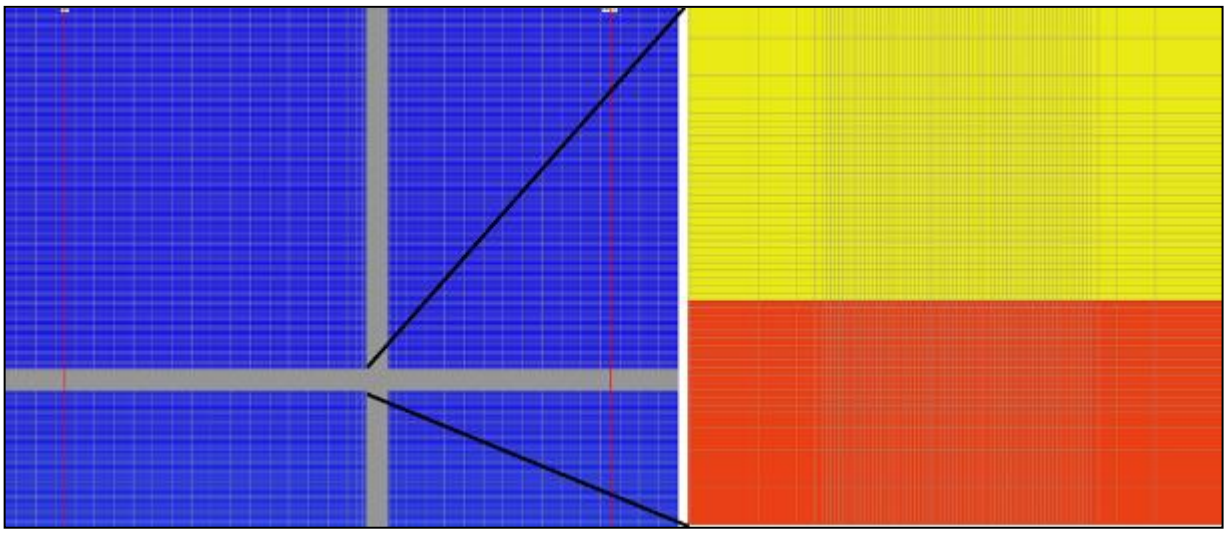

Figure 8.15 Location (grey area) and design of the grid refinement (right).

The placement of the test area is no coincidence. In order to be most assured matrix flow, the layer flooded last in the flooding sequence was chosen. This area is located in the Upper Tor Formation. The initial water saturation in the test area was 5 %. Permeability was 13 md in x-direction, and 5 md in z-direction. The porosity was 35 % for the upper 15 feet, and 40% for the lower 5 feet.

The reservoir temperature was fixed at 268 F. Allowing heat calculations lead to severe instability in the model; hence it was removed. This decision was supported by the fact that no cooling near C11 was seen during the last survey in 2012. It is safe to assume that no cooling effect will take place near the wellbore when injecting cold water into C11 at the

depth chosen. The slow injection rate combined with the large depth will most likely cause the water to be heated up close to reservoir temperature by the time it reaches the perforations.

9 Single Well Chemical Tracer Test (SWCTT)

This chapter addresses the general function of a tracer, a single well chemical tracer test (SWCTT) and how this can be used to determine the effect of a surfactant flood. Bear (1972) defined a tracer as a "labeled portion of the same liquid which may be identified by its density, color, electrical conductivity, etc." In this thesis the tracer is identified by its salinity, and solution chemistry and hydrolysis is not accounted for. The fine gridded area from Chapter 8 was used for the simulations.

9.1 The Function of a SWCTT

When considering mature oil fields for application of EOR, two of the main challenges are determining the amount of remaining oil, and evaluating the effect of EOR in pilot studies. Core analysis and well logging are the two most widely used methods for measuring the residual oil saturations. Major faults in both these methods is the small reservoir volume the results represent, as well as the large uncertainty involved (Deans *et. al.* 1973) and (Deans & Ghosh 1994). A SWCTT has proven to be a safer and more stable way of providing these unknowns. SWCTTs are a method of push-and-pull operation in a producer or injector. The test is based on injection of a reactive partitioning tracer, an ester, into the reservoir. The ester is displaced by tracer-free water to a target depth from the wellbore, and the well is shut in. The tracer will dissolve partly in the water phase and partly in the oil phase. During the shut-in period some of the ester dissolved in the water phase hydrolyses into alcohol. This product tracer is only soluble in water (Skrettingland *et al*. 2011). The hydrolysis is dependent on pH and temperature. Symbolically the reaction can be written as (Huseby *et al*. 2012);

$$R_1COOR_2 + H_2O \leftrightarrow R_2OH + R_1COOH \tag{9.1}$$

The test utilizes the difference in travel time between the injected ester and the alcohol generated in-situ by hydrolysis. Once back production starts, the product tracer will follow the water, while the passive tracer in the oil phase is delayed. The degree of this delay is

dependent on the oil saturation in place. A tracer profile is made from the returning tracer, and is compared to previously observed back produced concentrations to find the oil saturation. Figure 9.1 shows tracer profiles for an active tracer (EtOH) and a passive tracer (EtAc).

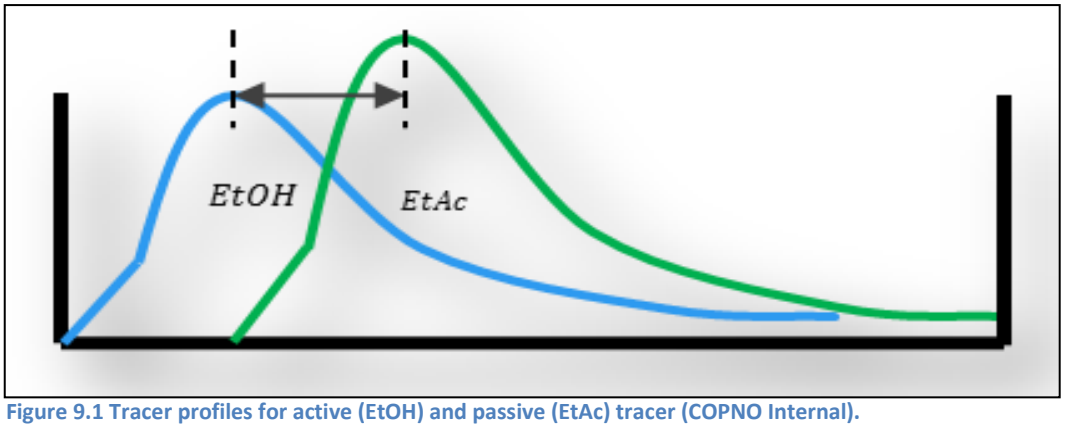

Figure 9.1 Tracer profiles for active (EtOH) and passive (EtAc) tracer (COPNO Internal).

If the oil saturation is close to the residual, which it often is in water-flooded regions, the low values of k_{ro} will make the oil flow rates negligible compared to the water flow rates. The oil saturation is then determined by the difference in retention time of an active and passive water tracer;

$$S_o = \frac{(t_{EtAc} - t_{EtOH})}{(t_{EtAc} - t_{EtOH}\,(1-K))} \tag{9.2}$$

Where t_{EtOH} and t_{EtAc} are the retention times of the active and passive tracer, respectively, S_o is the oil saturation, and *K* is the partition coefficient of the active tracer. The greater the oil saturation, the greater the difference in arrival times will be.

If this tracer test is done both prior to- and after an EOR implementation is carried out, a reduction in S_{orw} will be possible to observe. The tracer profile is measured in produced volume (m^3) vs. concentration of tracer (ppm). S_{orw} can be measured in a 10 meter radius from the well. A fundamental assumption for the SWCTT to be valid is that the tracers do not affect the phase transport. If this is the case, the simulation of tracer transport can be performed in a separate module decoupled from the reservoir simulation itself (Huseby *et al*. 2012). Two tracer pilot tests have been conducted on the Norwegian Continental Shelf; one in the Snorre field, and one in the Heidrun field.

The well options for the SWCTT are an existing injector, producer, infill injector or infill producer. If an existing injector is used for the test there is a reduced chance of non-pilot oil. On the other hand the near wellbore area has seen very high pressures and rates; hence could have a too low S_{orw}, be very cold and be extensively fractured. The injector would also need to have production capability for the back-production of the tracer. By using a producer for the SWCCT there is a high chance for non-pilot oil unless a new well or a high water cut well is used. The well would need to have injection capability. Injection into a hot near wellbore area will create a temperature profile, affecting the tracer profile. This temperature profile would most likely also be an issue with an infill producer, although not in the same scale. An infill injector would presumably also be positioned in a water flooded area like an existing injector, but with more intermediate temperatures (COPNO Internal).

9.2 Geological Effect on Tracer Curves

A simulation study was conducted with the aim to determine the geological effect on the shape of the back produced tracer curves. Two cases of tracer injection are presented. In one case, tracer was injected for 1.5 months followed by 0.5 months of chase water. In a second case, tracer was injected for 1 month followed by 1 month of chase water. In reality the tracer slug would be much smaller, but the large volume is chosen for viewing purposes. After the two months of injecting was complete, the well was switched from an injector to a producer. The tracer containing water was then back produced to obtain the tracer profile. The purpose of the chase water was to attain a curve with a distinct top. The back produced tracer was plotted as traced water (fraction) against time (days). The tests were carried out in an area flooded to the residual oil saturation.

9.2.1 Two Extreme Geological Base Cases

Several different geology scenarios were run for two extreme base cases: (1) a completely confined test area and (2) an unconfined test area. For the unconfined area, the tracer was free to flow in every direction from the injector, while fluid flow for the confined test area was restricted to flow within the horizontal boundaries of the 20 feet high perforation

interval. Fluid flow was restricted by applying a vertical permeability of 0.001 md to a single layer above and under the perforated interval. Figure 9.2 presents the water tracer propagation after injecting tracer for 1 month followed by 1 month of chase water. The scale from 0 to 1 incorporated into the picture is used for all the maps of tracer concentration in this chapter.

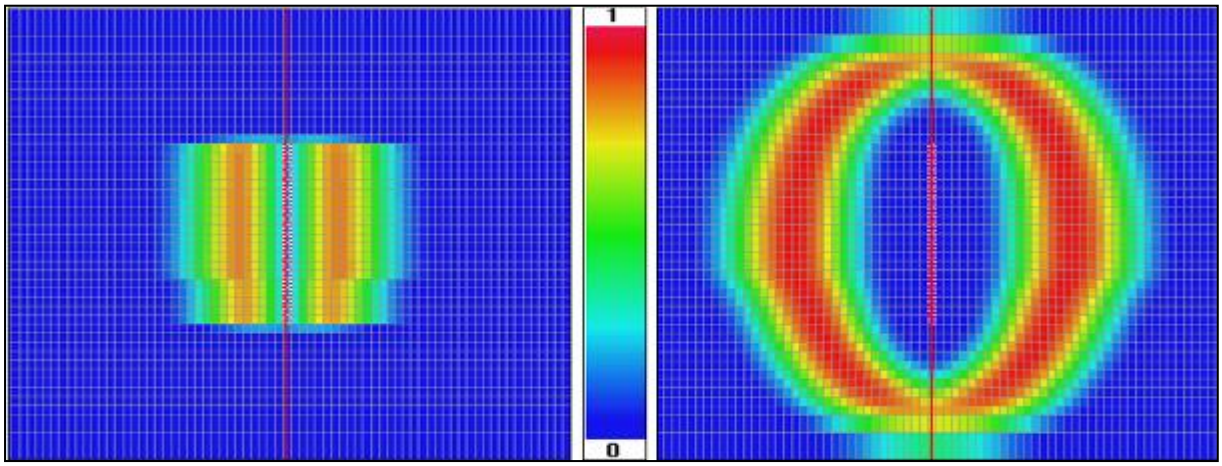

Figure 9.2 Tracer maps for confined (left) and unconfined (right) test areas after 2 months of injection.

When the fluid flow was not restricted to the height of the perforation interval, the flow propagated about 12 feet in z-direction from the top and bottom perforation. At the same time the tracer propagated further away from the wellbore in x-direction. This behavior suggests a higher injection rate for the unconfined case compared to the confined case.

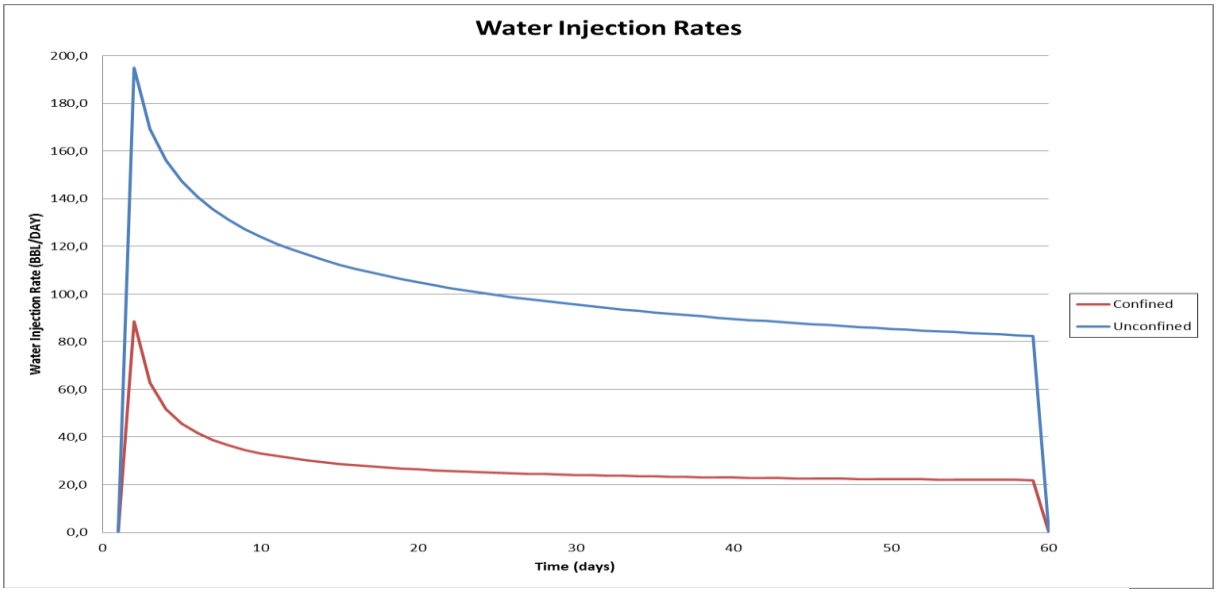

Figure 9.3 Water injection rate plotted against time for confined (red) and unconfined (blue) cases.

Injection data confirmed that the injectivity much higher for the unconfined case (Figure 9.3). A possible explanation is that for the unconfined test area, more volume in different

directions is susceptible to flow. This is supported by injection data for the separate perforations. For the confined case the injection rate is the same from all of the perforations. For the unconfined case, the top and bottom perforations contribute to more of the injectivity than the perforations in the middle.

Figure 9.4 shows the back produced tracer curves for the confined test area (in red) and the unconfined test area (in blue). Time in days on the x-axis is plotted against traced water fraction on the y-axis. The tails of the two curves are quite similar, but the tops differ in two distinct ways. Firstly, the top for the unconfined case reaches a higher value by a fraction of 0.1 compared to the confined case. The height of the top depends on the degree of dispersion near the wellbore. The graphs would suggest the tracer slug is more dispersed for the confined test area. Secondly, the top for the unconfined case appears later than for the confined case. This can be explained by the difference in injection volumes. Since injectivity is higher for the unconfined case, more chase water is injected. This consequently requires more chase water to be produced before the tracer can be produced.

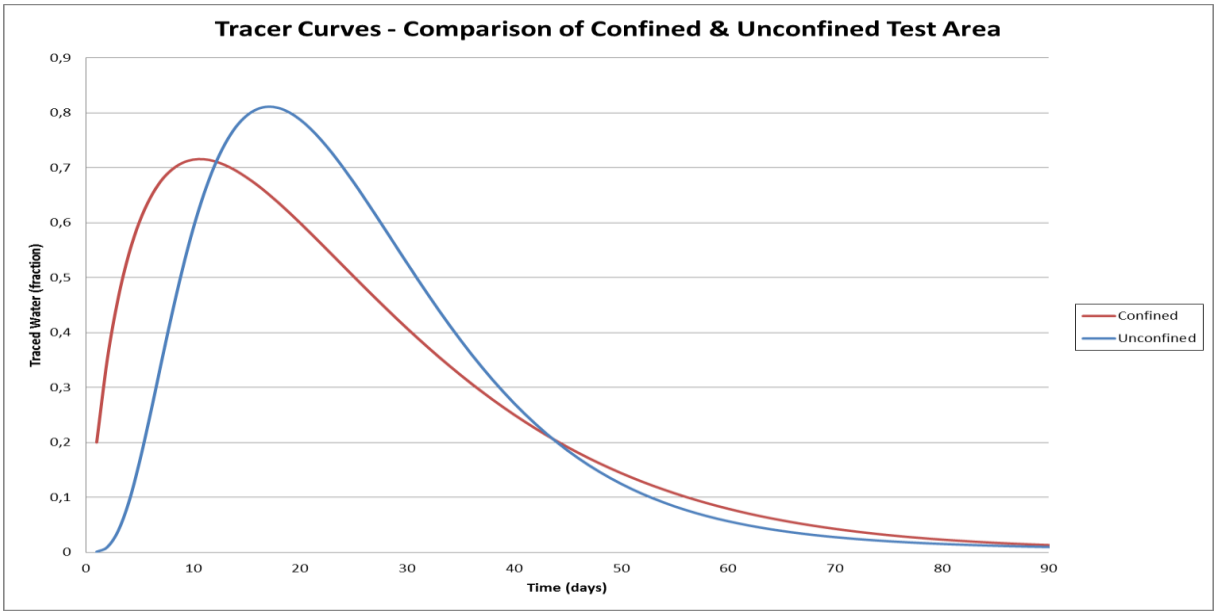

Figure 9.4 Tracer curves for confined and unconfined cases.

Figure 9.5 shows a comparison of the tracer curves for 1 month and 0.5 months of chase water (CW) injection. The total injection time for both cases was 2 months. When chase water was injected for 1 month it took longer time for the curve to reach a peak compared to injecting for 0.5 months. The two cases produce curves with similar tails. In the rest of this

chapter the case of 1 month tracer injection followed by 1 month of chase water will be used.

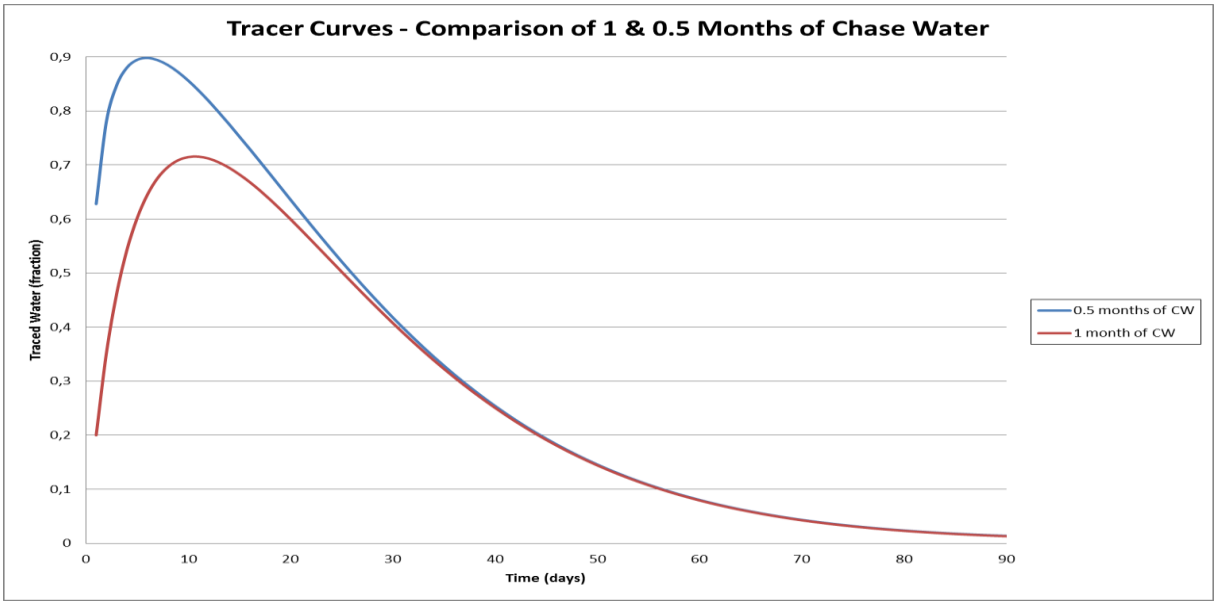

Figure 9.5 Tracer curves – Comparison of 1 & 0.5 months of chase water injection. Confined.

9.2.2 Introduction of a High Permeability Layer

One of the main points of research was how the tracer profile would be affected by a change in geology. A high permeability layer (a fracture like feature) was introduced to the test area. For the confined case, the fracture was incorporated into the middle of the test zone. The unconfined case was given a high permeability layer three feet above the top perforation. The horizontal permeability for this particular layer was varied between 20 md, 50 md, 200 md and 1000 md. Note that the horizontal permeability in the rest of the test area was 13 md. The vertical permeability was fixed at 5 md.

By simulating the different scenarios and viewing the tracer concentration map in CView (viewing program for PSim), an idea of how far the fluid propagated into the reservoir through the fracture was visualized. The results for the confined case can be seen in Figure 9.6. All of the images are captured after the 2 months of injection, and feature the scenario of 1 month of tracer injection followed by 1 month of chase water. The red boxes indicate the fine gridded test area of 70 feet times 40 feet.

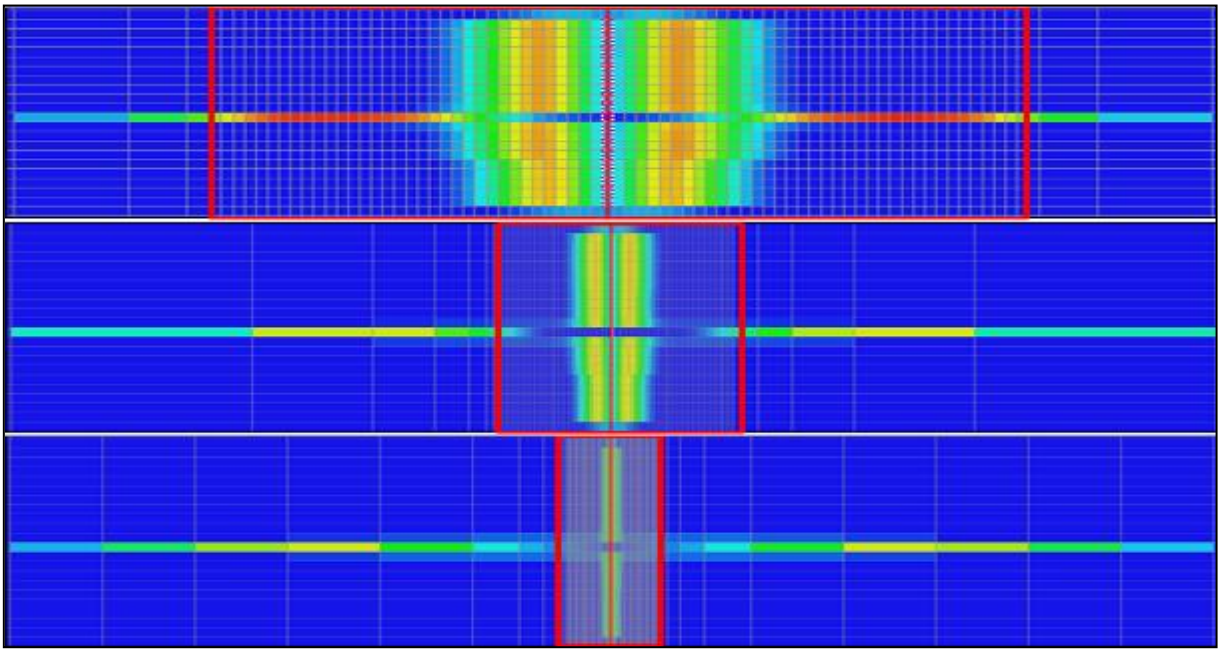

Figure 9.6 Tracer maps. Fracture with horizontal permeability 50 md (top), 200 md (middle) & 1000 md (bottom). Confined.

With the permeability of the fracture set to 20 md (not included in Figure 9.6), the tracer stayed inside the test area, while it only slightly exceeded the boundary for the case of 50 md. For fracture permeabilities of 200 md and 1000 md, the tracer propagated as far as 175 feet and 455 feet respectively away from the wellbore.

Figure 9.7 shows the tracer curves for the cases presented in Figure 9.5, along with the base case without the fracture. The case of the 50 md fracture produces a curve almost identical to that of the base case. As the permeability of the fracture increases, the maximum back produced tracer fraction decreases. The tops also shift slightly to the left. At the same time the tail experiences a less steep decline.

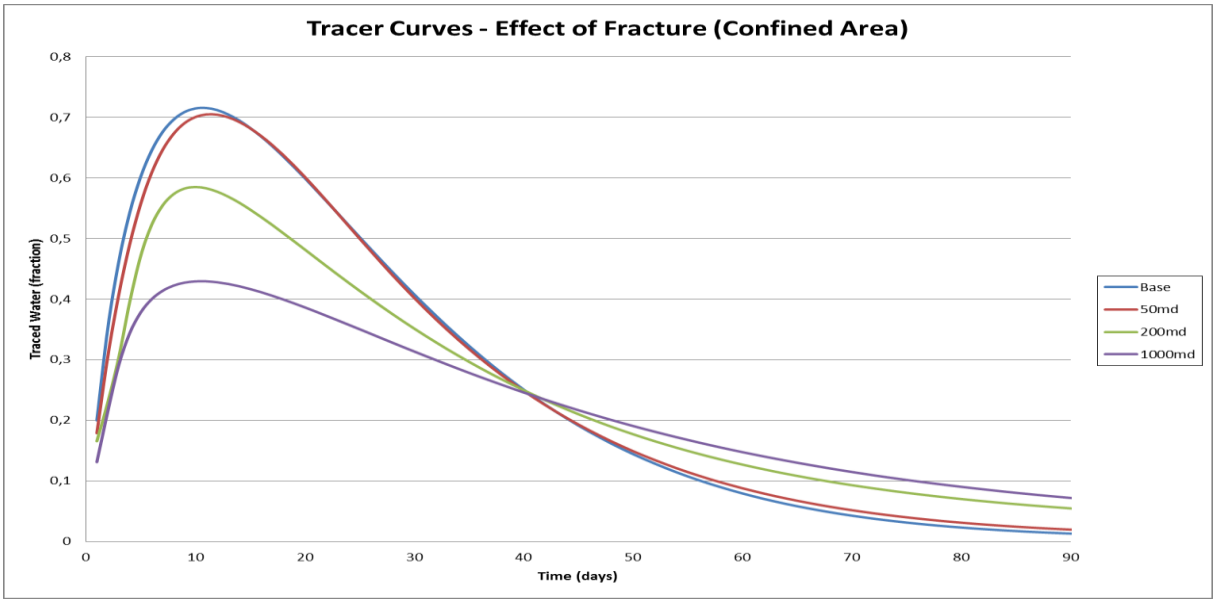

Figure 9.7 Tracer curves – Effect of fractures. Confined.

Similar trends were seen for the unconfined case with a fracture 3 feet above the perforation interval (Figure 9.8), although the tracer did not propagate quite as far from the test area.

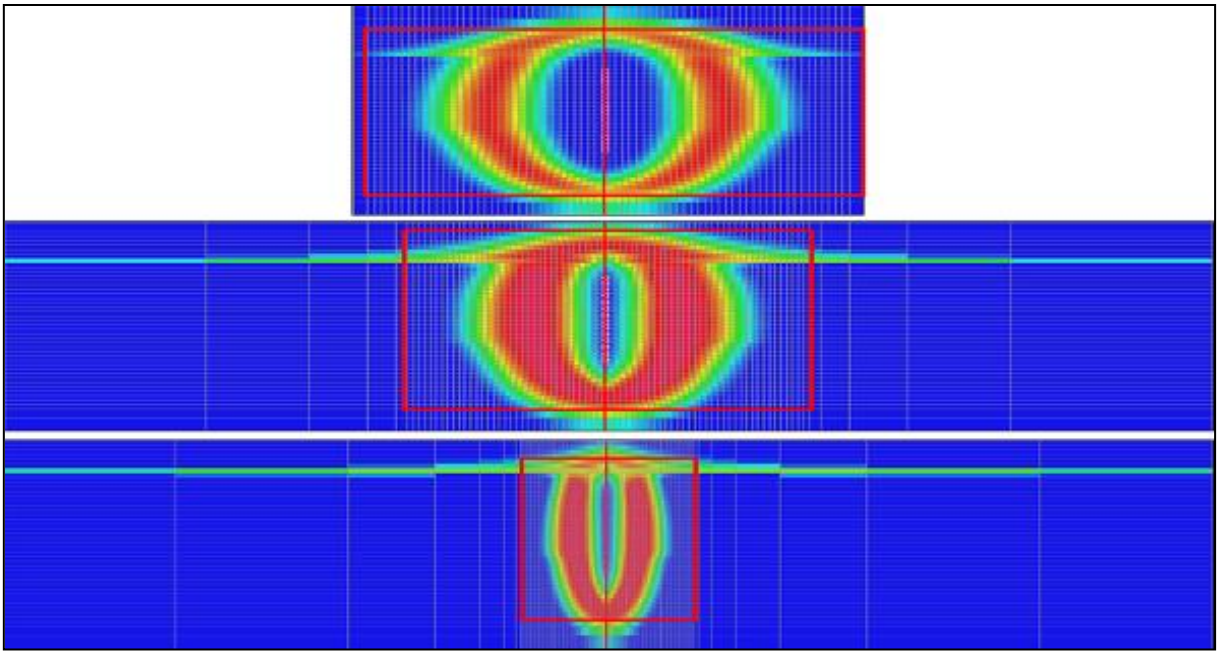

Figure 9.8 Tracer maps. Fracture with permeability 50 md (top), 200 md (middle) & 1000 md (bottom). Unconfined.

Figure 9.9 shows the tracer curves for the cases in Figure 9.8, along with the base case for the unconfined test area. Once again, the case of the 50 md fracture gives a similar curve as the base case. The trend for the higher permeabilities is also the same; the maximum traced water fraction decreases with increasing permeability, and the tops for the lower fractions are shifted slightly to the left. The high permeability of the fracture allows tracer to be produced earlier than for the base case.

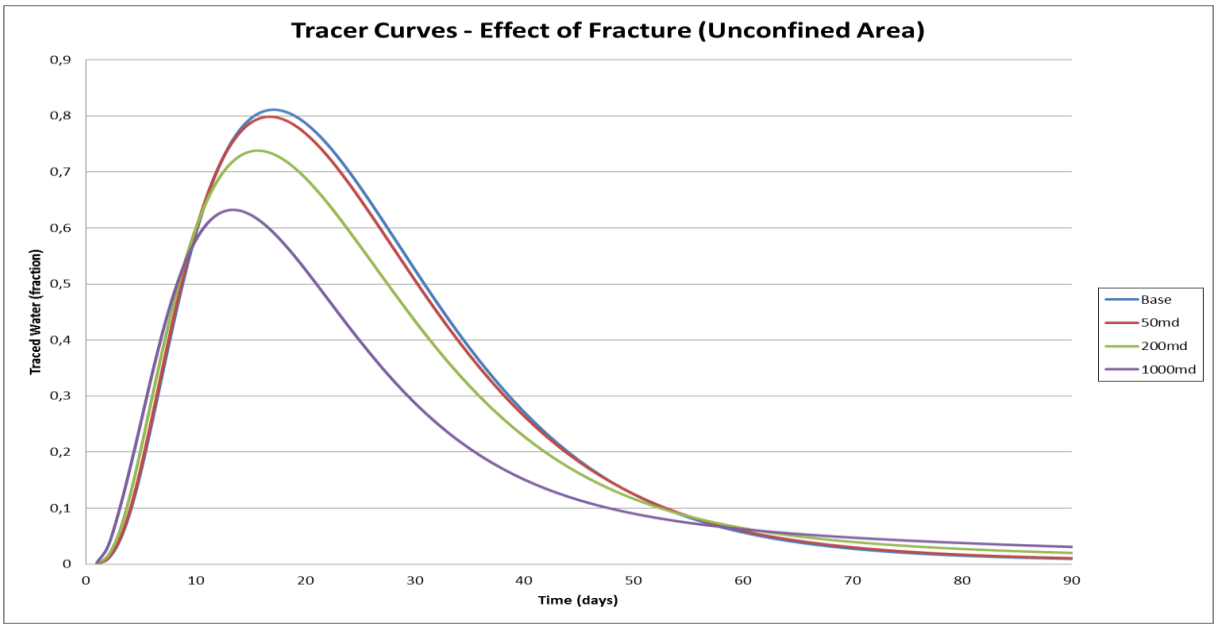

Figure 9.9 Tracer curves – Effect of fractures. Unconfined.

9.2.3 The Effect of Active Wells in the Vicinity of the Test Area

All of the previous tracer tests were executed in a static environment. This was created by shutting in the injector and producer on either side of C11 three years prior to the start of tracer injection in C11. By shutting the wells in, the model stabilizes. In a real field, conditions are not likely to be completely static. To see the effect of active wells around C11, the injector and producer were left active. Apart from this, the injection scheme was the same as for the previous cases. The results for the confined case are presented in Figure 9.10. Both images show the tracer maps after 2 months of injection, just prior to start of back production. As expected, a clear drift towards the right is observed. This happens because the net fluid flow in the model is from left to right when wells are active.

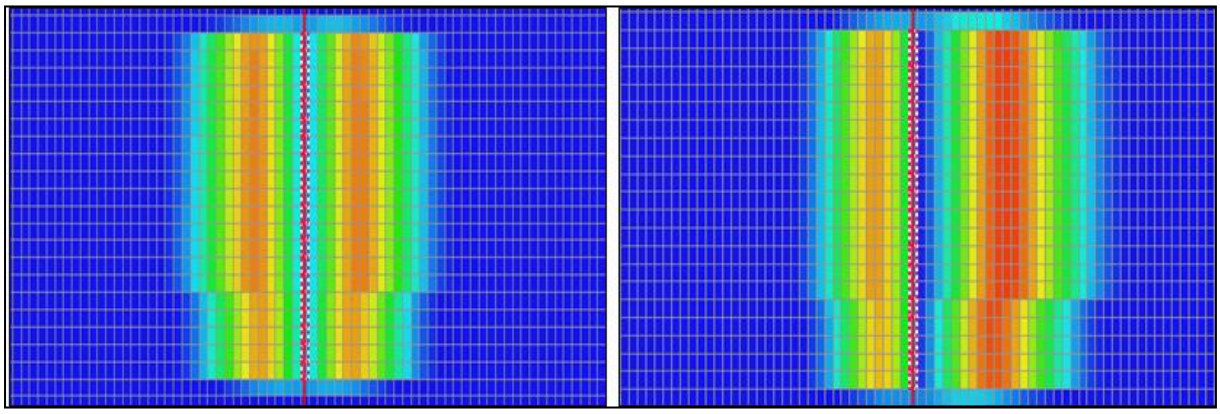

Figure 9.10 Tracer maps for when wells are shut in (left) and when wells are active (right). Confined.

Viewing the back produced tracer profiles featured in Figure 9.11, it is clear that the case of shut in wells reaches a higher top than the other case. The decline of the same curve is also steeper. However, the case of active wells reaches the peak somewhat earlier. This is due to the drift. Once tracer is injected on the left hand side of the well, it is met by a countercurrent net fluid flow. Figure 9.10 clearly shows that the tracer concentration on the left side of the well is higher for the case of active wells. When the tracer is back produced, more of the tracer is produced at once. The same trends were observed when the same scenario was run for the unconfined case.

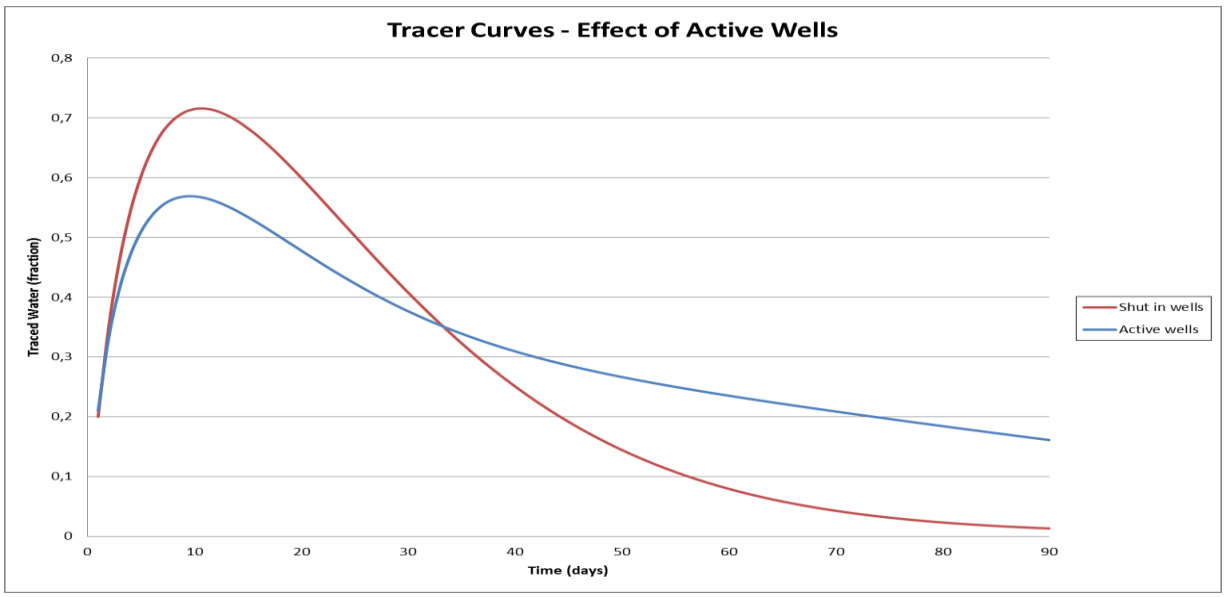

Figure 9.11 Tracer profiles for when wells are shut in (red) and when wells are active (blue). Confined.

Figure 9.12 shows the cumulative amount of tracer retrieved by back production, and confirms that more tracer is produced at once in the case of active wells. The total amount of back produced tracer is however higher for the case with static conditions. When wells are shut in, 99% of the tracer is produced after 3 months. In comparison, only 84% of the tracer is produced after 3 months when the wells in the vicinity are kept active. The drift to the right prevents all of the tracer from travelling back to the wellbore within the given production period.

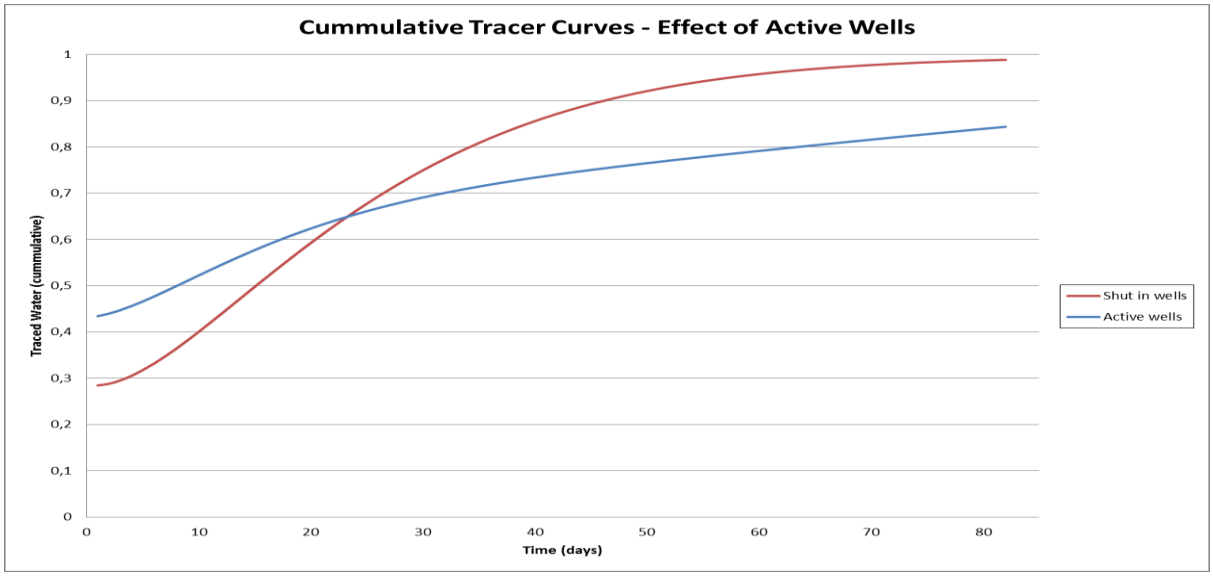

Figure 9.12 Cumulative tracer when wells are shut in (red) and when wells are active (blue). Confined.

10 Introducing Surfactants to the Model

This chapter includes an introduction to the basic logistics of a surfactant flood and surfactant modelling in both a 2D sector model and a 2D radial model. With the sector model the aim was to visualize how the surfactant slug mobilized a new oil bank. The goal with the radial model was to determine the volumes of chemicals and tracer needed to reach target depth from the well, and the time span of the operation.

10.1 The Basic Logistics of a Surfactant Flood

The three key parameters in the economics of a surfactant flood were defined by Spinler & Baldwin (2000) as incremental oil recovery, surfactant loss and surfactant cost. The incremental oil recovery is the measure of success for any EOR method. Surfactant loss is important because it affects the volume of chemicals needed for achieving an effective process.

Apart from cost, there are several other challenges related to the surfactant pilot test in Ekofisk. Low salinity water has previously not been injected into the field, and there is uncertainty around its compatibility with the chalk matrix. The location of the test area is another uncertainty. It could either be performed in the developed water flooded area as a tertiary recovery method, or in the unflooded South Ekofisk as a secondary recovery method. It is desirable to execute the test in an area without fractures, so that matrix flow is allowed. This is easier said than done, but seems more likely in the undeveloped South Ekofisk sector of the field.

The preferred optimum salinity for the surfactant formulation is in the range of 48 000 ppm to 62 500 ppm. By using a soft seawater formulation, the optimum salinity window becomes much wider than for that of normal seawater. In the early stages of the surfactant study on Ekofisk, the narrow optimum salinity window for seawater was a possible showstopper for the pilot test. The immobile oil saturation will not be as effectively reduced without the type 3 phase behavior in the optimum salinity region.

For normal seawater pH is in the range of 9 to 9.5, and the chalk surface is negatively charged. For the modified seawater formulation pH is 11.5, and the surface change of chalk is positive. The pH of the water was raised both to achieve optimum salinity and to reduce adsorption. The latest measured surfactant adsorption value was 0.40 mg/g at a temperature of 268 F. A previous value of 0.64 mg/g was measured at a lower temperature. Because these values were not measured from Ekofisk chalk, an adsorption value of 1.6 mg/g will also be used in this thesis - as a possible high value.

It is desired that the solubilization ratio should be 10 or higher. This corresponds to an IFT in the range of 0.003 dynes/cm or less (Levitt *et al.* 2009). A compromise must be made between maximum solubilization ratio (low IFT), low viscosity and other factors required for good transport. Polymer as a mobility buffer is not an option for Ekofisk due to the low matrix permeability. Polymer molecules are so large that shear degradation would quickly lower the viscosity to a point of inefficiency.

Another challenge is the temperature gradient that exists in the reservoir. The injection of unheated seawater over a long period of time has cause a temperature gradient. Cooling first appears in the vicinity of the injection wells, and a thermal front then moves through the reservoir. A decrease in temperature will lead to a decrease in IFT, which will benefit the viscous displacement of oil near the injection wells. The temperature gradient for Ekofisk ranges from 60 F to 268 F. The current surfactant formulation has proved to have good aqueous stability at both 155 F and 268 F. The thermal front should therefore not be an issue.

10.2 Surfactant Flooding in a 2D Sector Model

A surfactant flood model was created by including a CEOR module (see appendix) in the same model as for the tracer study in Chapter 9. Surfactant was injected for one month, and was then followed by one month of chase water. The following back production then lasted for 3 months. The bottom hole pressure (BHP) was 4000 psia for the producer and 7000 psia for the injector. Surfactant was added to water with a salinity of 58 000 ppm. The optimum salinity for the specific surfactant ranges between 0.821 meq/ml [48 000 ppm] (lower),

0.950 meq/ml [55 500 ppm] (optimum) and 1.070 meq/ml [62 500 ppm] (upper). The chase water had a salinity of 35 000 ppm. Surfactant adsorption was set to 0.40 mg/g and 1.6 mg/g at a surfactant concentration of 0.71 % for the 2D sector model.

10.2.1 Confined Test Area

Figures 10.1 and 10.2 are images of the fine gridded confined test area at the end of the 2 month injection period. The adsorption values were set to respectively 0.40 mg/g and 1.6 mg/g. They feature the oil saturation (S_o) distribution scaled according to the scale on the left hand side of the figures. The waterflood residual oil prior to the injection of surfactant was 0.264.

The blue area closest to the wellbore is completely flooded with water. This is where the surfactant has had a high enough concentration to be active. Both figures have a cut out in the water zone in the transition from the low porosity at the top (35%) to the higher porosity at the bottom (40%) of the test area. This can possibly be explained by gravitational forces. The water sinks downwards as it is injected. As the porosity changes in this zone, the lower grid blocks need more pore volume to be filled up. The accumulation is then simply a matter of grid block pore volume capacity.

There is a clear difference in how far from the well the water zone propagated. The main bulk of water extended 8.5 feet horizontally from the well in the case with low adsorption. When adsorption was increased, the same water bulk only extended 5 feet from the wellbore. A difference in oil saturation in the new oil bank was also observed. The oil saturation was 0.36 for the case with low adsorption, while it was 0.31 in the high adsorption case. This shows that more oil has been mobilized in the first case.

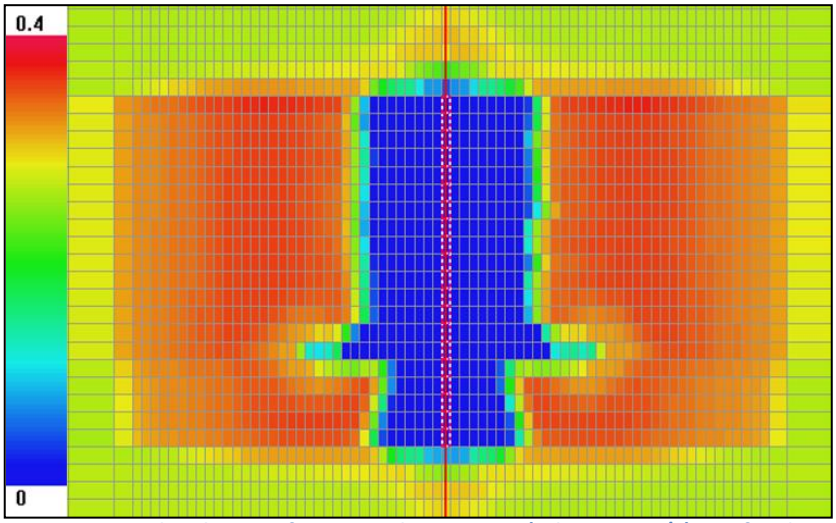

Figure 10.1 S_o distribution after 2 months injection. (Ads=0.40 mg/g). Confined.

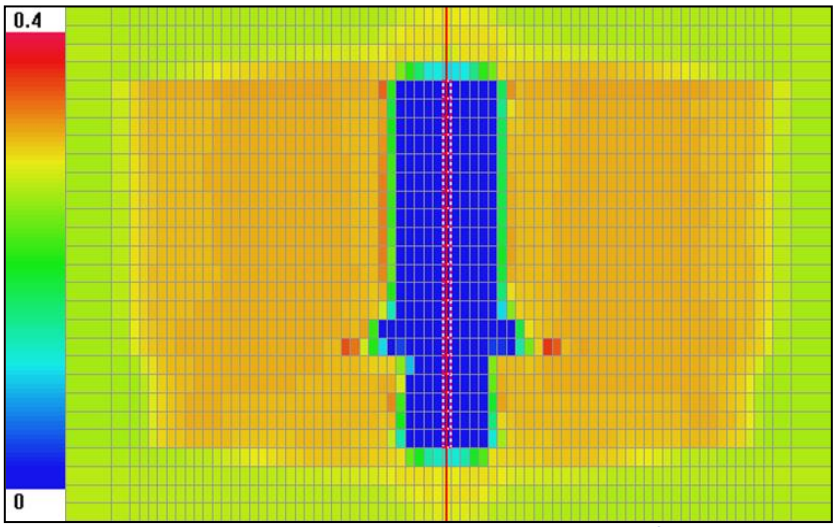

Figure 10.2 S_o distribution after 2 months injection. (Ads=1.6 mg/g). Confined.

10.2.2 Unconfined Test Area

Figures 10.3 and 10.4 show the S_o distribution for the unconfined case at the end of the injection period. The injection rate is higher for the unconfined case, meaning both the water zone and the oil bank has extended further away from the well than for the confined case. Here there were 3 cut outs in the completely swept zone. The middle one is probably the same as for the confined case. The top and bottom one could possibly be explained by the same concept. The injectivity is higher for the top and bottom perforations than for the middle ones. This water then sinks downwards, and since the permeability in x-direction is higher than in z-direction, it starts to propagate outwards.

The shape of the oil saturation distribution is similar for both the adsorption values. The case with the low adsorption has extended further from the well than the case of high adsorption. In addition, the oil saturation in the new oil bank was higher for the case of low adsorption – as in the confined cases. The oil saturation in the low adsorption case was 0.36, and extended 52 feet from the wellbore. The oil saturation was 0.31 in the new oil bank in the case of high adsorption; extending 42 feet from the well.

The main bulk of water extended 12 feet in x-direction where the low adsorption value was applied, whereas it extended 9 feet where the high adsorption was applied.

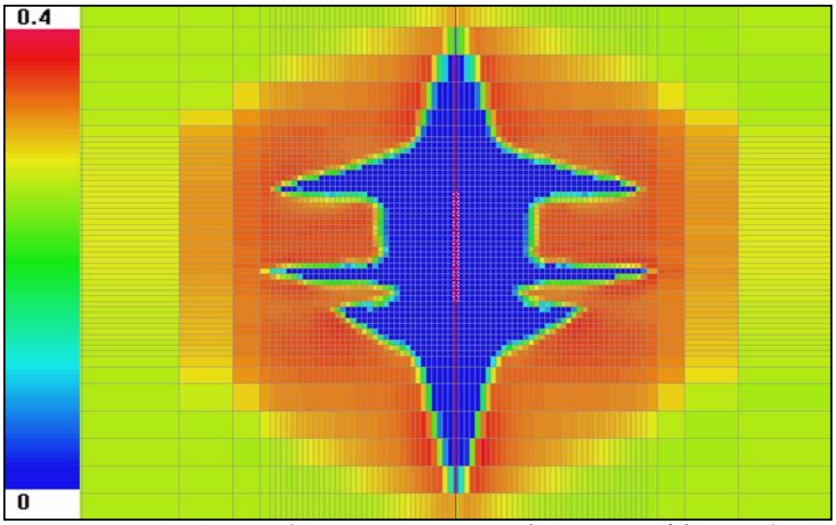

Figure 10.3 S_o distribution after 2 months injection. (Ads=0.40 mg/g). Unconfined.

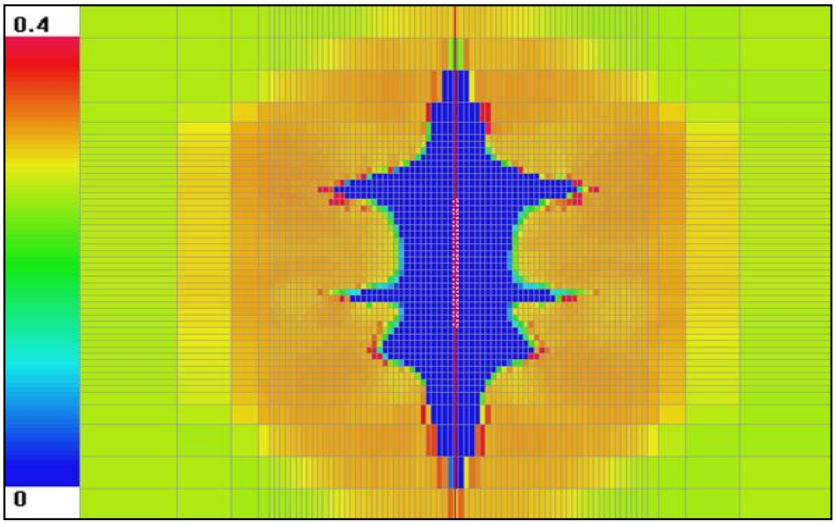

Figure 10.4 S_o distribution after 2 months injection. (Ads=1.6 mg/g). Unconfined.

Figures 10.5 and 10.6 display the water injection rates (blue) and oil production rates (green) for the confined cases (Figure 10.5) and unconfined cases (Figure 10.6) with and without the addition of surfactant. The full lines represent the cases with surfactant and an adsorption value of 0.40 mg/g, the dashed lines represent the cases with surfactant and an adsorption value of 1.6 mg/g, while the dotted lines represent water flooding without surfactant. Water- and oil rates are plotted against time in days.

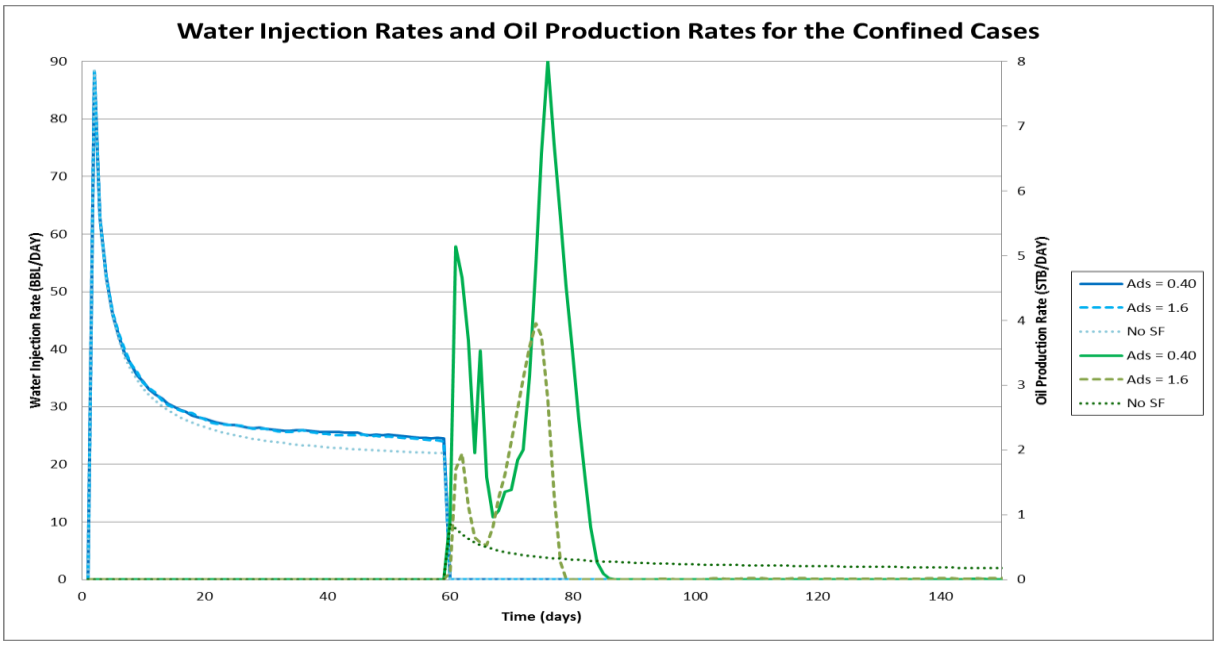

Figure 10.5 Water injection- and oil production rates for confined case with and without surfactant.

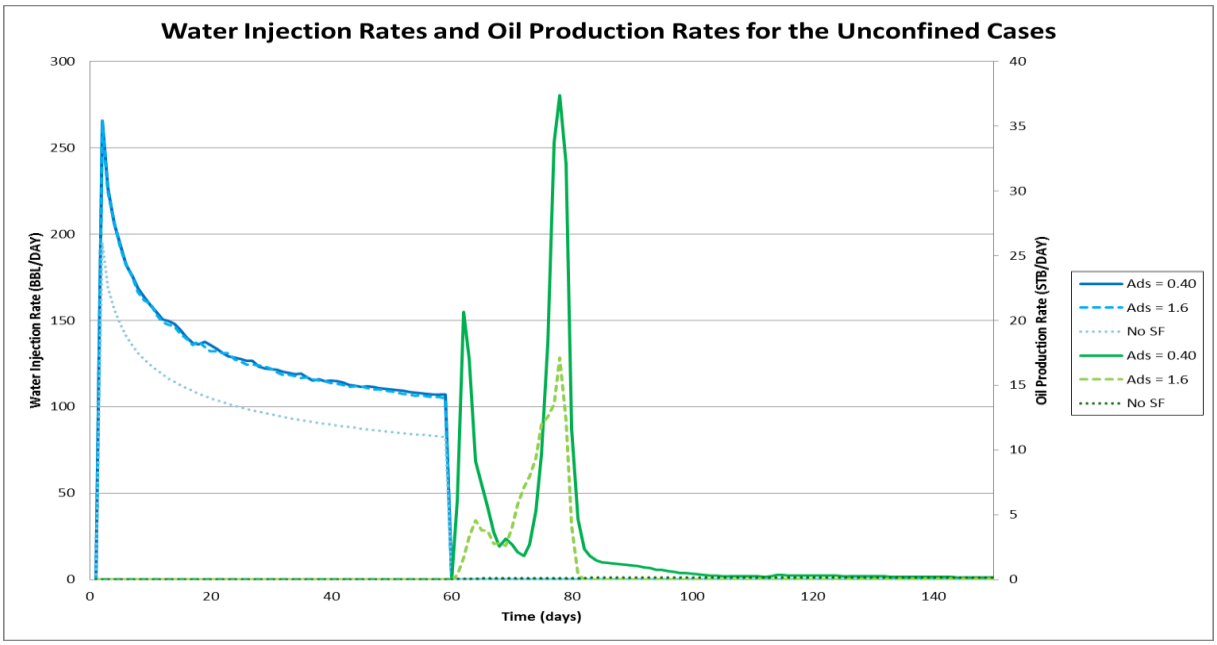

Figure 10.6 Water injection- and oil production rates for unconfined case with and without surfactant.

The same trends are observed for the two cases. Both water injectivity and oil production increased when surfactant is added to the system. The increase was largest for the unconfined case, and injection rates as well as production rates were overall higher. The oil rate increased because the surfactant slug mobilized a new oil bank which was later back produced.

The increase in injectivity can be explained by the behavior of the relative permeability curves. Because the surfactant causes the formation of microemulsions, the surfactant slug has higher viscosity than both oil and water. This would suggest that injectivity should be lower when chemicals are added to the water. The formation of a new oil bank is also a process working against increased injectivity. When the oil saturation increases, the position on the relative permeability curves is moved to the left. This behavior can be seen in Figure 10.7. When the relative permeability to water decreases, so does the effective permeability of water; making it harder to inject. Since this is not the case, a process must be overriding the said effects.

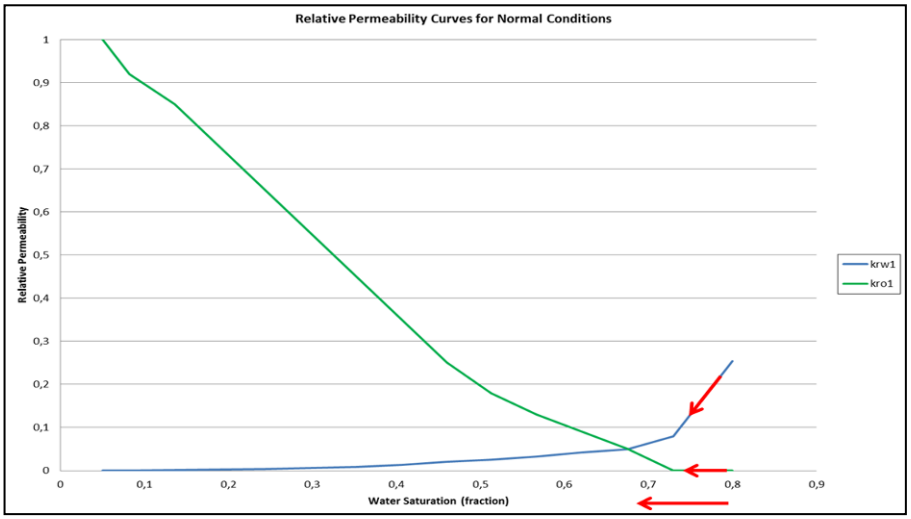

Figure 10.7 Relative permeability and the effect of decreasing water saturation.

When surfactant is added to the system, a new set of relative permeability curves becomes active in the region where the surfactant works. The curves applied during low IFT conditions are presented by dashed lines in Figure 10.8. They show that the residual oil saturation after the chemical flood, $S_{or,CEOR}$, is 0 % as long as the surfactant is active. As the water saturation

increases, the relative permeability to water increases drastically. This explains the increased injectivity observed from the graphs in Figure 10.5 and 10.6.

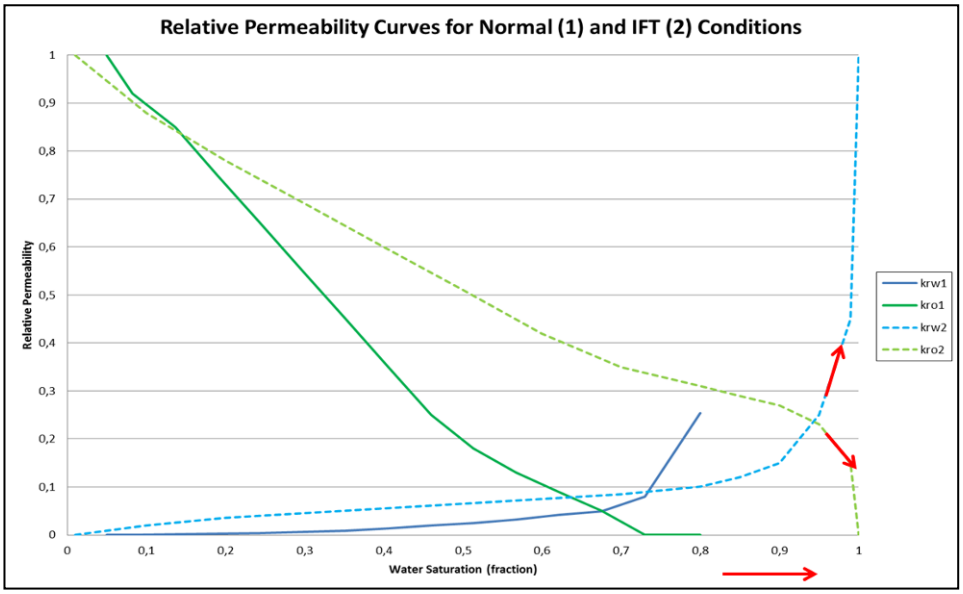

Figure 10.8 Relative permeability and the effect of low IFT conditions on water injectivity.

10.2.3 Residual Oil Distribution

Core experiments done in the Bartlesville laboratory showed less than 10 % residual oil saturation after the core had been flooded with surfactants. Moving forward, a S_{orw} of 9 % will be used for this thesis. However, how the S_{orw} was distributed inside the core was not initially recognized. It was first believed that the entire residual oil saturation was accumulated close to the producer. This concept is illustrated by Figure 10.9. The core in question was later sliced open. Visual inspection then indicated that the oil was evenly distributed throughout the length of the core. This latter concept is illustrated by Figure 10.10.

Figure 10.9 shows the concept being used in the simulation model. The water saturation is 100 %, governed by the low IFT relative permeability curves, as long as the surfactant concentration is high enough for it to be active. When the concentration falls below the critical value, the system switches back to the relative permeability curves for normal conditions. In this particular case, this leaves a residual oil saturation of 30 % in the rest of

the reservoir; summing up to a total of 9 % residual oil. It could be argued that this is a misleading representation of the situation.

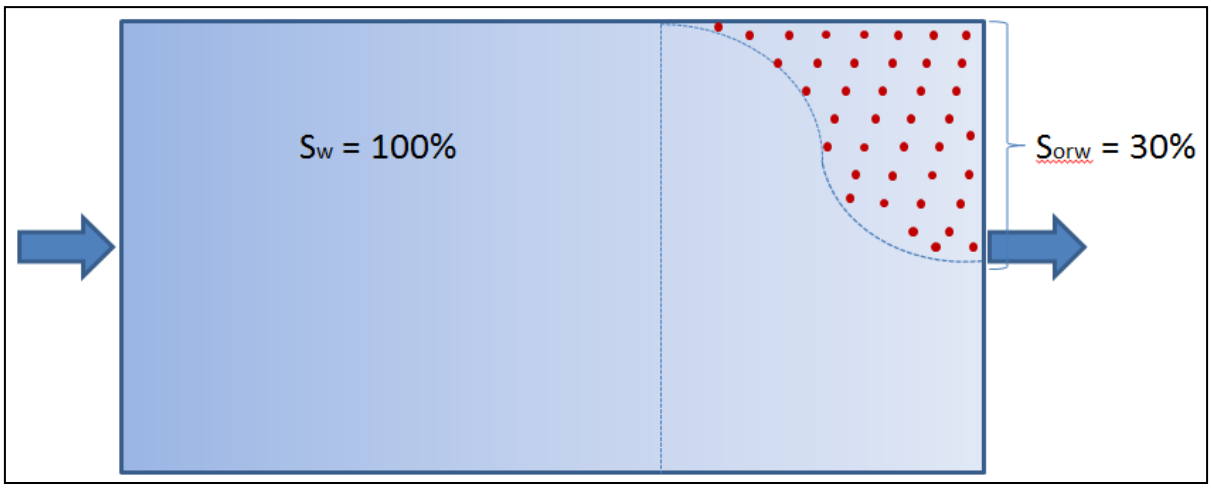

Figure 10.9 Model representation of the fluid distribution inside a core.

Applying this concept would mean that if the injector and producer are just placed close enough, the oil recovery would be 100 % in the whole reservoir. This may look wrong, knowing that there is supposed to be 9 % residual oil left after the surfactant flood. A more reasonable representation of the core can be seen in Figure 10.10.

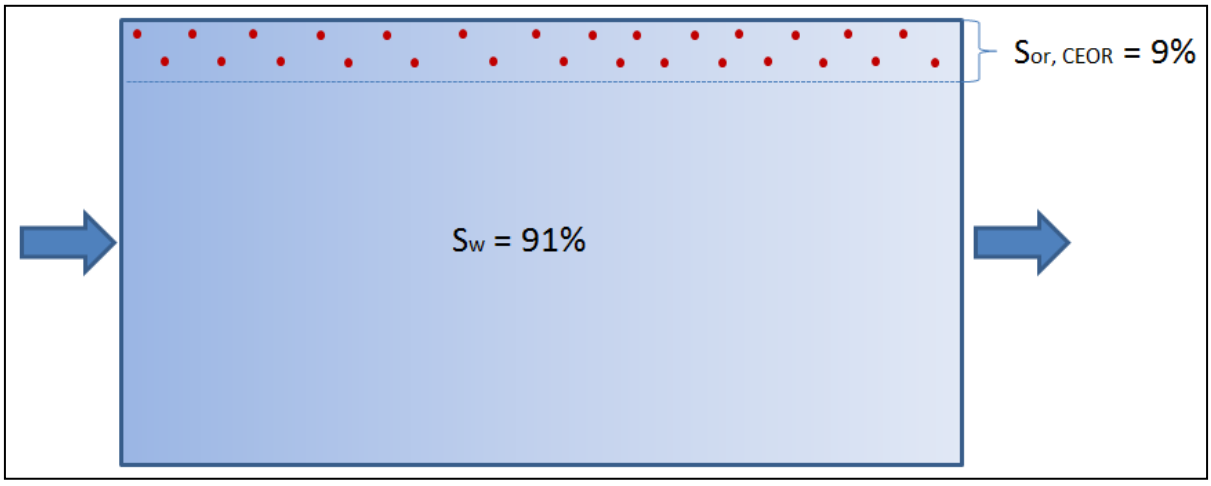

Figure 10.10 Presumably the correct representation of the fluid distribution inside a core.

In this latter figure, the residual oil is spread out uniformly through the entire core. To achieve this, a new set of relative permeability curves for low IFT conditions would need to be implemented. For this new curve the relative permeability to water should reach a maximum of 91 % water saturation. Present limitations in PSim prevent this from being applied to the model. It is currently being worked on by the developers of PSim.

10.3 Surfactant Flooding in a 2D Radial Model

The objective of studying a 2D radial model was to determine the volumes necessary to create an effective SWCTT. The injection scheme is presented in Table 10.1. The middle of the tracer slugs should be displaced 10 feet into the reservoir. This proved to correspond to the end of the slug being placed 12 feet away from the well. The surfactant slug should be displaced 20 feet from the well. Predetermined slug volumes of 0.1 PV for both tracers were to be injected prior to – and after the surfactant slug. In the field, two short shut in periods after the tracer placement would be required for tracer hydrolysis. The tracer in the simulation model does however not react; hence it does not need the shut in period.

A 2D radial model for Ekofisk was created with 200 cells in x-direction (2000 feet) and three layers. Since the model is radial, the volumes of the grid blocks increase exponentially away from the well. A single well, placed in the middle of the model, operated as both injector and producer. The applied salinity gradient ranged between 58 000 ppm and 28 000 ppm. Water viscosity was set to 0.2214, and initial water saturation was 70 %. This implied that the area in question had already been flooded with water. Porosity was 40 % in all layers, permeability in x- and z-direction was 4 md, and transmissibility was 1 in both directions.

Two different values for surfactant adsorption were used for the surfactant concentration of 0.71 %; 0.40 mg/g and 1.6 mg/g. These adsorption values correspond to retention numbers of 0.16% and 0.64% respectively. The values are within the range determined by laboratory core experiments and simulation studies done in Bartlesville, OK.

10.3.1 Flow Scheme to Determine Slug Volumes

A flow scheme for the SWCTT was created based on the core experiments and simulation studies. The pore volume of surfactant needed to reach a distance of 20 feet from the well is highly dependent on the retention number. To determine the effect of adsorption, two scenarios of retention numbers were run.

Since the test zone was confined to a 20 x 20 feet radial interval, one pore volume (PV) can be calculated as;

$$PV = (\pi r^2 h \varphi) \times 0.17811 \frac{bbl}{cu.ft} \quad (10.1)$$

$$PV = (\pi \times (20\ ft)^2 \times 20\ ft \times 0.4\ ) \times 0.17811 \frac{bbl}{cu.ft} = 1790\ bbl$$

Water injection rate was fixed to 35 bbls/day. This rate was based on earlier simulation studies. Table 10.1 shows the schedule for the single well chemical tracer test with 0.40 mg/g adsorption. The bold numbers in the PV column are fixed volumes, and were not altered to get the slugs to the desired distance from the well. The volume of chase water behind the tracer slugs was, however, altered to place the tracer at the right distance. The pore volume of chase water behind the surfactant slug was also fixed. A larger volume of this slug proved to make no difference in placing the surfactant slug further from the well. Adsorption reduced the tracer concentration to ineffective long before the entire PV of placement water had been injected.

Table 10.1 Schedule for the SWCTT (Adsorption = 0.4 mg/g)

Step	Operation	PV	BBLS	DAYS	L res.
Preflush	INJ	**0,50**	895	25,6	
Tracer 1	INJ	**0,10**	179	5,1	12
Placement 1	INJ	0,18	322,2	9,2	
Flowback 1	PROD	0,38	680,2	19,4	
Cleaning	INJ	**0,50**	895	25,6	
SF Slug	INJ	**0,40**	716	20,5	18
Placement SF	INJ	**1,05**	1880	53,7	
Tracer 2	INJ	**0,10**	179	5,1	12
Placement 2	INJ	0,27	483,3	13,8	
Flowback 2	PROD	0,19	340,1	9,7	
Total	**INJ**	3,1	5549	159	
Total	**PROD**	0,6	1020	29	
Total	**INJ&PROD**	3,7	6569	188	

The reservoir was preflushed with 0.5 PV of 35 000 ppm salinity water. The preflush was followed by 0.1 PV of tracer in form of 58 000 ppm salinity water. The tracer was displaced 12 feet from the well by 0.18 PV of 35 000 ppm salinity water. The injector was then switched to a producer for a 0.33 PV back production of the tracer. The next step was a cleaning process by means of injecting 0.5 PV of 35 000 ppm salinity water. This was

followed by the injection of the surfactant slug in 58 000 ppm salinity water. Applying the adsorption value of 0.40 mg/g proved to displace the effective surfactant slug out to a radius of 18 feet. After the placement of the surfactant slug, the second tracer of 0.1 PV was injected. This was displaced by 0.27 PV for the middle of the slug to reach a depth of 10 feet from the well. The injector was again switched to a producer; back producing 0.19 PV.

Using the same volumes and an adsorption value of 1.6 mg/g proved to only displace the surfactant slug to a depth of 13 feet from the well (see appendix). A third scenario with an adsorption value of 0.64 mg/g can also be found in the appendix. The whole process took 6 months to complete.

Figure 10.11 shows the oil saturation (dashed red), water salinity (green) and surfactant concentration partitioned in the water phase (black) plotted against time (days). The oil saturation and water salinity scale is featured on the left hand side, while the scale on the right hand side is for the surfactant concentration.

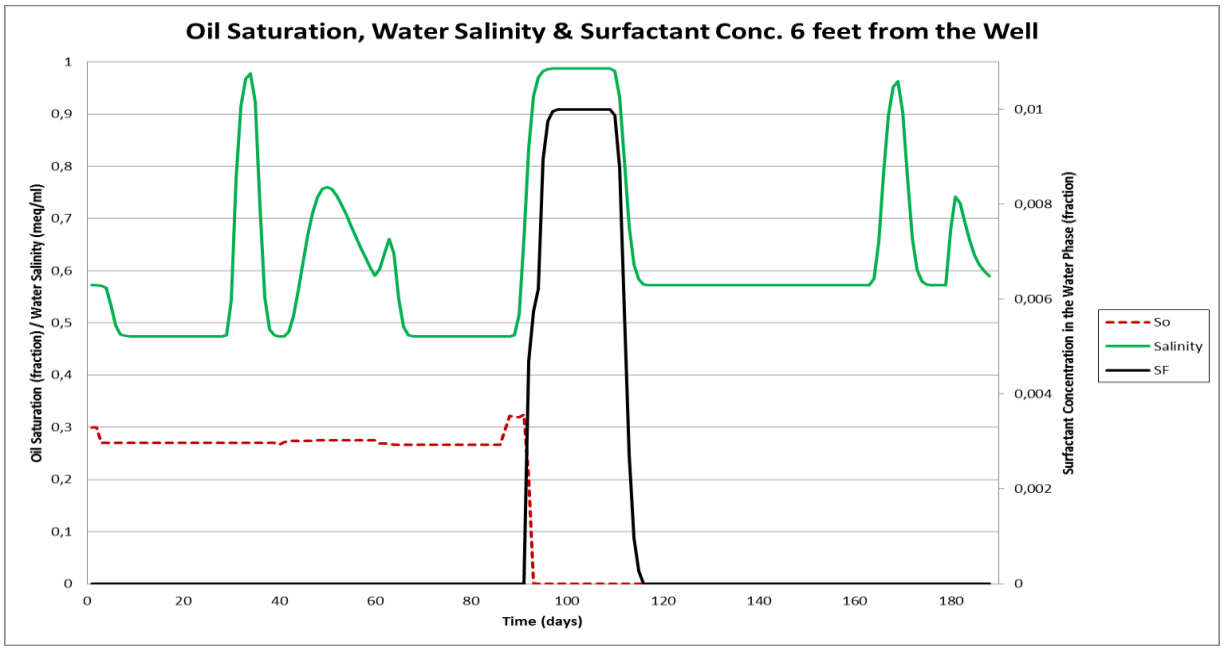

Figure 10.11 S_o, water salinity and SF concentration in the water phase 6 feet from the well. (Adsorption = 0.4 mg/g)

These values were taken 6 feet from the wellbore. The first two green tops represent the concentration of Tracer 1 as it is injected (first top) and back produced (second top). The second tracer is not completely back produced, which is the reason for the second bump at the end of it. The two last green tops represent injection and production of Tracer 2. The

tracer comprises of high salinity water, which was also used for the injection of the surfactant slug. The surfactant concentration top and the high salinity top nearly coincide completely in terms of time. A small oil bank is pushed slightly ahead of the surfactant slug. The oil saturation is immediately reduced to zero as the surfactant in combination with the high salinity water reaches the depth of interest after 90 days.

Figure 10.12 shows the same scenario as Figure 10.11, but at a larger depth from the wellbore. The surfactant slug is much more dispersed at a distance of 16 feet from the well, and the fraction of high concentration surfactant is drastically reduced. It still manages to reach a high enough concentration to effectively reduce the oil saturation to zero around day 120.

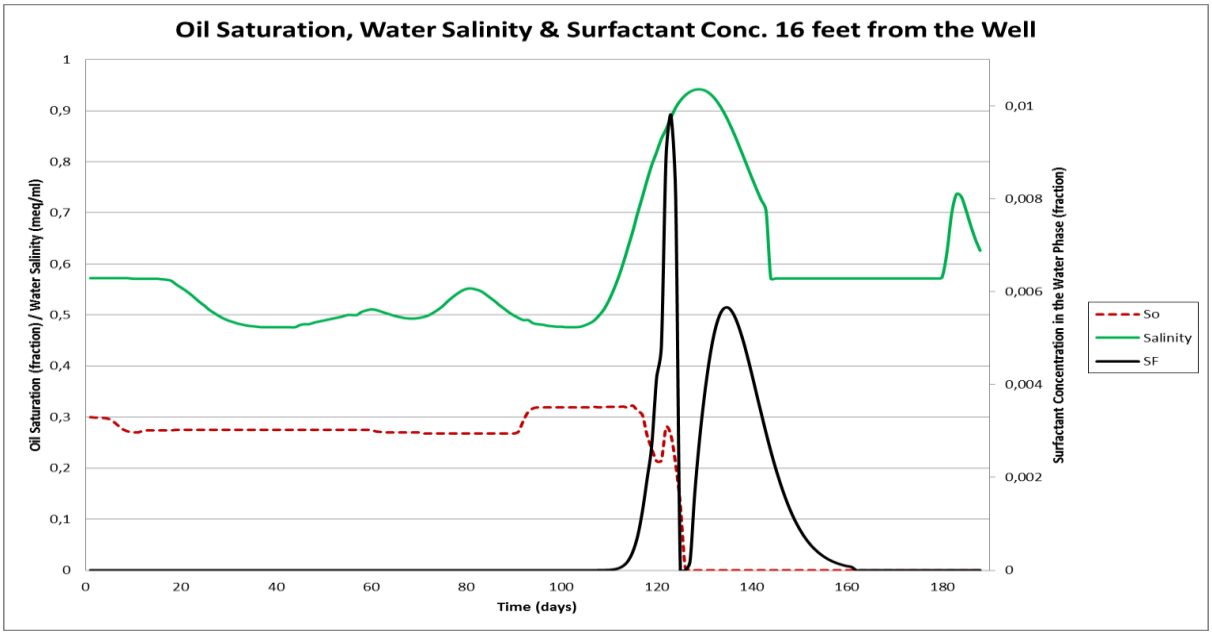

Figure 10.12 S_o, water salinity and SF concentration in the water phase 16 feet from the well. (Adsorption = 0.4 mg/g)

The same type of profiles for adsorption values of 0.64 mg/g and 1.6 mg/g showed the same trends. The surfactant was reduced to a concentration under the critical at distances of 16 feet and 13 feet from the well, respectively.

The resulting back produced tracer curve is presented in Figure 10.13. It shows the traced water fraction plotted against time in days. The first top is for Tracer 1, while the second is for Tracer 2. The second tracer is slightly more dispersed than the first tracer; drawn out from the lower value of the top. This can be linked to the larger volume of chase water needed to displace the second slug to the desired depth.

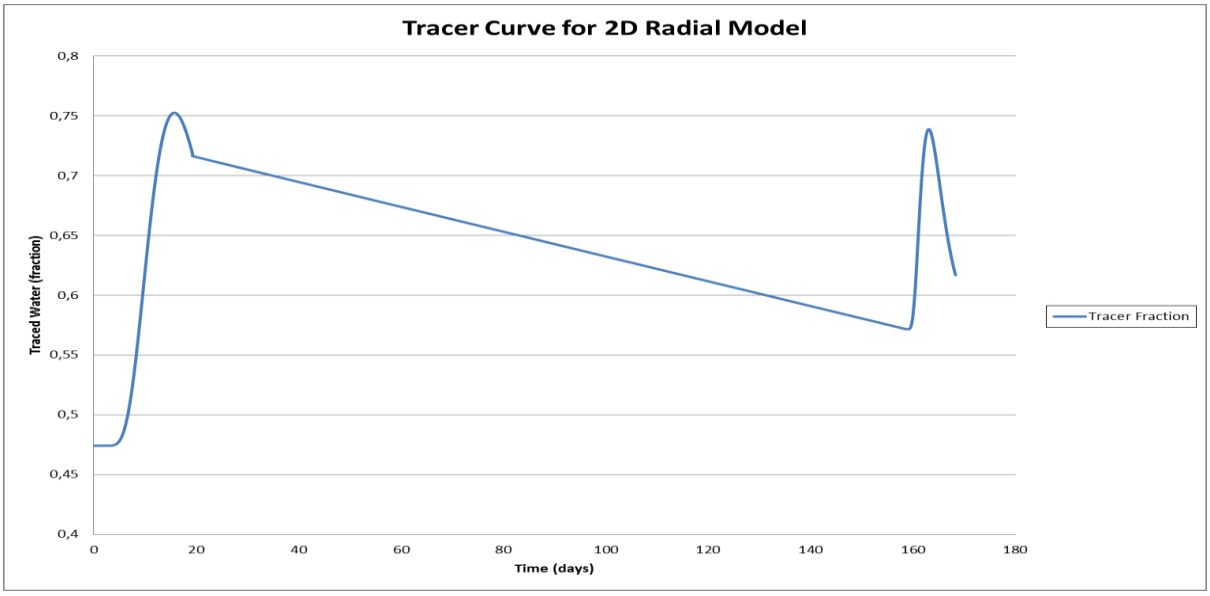

Figure 10.13 Back produced tracer curve for 2D radial model.

11 Conclusion and Discussion

To sum up the findings in this thesis, the following conclusions can be made:

1. The height of the tracer curve top depends on the degree of dispersion near the wellbore. If the tracer slug becomes highly dispersed by water close to the well, the top will reach a lower value than a more concentrated tracer slug.

2. The length and shape of the tracer curve tail depends on the degree of dispersion in the tracer furthest away from the well. A higher degree of dispersion produces a tail with higher traced water fraction than a lower degree of dispersion does.

3. The degree of dispersion increases with increasing heterogeneity, but does not affect the smoothness of the curve.

4. Retention plays a major role in the volume of surfactant needed to design an efficient SWCTT.

5. The surfactant slug becomes increasingly dispersed as it travels further from the well.

6. The surfactant slug reaches a depth of 18 feet with an adsorption of 0.4 mg/g with a surfactant slug of 0.4 PV. A depth of 13 feet is reached with the same volumes and an adsorption value of 1.6 mg/g. The total process takes 6 months.

Dispersion can be explained as the mixing caused by a single-phase fluid moving through a porous medium. In a multiphase system diffusivity refers to the mixing of tracer within the flow path of a given phase, not the mixing of the phases themselves (Miller 2010). The tracer starts out with an abrupt interface, which gradually evolves into an ever-widening transition zone. Across the transition zone the tracer concentration varies between that of the tracer to that of the other liquid (Bear 1972).

Figure 11.1 features two breakthrough curves for one-dimensional flow in a sand column. Relative tracer distribution (ε) on the y-axis is plotted against time (Q_t/U_0), where U_0 is the pore volume of the column and Q_t is the constant discharge rate. The dashed line represents an ideal flow without dispersion. This kind of flow front is called a shock front. The full line represents the actual flow front with dispersion, and is characterized by an S-shaped curve.

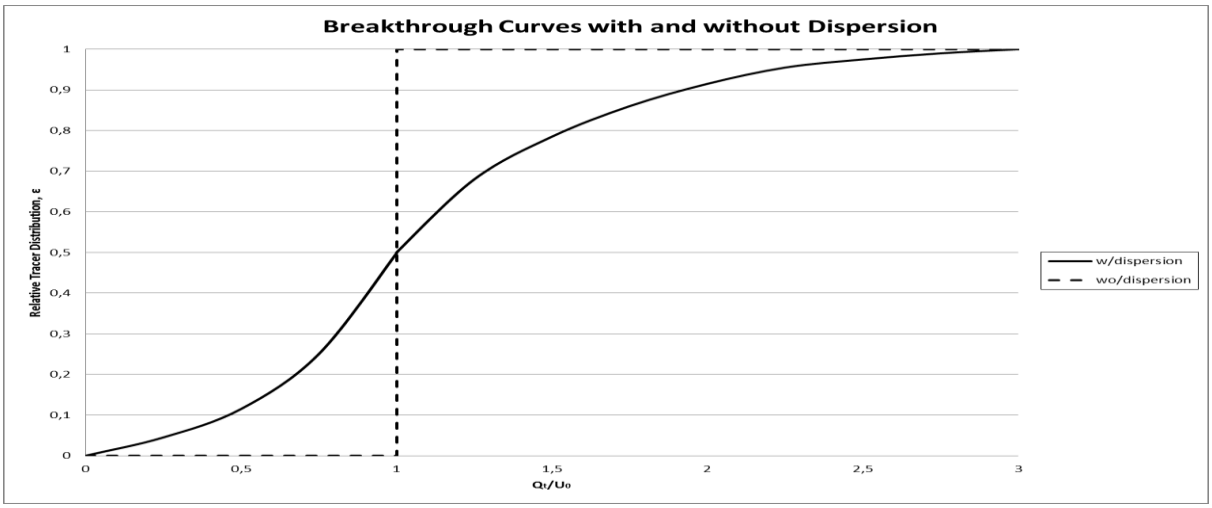

Figure 11.1 Breakthrough curves in a 1D flow in a sand column. After Bear (1972).

The effect of fractures was seen clearly for both the confined and the unconfined test area. As the fracture permeability increased, more tracer bearing water escaped from the test area; reducing the height of the tracer curve tops. The traced water fraction of the tail increased as the fracture permeability increased. These two features indicate a higher degree of dispersion in both ends of the tracer slug as the permeability of the fracture increased. This coincides with the statement from the literature that heterogeneity leads to more dispersion. The increase in dispersion as heterogeneity increased was largest for the confined test area. This may be due to the difference in placement of the fracture for the two cases, or the fact that a smaller area is more sensitive to change.

The result of active wells in the vicinity of the test area was a clear drift in the net fluid flow direction. Based on the tracer curves for this case, the drift caused a high degree of dispersion in both ends of the slug. This effect was most prominent for the rear of the slug. The shape of the curve will also be a function of the drift rate and shut-in time. The tracer response could possibly separate into two tops with a high drift and a long shut-in time.

All the tracer curves presented in this thesis are smooth with a single top. In some cases tracer curve tops with structure are experienced, as can be seen in Figure 11.2.

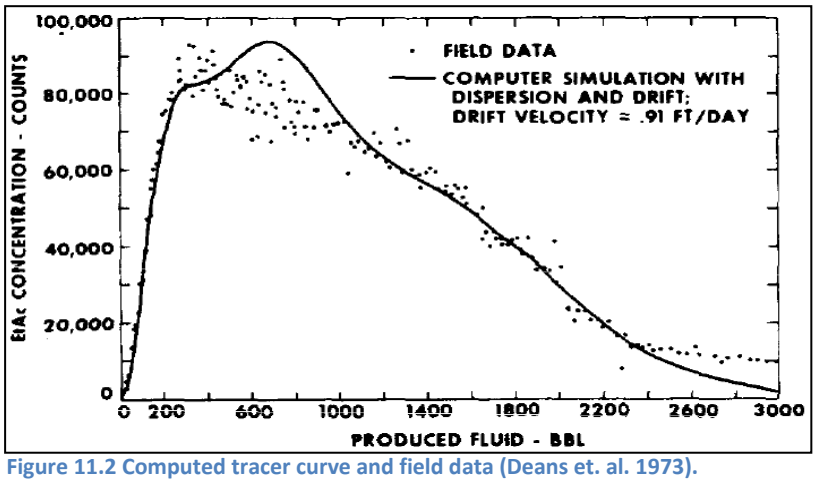

Figure 11.2 Computed tracer curve and field data (Deans et. al. 1973).

This simulation study suggests that reservoir heterogeneity will not produce tracer curves with multiple tops. It should be noted that solution chemistry was not applied in the model, hence it was suggested that multiple tops on tracer curves can be a result of the hydrolysis that takes place either before or after the tracer slug has been displaced to the preferred depth. Hydrolysis of the tracer starts immediately after the tracer comes in contact with water; not only during the shut in period. The shape of the produced tracer profiles is changed by the variations of hydrolysis rate with pH. The reaction velocity of an ester, the hydrolysis rate, is catalyzed by both acids and bases. The rate increases both ways from a pH of 6.5; where the rate is at a minimum (Deans & Ghosh 1994).

Acetic acid is produced during hydrolysis. If the rock does not have enough buffer capacity to absorb the acid, the environment will become increasingly acidic; hence increasing the hydrolysis rate. A consequence of the pH rate dependence of ester hydrolysis is that transit-generated tracer may dominate the response; making the test insensitive to oil saturation. It is desired that most of the tracer undergoes hydrolysis during the shut in period.

For the SWCTT to be applicable on Ekofisk, the time to complete the test needs to be reduced. It lasts for 6 months as it is presented here. The preferred time is maximum 1-2 months. More studies on injection rate and adsorption need to be performed. If injection is not substantially higher than the 35 bbl/day presented in this thesis, the depth at which the slugs are to be displaced needs to be reduced.

11.1 Future Work and Limitations

Future work involves finding the final optimum surfactant formulation for Ekofisk chalk with regards to environmental regulations, retention values, cost and availability. Ekofisk chalk cores are being prepared for surfactant flooding as this thesis is being written. When the results from these test become available, a more accurate model can be made with respect to recovery and adsorption.

The appropriate flow scheme and necessary volumes need to be made clear. The volumes presented in this thesis are clearly too large. This could indicate that the chosen injection rate is too low. Further studies need to be done regarding the injection rate that can be expected for the appropriate well. The desired time for the entire SWCTT is 1 – 2 months. Shorter displacement lengths of the slugs should be considered if the injection rates turn out to be within the range presented in this thesis.

A location for the SWCTT needs to be chosen. The two main options currently being considered are the water flooded areas or the unflooded areas of Ekofisk South. An ideal test zone for the SWCTT should be thin and isolated with matrix flow. In reality there is no way to assure that the chosen zone is ideal, and flow out of the zone is likely to occur. If an existing well or a new well is to be drilled, also needs to be determined.

A choice also needs to be made with regards to performing a secondary or tertiary surfactant flood. This choice is clearly co-dependent on the choice for well location. Secondary recovery could be performed in the unflooded section of the reservoir, while tertiary could be performed in the flooded areas.

Figure 11.3 shows the steps in a screening process for a general EOR technique. The process uncertainty decreases as more steps are performed. The effort and investment also increases significantly with each step in the process.

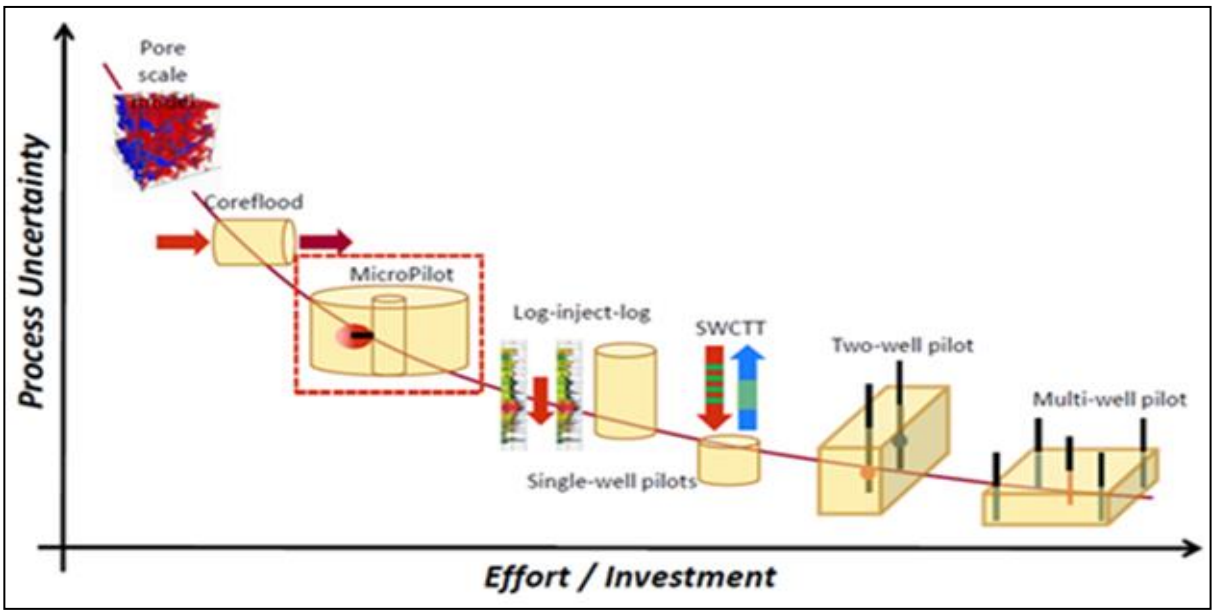

Figure 11.3 Illustration of a flow chart for an EOR screening process (Schlumberger 2014).

The natural next step after the Ekofisk SWCTT would be a second SWCTT, a two-well pilot or a multi well pilot. The two latter pilot tests are very costly. They take a lot of time; both the planning, execution and the time it takes to see the response. The main goal of a two-well pilot or a multi well pilot is to estimate the impact of heterogeneity.

A large amount of limitations are associated with the practical field implementation of a surfactant flood. A great quantity of equipment and logistics is involved in the process. One particular limitation is the logistics around finding a practical way to separate the emulsions formed during a surfactant flood. If the water is to become clean enough to be discarded back into the sea, these emulsions need to be efficiently handled.

12 References

Abe, M., Schechter, D., Schechter, R.S., Wade, W.H., Weerasooriya, U. and Yiv, S. 1986. *Microemulsion with Branched Tail Polyoxyethelene Sulfonate Surfactants.* Journal of Colloid and Interface Science 114 (2): 342-356.

Ahmed, T. and Meehan, D.N. 2012. *Chapter 6 – Introduction to Enhanced Oil Recovery.* In: Ahmed, T. and Meehan, D. N. (eds.) Advanced Reservoir Management and Engineering (Second Edition). Boston: Gulf Professional Publishing.

Ashraf, A., Hadia, N., Torsæter, O. and Tweheyo, M.T. 2010. *Laboratory Investigation of Low Salinity Waterflooding as Secondary Recovery Process: Effect of Wettability*. Paper SPE 129012 presented at the SPE Oil and Gas India Conference and Exhibition, Mumbai, India, 20-22 January 2010.

Austad, T. 2013. *"Smart Water" Flooding in Carbonates and Sandstones: A New Chemical Understanding of the EOR-potential*. UiS, Norway. Presented at the FORCE education Seminar NPD, Nov. 6-7., 2013.

Austad, T., Strand, S., Madland, M. V., Puntervold, T. and Korsnes, R. I. 2008. *Seawater in Chalk: An EOR and Compaction Fluid.* Paper IPTC 11370/ SPE 118431 presented at the 2007 International Petroleum Technology Conference, Dubai, 4-6 December.

Austad, T. and Milter, J. 1997. *Spontaneous Imbibition of Water into Low Permeable Chalk at Different Wettabilities Using Surfactants*. Paper SPE 37236 presented at the International Symposium on Oilfield Chemistry, Houston, TX, 18-21 February 1997.

Awan, A.R., Teigland, R. and Kleppe, J. 2008. *A Survey of North Sea Enhanced-Oil-Recovery Projects Initiated During the Years 1975 to 2005*. Paper SPE 99546 presented at the 2006 SPE/DOE Symposium on Improved Oil Recovery, Tulsa 22-26 April.

Bear, J. 1972. *Dynamics of Fluids in Porous Media*: American Elsevier Science Publishing Co., Inc. New York.

Brown, L.R., Vadie, A.A. and Stephens, O.J. 2002. *Slowing Production Decline and Extending the Economic Life of an Oil Field: New MEOR Technology*. Paper SPE 75355 presented at the 2000 SPE/DOE Improved Oil Recovery Symposium, Tulsa, 3–5 April.

Boyce, B.M. 1972. *Ekofisk Phase 1 Production Looks Good*, Oil & Gas J. (June 12, 1972)

Bryant, S.L. and Lockhart, T.P. 2002. *Reservoir Engineering Analysis of Microbial Enhanced Oil Recovery*. Paper SPE 79719 presented at the 2000 SPE Annual Technical Conference and Exhibition, Dallas, 1–4 October.

Cinar, Y. Lectures in PTRL 4012/5012, *Enhanced oil and gas recovery*. UNSW. Spring 2013.

ConocoPhillips n.d. *The Greater Ekofisk Area*. Available at: www.conocophillips.no. [26 March 2014].

COPNO Internal, Internal Database at ConocoPhillips Norwegian Business Unit. [January-June 2014].

Cuiec, L., Bourbiaux, B. and Kalaydjian, F. 1994. *Oil Recovery by Imbibition in Low-Permeability Chalk*. Paper SPE 20259 presented at the 1990 SPE/DOE Symposium on Enhanced Oil Recovery in Tulsa, April 22-25.

Deans, H.A., Tomich, J.F., Dalton, R.L. and Shallenberger, L.K. 1973. Single-Well Tracer Method To Measure Residual Oil Saturation. Paper SPE 3192 presented at SPE Symposium on Improved Oil Recovery, Tulsa, April 16 – 19, 1972.

Deans, H.A. and Ghosh, R. 1994. *pH and Reaction Rate Changes During Single-Well Chemical Tracer Tests*. Paper SPE/DOE 27801 presented at the SPE/DOE Ninth Symposium on Improved Oil Recovery, Tulsa 17 – 20 April, 1994.

Elshahawi, H., Fathy, K. and Hiekal, S. 1999. *Capillary Pressure and Rock Wettability Effects on Wireline Formation Tester Measurements.* Paper SPE 56712 presented at the 1999 SPE Technical Conference and Exhibition held in Houston, Texas, 3-6 October 1999.

Ersland, G., Ferno, M. A., Graue, A., Baldwin, B.A. and Stevens, J. 2010. *Complementary imaging of oil recovery mechanisms in fractured reservoirs.* Chemical Engineering Journal, 158, 32-38.

FORCE Report 2011*, Assessment of Environmental Impact from EOR Chemicals for the Norwegian Continental Shelf*, Available from: www.force.org. [25 February 2014].

Grigg, R.B. and Mikhalin, A.A. 2007. *Effects of Flow Conditions and Surfactant Availability on Adsorption*. Paper SPE 106205 presented at the 2007 SPE International Symposium on Oilfield Chemistry, Houston, Tx, 28 February – 2 March.

Hallenbeck, L.D., Sylte, J.E., Ebbs, D.J. and Thomas, L.K. 1991. *Implementation of the Ekofisk Field Waterflood.* Paper SPE 19838 presented at the 1989 SPE Annual Technical Conference and Exhibition, San Antonio.

Healy, R.N. and Reed, R.L. 1974. *Physiochemical Aspects of Microemulsion Flooding*. Paper SPE 4583 presented at the SPE-AIME 48th Annual Fall Meeting, Las Vegas, Nev., Sept. 30 – Oct. 3, 1973.

Hearn, C.L. 1971. *Simulation of Stratified Waterflooding by Pseudo Relative Permeability Curves*. Paper SPE 2929 presented at SPE 45th Annual Fall Meeting, Houston, Oct. 4 – 7, 1970 and at SPE Petroleum Technology Symposium, Hobbs, Oct. 29 - 30, 1970.

Hermansen, H., Landa, G. H., Sylte, J. E. and Thomas, L. K. 2000. *Experiences after 10 years of waterflooding the Ekofisk Field, Norway*. Journal of Petroleum Science and Engineering, 26, 11-18.

Hirasaki, G.J., Miller, C.A. and Puerto, M. 2011. *Recent Advances in Surfactant EOR*. Paper SPE 115386 presented at the SPE Annual Technical Conference and Exhibition, Denver, 21-24 September 2008.

Horikx, J.T., Timmermans, P., Daudin, R., O`Neill, N. and Sorriaux, F. M. 2013. *A Specific Way of Assessing Target Recovery Factor (Chalk Oil Fields).* Paper IPTC 16925 presented at the 2013 International Petroleum Technology Conference, Beijing, China, 26-28 March.

Huseby, O.K., Sagen, J. & Dugstad, O. 2012. *Single Well Chemical Tracer Tests – Fast and Correct Simulations.* Paper SPE 155608 presented at the SPE EOR Conference at Oil and Gas West Asia held in Muscat, Oman, 16-18 April 2012.

Jensen, T.B., Harpole, K. J. and Østhus, A. 2000. *EOR Screening for Ekofisk*.Paper SPE 65124 presented at the SPE European Conference held in Paris, France, 24-25 October 2000.

Lake, L.W. 1987. *Chemical Flooding* (1987 PEH Chapter 47) U. of Texas 1987-47-PEH 1987. Society of Petroleum Engineers PEH SPEBOOK.

Lake, L.W. 1989. *Enhanced Oil Recovery*. Englewood Cliffs, New Jersey: Prentice Hall.

Levitt, D.B., Jackson, A.C., Heinson, C., Britton, L.N., Malik, T., Dwarakanath, V. and Pope, G.A. 2009. *Identification and Evaluation of High-Performance EOR Surfactants*. Paper SPE 100089 presented at the SPE/DOE Symposium on Improved Oil Recovery, Tulsa 22-26 April 2006.

Miljødirektoratet 2013, *Olje og Gass*. Available from: http://www.miljostatus.no/Tema/Hav-og-kyst/Olje-og-gass. [25 February 2014].

Miller, M. 2010. Naturally Fractured Reservoir Engineering Course Material. HOT course held in Vienna, Austria, Sept. 27 – Oct. 1, 2010.

Morrow, N. and Buckley, J. 2011. *Improved Oil Recovery by Low-Salinity Waterflooding*. Paper SPE 129421. Distinguished Author Series.

Morrow, N.R. and Mason, G. 2001. *Recovery of Oil by Spontaneous Imbibition*. Current Opinion in Colloid & Interface Science, 6, 321-337.

Nelson, R.C., Lawson, J.B., Thigpen, D.R. and Stegemeier, G.L. 1984. *Cosurfactant-Enhanced Alkaline Flooding.* Paper SPE 12672 presented at the SPE Enhanced Oil Recovery Symposium, Tulsa, 15-18 April.

Newman, G.H. 1983. *The Effect of Water chemistry on the Laboratory Compression and Permeability Characteristics of Some North Sea Chalks*. Paper SPE 10203 presented at the 1981 SPE Annual Technical Conference and Exhibition, San Antonio, Oct. 5-7.

NPD, Norwegian Petroleum Directorate. Available from: www.npd.no. [19 February].

Robertson, S.D. 1988. *An Empirical Model for Microemulsion Phase Behavior*. Paper SPE 14909 presented at the 1986 SPE Symposium on Enhanced Oil Recovery in Tulsa, April 20-23.

Saud, S.A. and Abdulaziz, A.A. 1998. Factors affecting pseudo relative permeability curves. Journal of Petroleum Science and Engineering, Volume 21, Issue 3 – 4, [249-261].

Schlumberger, 2014. Available from: www.slb.com. [3 June 2014].

Sheng, J.J. 2013. *Chapter 12 – Surfactant Enhanced Oil Recovery in Carbonate Reservoirs*. In: Sheng, J.J. (ed.) Enhanced Oil Recovery. Field case studies. Boston: Gulf Professional Publishing.

Sheng, J.J. 2012. *Synergistic Mechanisms of ASP Flooding*. Available from: http://www.upstreampumping.com/article/production/synergistic-mechanisms-asp-flooding. [16 November 2013].

Sheng, J.J. 2011. *Chapter 7 – Surfactant Flooding*. In: Sheng, J.J. (ed.) Modern Chemical Enhanced Oil Recovery. Boston: Gulf Professional Publishing.

Siggel, L., Santa, M., Hansch, M, Nowak, M., Ranft, M., Weiss, H., Hanjal, D., Schreiner, E., Oetter, G. and Tinsley, J. 2012. *A New Class of Viscoelastic Surfactants for Enhanced Oil Recovery.* Paper SPE 153969 presented at the Eighteenth SPE Improved Oil Recovery Symposium held in Tulsa, Oklahoma, USA, 14-18 April 2012.

Skauge, A. 2013*. EOR-Introduction*. Presented at the FORCE – EOR Competence Building Seminar, 6-7 November, Stavanger, Norway. Available from: www.force.og.[24 February].

Skrettingland, K., Holt, T., Tweheyo, M. T. and Skjevrak, I. 2011. *Snorre Low Salinity Water Injection –Core Flooding and Single Well Field Pilot*. Paper SPE 129877, SPE Reservoir Evaluation & Engineering, Vol 14, No. 2, pp. 182-192, 2011.

Solairaj, S., Britton, C., Kim, D.H., Weerasooriya, U. and Pope, G. A. 2012. *Measurement and Analysis of Surfactant Retention*. Paper SPE 154247 presented at the Eighteenth SPE Improved Recovery Symposium, Tulsa, Oklahoma, USA, 14-18 April 2012.

Spinler, E.A. and Baldwin, B.A. 2000. *Surfactant Induced Wettability Alteration in Porous Media*. In: L.L. Schramm (Editor), Surfactant Fundamental and Application in the Petroleum Industry. Cambridge University Press, pp. 159-202.

SSB 2014, *Oil and gas activities, production, Q4 2013*. Statistics Norway. Available from: www.ssb.no. [15 May 2014].

Sulak, R.M. 1990. *Ekofisk Field: the first twenty years*. Paper SPE 20773 presented at the 1990 SPE Annual Technical Conference, New Orleans, September 23-26.

Surkalo, H. 1990. *Enhanced Alkaline Flooding*. Paper SPE 19896. Technology Today Series.

Taber, J.J., Martin, F.D. and Seright, R.S. 1997. *EOR Screening Criteria Revisited - Part 1: Introduction to Screening Criteria and Enhanced Recovery Field Projects*. Paper SPE 35385 presented at the 1996 SPE/DOE Improved Oil Recovery Symposium, Tulsa, Oklahoma, 21-24 April.

Tiab, D. and Donaldson, E.C. 2012. *Chapter 5 – Capillary Pressure*. Petrophysics (Third Edition). Boston: Gulf Professional Publishing.

Van den Bark, E. and Thomas, O.D. 1980. *Ekofisk: First of the Giant Oil Fields in Western Europe*. Giant Oil and Gas Fields of the Decade, AAPG, Tulsa (1980) Memoir 30, 195-224.

Wang, J., Dong, M. and Arhuoma, M. 2010. *Experimental and Numerical Study of Improving Heavy Oil Recovery by Alkaline Flooding in Sandpacks*. Paper SPE 134248 presented at the 9th Canadian International Petroleum Conference June 17–19, 2008, Calgary, Alberta.

Warren, J.E. and Root, P.J. 1963. *The Behavior of Naturally Fractured Reservoirs*. Paper SPE 426 presented at the Fall Meeting of the Society of Petroleum Engineers Oct. 7-10, 1962, Los Angeles. Pittsburgh: Gulf Research & Development Co.

Winsor, P.A 1954. *Solvent Properties of Amphiphilic Compounds*. London: Butterworth`s Scientific Publications.

Zahid, A., Stenby, E.H. and Shapiro, A.A. 2010. *Improved Oil Recovery in Chalk: Wettability Alteration or Something Else?* Paper SPE 131300 presented at the SPE EUROPEC/EAGE Annual Conference and Exhibition held in Barcelona, Spain, 14-17 June 2010.

Zhang, R. and Somasundaran, P. 2006. *Advances in Adsorption of Surfactants and their Mixtures at Solid/Solution Interfaces*. Elsevier: Advances in Colloid and Interface Science.

Zolotukhin, A.B. and Ursin, J. 2000. *Introduction to Petroleum Reservoir Engineering*. Høyskoleforlaget, Norwegian Academic Press.

Appendices

Flow Schemes at Different Adsorption Values

A.X Schedule for the SWCTT (Adsorption = 1.6 mg/g)

Step	Operation	PV	BBLS	DAYS	L res.
Preflush	INJ	**0,50**	895	25,6	
Tracer 1	INJ	**0,10**	179	5,1	12
Placement 1	INJ	0,18	322,2	9,2	
Flowback 1	PROD	0,38	680,2	19,4	
Cleaning	INJ	**0,50**	895	25,6	
SF Slug	INJ	**0,40**	716	20,5	13
Placement SF	INJ	**1,05**	1880	53,7	
Tracer 2	INJ	**0,10**	179	5,1	12
Placement 2	INJ	0,27	483,3	13,8	
Flowback 2	PROD	0,19	340,1	9,7	
Total	**INJ**	3,1	5549	159	
Total	**PROD**	0,6	1020	29	
Total	**INJ&PROD**	3,7	6569	188	

A.X Schedule for the SWCTT (Adsorption = 0.64 mg/g)

Step	Operation	PV	BBLS	DAYS	L res.
Preflush	INJ	**0,50**	895	25,6	
Tracer 1	INJ	**0,10**	179	5,1	12
Placement 1	INJ	0,18	322,2	9,2	
Flowback 1	PROD	0,38	680,2	19,4	
Cleaning	INJ	**0,50**	895	25,6	
SF Slug	INJ	**0,40**	716	20,5	16
Placement SF	INJ	**1,05**	1880	53,7	
Tracer 2	INJ	**0,10**	179	5,1	12
Placement 2	INJ	0,27	483,3	13,8	
Flowback 2	PROD	0,19	340,1	9,7	
Total	**INJ**	3,1	5549	159	
Total	**PROD**	0,6	1020	29	
Total	**INJ&PROD**	3,7	6569	188	

PSim Data Input File

```
TITLE
             Ekofisk sector model 2 from south Ekofisk (P50 model)
             Horizontal wells at 4000 bbl/day injection rate
             Surfactant adsorption = 0.55 mg/g at surf conc. 0.71%
             With salinity gradient: 80,000 ppm, 50,000 ppm, and 35,000 ppm
ENDTITLE

C ================================================================================
GRID 112  1  234
FIELDNAME Ekofisk sector 1
C ================================================================================

KEYWORD
DATE 1 1 1986

HISTORYFILE
C11_R_2.history

C ================================================================================
C      ===   GENERAL FLUID PROPERTIES
C ================================================================================

C ------------------------------------------------------
C                    Water and rock properties
C ------------------------------------------------------
MISC  1.07  3.4e-006  59.554  0.2214  1e-005  14.7        ! Bwi  cw  denw  visw  Cr
Pref

C ---------------------------------------
C    Standard pressure and temperature
C ---------------------------------------
PSTD 14.7
TSTD 60

C ============================
C     Fluid EOS Properties
C ============================
PVTEOS
268.
CPT       MW      TC      PC      AC     ZCRIT   SHIFT   PCHOR   OMEGA    OMEGB
OMEGAS   OMEGBS
C1N2      16.12  341.7  665.8  .0119   .3594  -.15920    76.8 .5051080 .0777805
.5051080 .0777805
C2C3      35.70  596.6  703.6  .1257   .3290  -.10032   119.1 .4303043 .0796165
.4303043 .0796165
C4F1      79.48  908.4  468.9  .2619   .2361  -.00372   251.1 .4262349 .0749099
.4262349 .0749099
F2F3     180.89 1273.6  289.6  .5357   .2292   .11424   520.2 .4415066 .0758590
.4415066 .0758590
F4F5     408.17 1609.2  159.6 1.0469   .2460   .17074   944.4 .4382145 .0766369
.4382145 .0766369
BIN             Interaction Parameters
.00988    .01270    .02670    .13800
.01050    .01180    .01180
.00000    .00000
.00000

HEATBALANCE !    3
C cpw           rocpf            k                tginj       twinj    rowinj
slope_bw0           res_ti
1.                  37.2             30.                 268.       268.      62.43
-.000336             268.
5.00000E-01  5.00000E-01  5.00000E-01  5.00000E-01  5.00000E-01
53.96        1.308
59           1.216
```

```
68          1.076
77          0.962
86          0.867
95          0.787
104         0.720
113         0.662
122         0.613
131         0.571
140         0.535
149         0.504
158         0.477
167         0.454
176         0.435
185         0.418
194         0.405
203         0.394
212         0.385
221         0.378
230         0.373
268         0.372
C ============================================================================
C      ===   REL PERM AND CAP PRESSURE
C ============================================================================

!--------------------------------
!  Water flood relative perm
!--------------------------------
SWT 1
0.05        0     1           0 0
0.082       0     0.92        0 0
0.136       0.0012      0.85        0 0
0.19        0.0025      0.75        0 0
0.244       0.0042      0.65        0 0
0.298       0.006 0.55        0 0
0.352       0.009 0.45        0 0
0.406       0.013 0.35        0 0
0.46        0.02  0.25        0 0
0.513       0.025 0.18        0 0
0.567       0.032 0.13        0 0
0.621       0.042 0.09        0 0
0.675       0.049 0.05        0 0
0.73        0.08  0.000       0 0
0.8         0.254 0           0 0

SGT 1
SGTR 0.25
0     0                 1                 0             0
0.04        0.013               0.86        0           0
0.081       0.025               0.71        0           0
0.121       0.04                0.57        0           0
0.161       0.055               0.45        0           0
0.2         0.06                0.34        0           0
0.242 0.07175     0.26        0           0
0.282       0.0741              0.195       0           0
0.323       0.0773              0.156538    0           0
0.363       0.0789              0.134267    0           0
0.404       0.0813              0.111995    0           0
0.64  0.08765     0           0                   0     0
0.74        1           0                 0           0
0.95        1           0                 0           0

!--------------------------------
!   Relative perm at low IFT
!--------------------------------

SWT 2
0.01  0.00  1.00  0.00  0.00
0.10  0.10  0.90  0.00  0.00
```

```
0.20   0.20   0.80   0.00   0.00
0.30   0.30   0.70   0.00   0.00
0.40   0.40   0.60   0.00   0.00
0.50   0.50   0.50   0.00   0.00
0.60   0.60   0.40   0.00   0.00
0.70   0.70   0.30   0.00   0.00
0.80   0.80   0.20   0.00   0.00
0.90   0.90   0.10   0.00   0.00
0.99   1.00   0.00   0.00   0.00

SGT 2
SGTR 0.00
0.00      0.00       1.00       0.00    0.00
0.10      0.10       0.90       0.00    0.00
0.20      0.20       0.80       0.00    0.00
0.30      0.30       0.70       0.00    0.00
0.40      0.40       0.60       0.00    0.00
0.50      0.50       0.50       0.00    0.00
0.60      0.60       0.40       0.00    0.00
0.70      0.70       0.30       0.00    0.00
0.80      0.80       0.20       0.00    0.00
0.90      0.90       0.10       0.00    0.00
0.99      1.00       0.00       0.00    0.00

SWT 3
0.05         0            1            300          300
0.082        0            0.905        170          170
0.136        0.0012       0.757        100          100
0.19         0.0025       0.624        80           80
0.244        0.0042       0.504        72           72
0.298        0.007        0.398        66           66
0.352        0.013        0.305        64           64
0.406        0.023        0.225        61           61
0.46         0.039        0.158        58           58
0.513        0.061        0.104        56           56
0.567        0.092        0.061        54           54
0.621        0.133        0.03         52           52
0.675        0.186        0.011        50           50
0.73         0.254        0                         0
0.8          0.254        0            -300         -300


SGT 3
SGTR 0.25
0                  0                  1                  0         0
0.04               0.013        0.86                 0         0
0.081              0.025        0.71                 0         0
0.121              0.04               0.57           0         0
0.161              0.055              0.45           0         0
0.202              0.06               0.34           0         0
0.242        0.07175            0.26                 0         0
0.282              0.0741             0.195          0         0
0.323              0.0773             0.156538       0         0
0.363              0.0789             0.134267       0         0
0.404        0.0813             0.111995             0         0
0.64         0.08765            0                    0         0
0.74         1                  0                    0         0
0.95         1                  0                    0         0

C ========================================================================
C ===  Read PETREL EXPORTED GRID AND GRID PROPERTIES
C ========================================================================
C grid
DELX XVAR
      18*70.0
      35
      18
```

```
       10
       5
       2
       70*1
       2
       5
       10
       18
       35
       14*70.0

DELY CON
       70.0

DEPTH LAYER
       525*9373

THICKNESS ZVAR
       139*5
       3
       2
       40*1
       2
       3
       51*5

POROS ZVAR
       27*0.2
       3*0.3
       4*0.34
       6*0.38
       4*0.43
       3*0.4
       8*0.35
       3*0.4
       4*0.35
       48*0.4
       2*0.35
       2*0.3
       0.2
       6*0.23
       2*0.15
       5*0.35
       4*0.4
       7*0.35
       27*0.35
       17*0.4
       2*0.4
       8*0.35
       3*0.25
       3*0.3
       16*0.25
       6*0.3
       8*0.25
       5*0.2

KX ZVAR
       27*0.001
       1*0.1
       8*13
       8*15
       40*17
       4*46
       6*21
       20*7
       9*100
       34*13
       46*13
```

```
       8*20
       23*9

KY EQUALS KX
KZ ZVAR
       20*0.001
       8*1
       75*5
       28*7
       1*5
       18*5
       1*0.001
       20*5
       1*0.001
       62*5

KVSTRESS 200.0 0.88 1
       2000   1.0
       6000   0.98


C ================================================================================
C === transmissbility multipliers
C ================================================================================
TXF ZVAR
       44*0.5
       34*0.5
       156*0.5

TYF CON
       1

TZF ZVAR
       28*0.0001
       70*0.1
       5*0.01
       12*0.1
       7*0.1
       9*0.2
       1*0.0001
       9*0.2
       40*0.8
       53*0.2

C ================================================================================
C ===  DEFINE REGIONS
C ================================================================================


ROCKTYPE ZVAR
 103*1
 28*3
 69*1
 34*1

C ================================================================================
C ===  DEFINE INITIAL
C ================================================================================
INITIAL 1
DEPTH
10100.000000 1990.000000 0.293348 0.110178 0.167479
  0.268780 0.160216

PINIT 4000
ZINIT 10210

SWINIT ZVAR
       25*0.79
```

```
       3*0.4
       2*0.2
       4*0.1
       4*0.05
       35*0.08
       41*0.05
       9*0.5
       36*0.05
       34*0.05
       36*0.1
       5*0.15
TEMP CON
       268

REGION CON
       1

ENDINIT

MODIFY PV
       1 35 1 1 1 10 * 10000
       1 35 1 1 11 20 * 1000

C ================================================================================
C ===  output
C ================================================================================

NOECHO
SCREENPRT 1
PRINTZERO 1
PRINTTHP 0
SUMFREQ 1
ANNUALSUM
WELLFREQ 1
PRINTSUM 1 0 0 0 1 1
MAPSFILE SW SO SG P PSAT
MAPSFILEFREQ 1

WELL
I      J      K      SKIN   RW
PROD
109    1      33     -2.5   0.354
109    1      34     -2.5   0.354
109    1      45     -2.5   0.354
109    1      46     -2.5   0.354
109    1      57     -2.5   0.354
109    1      58     -2.5   0.354
109    1      69     -2.5   0.354
109    1      70     -2.5   0.354
109    1      81     -2.5   0.354
109    1      82     -2.5   0.354
109    1      93     -2.5   0.354
109    1      94     -2.5   0.354
109    1      103    -2.5   0.354
109    1      104    -2.5   0.354
109    1      113    -2.5   0.354
109    1      114    -2.5   0.354
109    1      125    -2.5   0.354
109    1      126    -2.5   0.354
109    1      137    -2.5   0.354
109    1      138    -2.5   0.354
109    1      185    -2.5   0.354
109    1      186    -2.5   0.354
109    1      195    -2.5   0.354
109    1      196    -2.5   0.354
109    1      206    -2.5   0.354
109    1      207    -2.5   0.354
109    1      217    -2.5   0.354
```

```
109     1       218     -2.5    0.354
109     1       226     -2.5    0.354
109     1       227     -2.5    0.354

WELL
I       J       K       SKIN    RW
C11PROD
58      1       152     -2.5    0.354
58      1       153     -2.5    0.354
58      1       154     -2.5    0.354
58      1       155     -2.5    0.354
58      1       156     -2.5    0.354
58      1       157     -2.5    0.354
58      1       158     -2.5    0.354
58      1       159     -2.5    0.354
58      1       160     -2.5    0.354
58      1       161     -2.5    0.354
58      1       162     -2.5    0.354
58      1       163     -2.5    0.354
58      1       164     -2.5    0.354
58      1       165     -2.5    0.354
58      1       166     -2.5    0.354
58      1       167     -2.5    0.354
58      1       168     -2.5    0.354
58      1       169     -2.5    0.354
58      1       170     -2.5    0.354
58      1       171     -2.5    0.354

WELL
I       J       K       SKIN    RW
C11INJ
58      1       152     -2.5    0.354
58      1       153     -2.5    0.354
58      1       154     -2.5    0.354
58      1       155     -2.5    0.354
58      1       156     -2.5    0.354
58      1       157     -2.5    0.354
58      1       158     -2.5    0.354
58      1       159     -2.5    0.354
58      1       160     -2.5    0.354
58      1       161     -2.5    0.354
58      1       162     -2.5    0.354
58      1       163     -2.5    0.354
58      1       164     -2.5    0.354
58      1       165     -2.5    0.354
58      1       166     -2.5    0.354
58      1       167     -2.5    0.354
58      1       168     -2.5    0.354
58      1       169     -2.5    0.354
58      1       170     -2.5    0.354
58      1       171     -2.5    0.354

WELL
I       J       K       SKIN    RW
INJ
1       1       33      -2.5    0.354
1       1       34      -2.5    0.354
1       1       45      -2.5    0.354
1       1       46      -2.5    0.354
1       1       57      -2.5    0.354
1       1       58      -2.5    0.354
1       1       69      -2.5    0.354
1       1       70      -2.5    0.354
1       1       81      -2.5    0.354
1       1       82      -2.5    0.354
1       1       93      -2.5    0.354
1       1       94      -2.5    0.354
1       1       103     -2.5    0.354
```

```
1      1      104    -2.5   0.354
1      1      113    -2.5   0.354
1      1      114    -2.5   0.354
1      1      125    -2.5   0.354
1      1      126    -2.5   0.354
1      1      137    -2.5   0.354
1      1      138    -2.5   0.354
1      1      185    -2.5   0.354
1      1      186    -2.5   0.354
1      1      195    -2.5   0.354
1      1      196    -2.5   0.354
1      1      206    -2.5   0.354
1      1      207    -2.5   0.354
1      1      217    -2.5   0.354
1      1      218    -2.5   0.354
1      1      226    -2.5   0.354
1      1      227    -2.5   0.354

WELLTYPE
PROD STBOIL
C11PROD STBOIL
C11INJ STBWATINJ
INJ STBWATINJ
INJ STBWATINJ

RATE
PROD          1E20
C11PROD       -1
C11INJ        -1
INJ           50000.0

BHP
INJ           8000
PROD          4000
C11PROD       20000
C11INJ        6500

!----------------------------------------------------------------------
!                              Timestep control
!----------------------------------------------------------------------
DTIMPES 0.5               ! Use IMPES stable time stepping, CFL multiplier
DTMIN 0.0003              ! Minimum time step size, days
DTMAX 5.00                      ! Maximum time step size, days
MAXITN 12                 ! Maximum number of Newton iterations before cutting time
step



!----------------------------------------------------------------------
!                              Output control
!----------------------------------------------------------------------
MAPSFREQ -1
MAPSFILEFREQ YEAR
MAPSFILE P SW SO SG VISO VISW KRW KRO TEMP TRACER

SUMFREQ 1                 ! controls frequency of lines in the eor summary (.out)
and the .PLTDAT file
STEPFREQ -1               ! controls frequency of time step table and region table
in the .out file
PRINTZERO 0               ! Include lines of 0 rate in eor summary file

!----------------------------------------------------------------------
!                           Proceed to time (days)
!----------------------------------------------------------------------
HEATCALCS OFF
DATE 1 2  1986
```

```
MODR KVSTR
      1      9      1      1      33     33     =      2
      1      9      1      1      34     34     =      2
      1      9      1      1      45     45     =      2
      1      9      1      1      46     46     =      2
      1      9      1      1      57     57     =      2
      1      9      1      1      58     58     =      2
      1      9      1      1      69     69     =      2
      1      9      1      1      70     70     =      2
      1      9      1      1      81     81     =      2
      1      9      1      1      82     82     =      2
      1      9      1      1      93     93     =      2
      1      9      1      1      94     94     =      2
      1      9      1      1      103    103    =      2
      1      9      1      1      104    104    =      2
      1      9      1      1      113    113    =      2
      1      9      1      1      114    114    =      2
      1      9      1      1      125    125    =      2
      1      9      1      1      126    126    =      2
      1      9      1      1      137    137    =      2
      1      9      1      1      138    138    =      2
      1      9      1      1      149    149    =      2
      1      9      1      1      150    150    =      2
      1      9      1      1      161    161    =      2
      1      9      1      1      162    162    =      2
      1      9      1      1      172    172    =      2
      1      9      1      1      173    173    =      2
      1      9      1      1      183    183    =      2
      1      9      1      1      184    184    =      2
      1      9      1      1      192    192    =      2
      1      9      1      1      193    193    =      2

DATE   1      7      1997
……
DATE   1      1      2024

RATE
PROD          -1
INJ           -1

DATE   1      2      2024
……
DATE   1      1      2027

RATE
C11PROD       -1
C11INJ                20000

BHP
C11PROD       4000
C11INJ                7000

MAPSFILEFREQ 1

WELLTRACER
C11INJ WATR
0.0    1.0

DATE   2      1      2027
……
DATE   31     1      2027

WELLTRACER
C11INJ WATR
1.0    0.0

DATE   1      2      2027
……..
```

```
DATE   28     2      2027

RATE
C11PROD       20000
C11INJ                -1

BHP
C11PROD       4000
C11INJ                7000


DATE   1      3      2027
……
DATE   31     5      2027

END
```

CEOR Module

```
!---------------------------------------------------------------------
!                        CEOR Module
!---------------------------------------------------------------------
!  Tracer Definitions
TRACER 1
   3              WATR                                                ! salt,
polymer, surfactant
   1              F4F5                                                !
surfactant

! ---- Tracer Initial Concentrations - Define TRACERF for each tracer ----
TRACERF CON 1
  1          WATR                                                    ! Salt
  0.5715                                                ! Concentration - meq/ml

TRACERF CON 1
   2          WATR                                                    ! Polymer
   0.0                                                               !
Concentration - wt%

TRACERF CON 1
   3          WATR                                                    !
Surfactant
   0.0                                                               !
Concentration - vol%

 TRACERF CON 1
   1          F4F5                                                    !
Surfactant
   0.0                                                               !
Concentration - vol%

 !!  Salt - Define once
 SALT  1                                                             !
(reservoir number)
   SALTTRACER       1                                      ! Salt tracer
number (assumed in WATR phase)
 ENDSALT


!  Adsorption  - one value must be entered for each tracer
  ADSORPTION 1                                    ! (reservoir number)
  ADSPHASE          WATR
  ADSKEQ            0.0   100     1000                    ! Adsorption Equilibrium
Constant Keq (1/[concentration])
  ADSKS             0.0   0.0       0.0                   ! Adsorption Rate
 Constant Ks (1/[concentration]/day, second order) --> Zero means use equilibrium
 adsorption
 ADSCMAX     0.0   0.0097    0.00256          ! Maximum adsorbed concentration
 ([concentration]) (ADSCMAX:       ADSCPOLY= AD41/B4D, ADSCSURF=AD31/B3D)
 ADSSALT     0.0   0.0100    0.00050    ! Maximum adsorption concentration salinity
 dependance (ADSCMAX+ADSSALT*CSE) (ADSALT=AD42/B4D, AD32/B3D)  (original -> 0.0
 0.0050    0.00025)
 ADSDENS     0.0   0.0       0.0                   ! Density of adsorbed
 components (lbm/STB) - used to reduce porosity
ENDADSORPTION

!  Surfactant
SURFACTANT  1                                     ! (reservoir number)
  SURFWATERTRACER   3                           ! Surfactant tracer number
(assumed in WATR phase)
  SURFOILTRACER   F4F5    1                               ! Surfactant tracer
number (assumed in WATR phase)
  SURFCMC           0.0005                                ! Surfactant CMC at
optimum salinity (critical micelle concentration)
```

```
  SURFIFTBASE     30                                  ! Base oil/water IFT (with no
surfactant)
  SURFNCBASE     1.0e-7                               ! Reference capillary number
6.0e-6
  SURFCAPNUM   1865.0      59074      364.2   ! NC_ref, NC_hf - Base capillary
number; capillary number at half desaturation (T11, T22, T33 or 1/Tii) 5.36e-4
1.69e-5  2.75e-3
  SURFLOWNCTAB    2                                   ! SWT index corresponding to
sigma_min
  SURFSALINITY      0.821     0.950     1.070        ! CSEL, CSOPT, CSEU -- Lower
salinity for type III, Optimum salinity, and Upper salinity for type III CSEO

! Full Surfactant phase behavior
  SURFPLAIT         0.001     0.999                          ! C2_PL, C2_PR -- Oil
coordinate of left plait point (for Type II) and right plait point (for Type I)

  SURFVISALPHA      0.5  0.5  0.0  0.9  0.7          ! Microemulsion viscosity
correlation Parameters

ENDSURFACTANT

MAPSFILE SO SW SG P POROS KX KZ SWINIT PSAT
```